Fachbereich Veterinärmedizin der
Freien Universität Berlin
Institut für Veterinär-Physiologie

Ionic Conductances of the Ruminal Epithelium

Habilitationsschrift
Zur Erlangung der Lehrbefähigung
am Fachbereich Veterinärmedizin
der Freien Universität Berlin

eingereicht von
Dr. med. Friederike Stumpff

Berlin 2010

Gutachter:

Prof. Dr. Gerhard Breves

Prof. Dr. Martin Diener

Prof. Dr. Michael Fromm

Deskriptoren (nach CAB Thesaurus):

rumen, omasum, ion channels, ion transport, ionophores, sodium, potassium, chloride, magnesium, ammonium, ammonia, urea, acetates, acetic acid, propionates, butyrates, butyric acid, short chain fatty acids, volatile fatty acids, epithelium, electrophysiology, cell culture, sheep, ruminants, cattle, physiology

Tag des öffentlich-wissenschaftlichen Vortrags:

18. Februar 2011

Bibliografische Information der *Deutschen Nationalbibliothek*
Die Deutsche Nationalbibliothek verzeichnet diese Publikation in der Deutschen Nationalbibliografie; detaillierte bibliografische Daten sind im Internet über <http://dnb.ddb.de> abrufbar.

ISBN: 978-3-86664-961-3
Zugl.: Berlin, Freie Univ., Habil., 2010
Habilitation, Freie Universität Berlin
D 188

Choriner Str. 85 – 10119 Berlin – verlag@menschundbuch.de – www.menschundbuch.de

To

Günter,Yamina and Nils

in gratitude

CONTENTS

1 INTRODUCTION 1

2 OPEN QUESTIONS 2

3 THE FORESTOMACH SYSTEM: AN OVERVIEW 5

3.1.1 Histology and organogenesis of the forestomachs 5
3.1.2 Saliva 7
3.1.3 Release of cations and anions into the rumen by fermentational processes 8
3.1.4 Clinical importance of maintaining ruminal homeostasis 11
3.1.5 Clinical importance of omasal absorption 11
3.1.6 Importance of developing transport models across forestomach epithelia 12

4 LITERATURE 13

4.1 Paracellular pathway 13
4.1.1 Transport of chloride across forestomach epithelia: a transcellular process 14
4.1.2 Paracellular transport: the rumen 15
4.1.3 Paracellular transport: the omasum 16
4.1.4 Paracellular transport: the reticulum 17
4.1.5 Open questions 18

4.2 The stratum corneum and the apical microclimate 18
4.2.1 The functional significance of the apical microclimate 18
4.2.2 Open questions 19

4.3 Basolateral extrusion of Na^+ via the Na^+/K^+-ATPase 20

4.4 Apical uptake of sodium via Na^+/H^+- exchange (NHE) 20
4.4.1 Stimulation of NHE by CO_2 and short chain fatty acids (SCFA) 21
4.4.2 Open questions 22

4.5 Electrogenic Na^+ conductance of the rumen 23
4.5.1 Interactions of Na^+ conductance with Ca^{2+} and Mg^{2+} 24
4.5.2 Effects of voltage on electrogenic Na^+ transport 25
4.5.3 Open questions 26

4.6 Transport of magnesium 26
4.6.1 Apical uptake of magnesium 27
4.6.2 Basolateral efflux of Mg^{2+} 28
4.6.3 Open questions 28

4.7 Transport of potassium 28
4.7.1 Potassium conductances of the rumen 29
4.7.2 The inverse regulation of ruminal Na^+ and K^+ concentration 29
4.7.3 Open questions 29

4.8 Transport of nitrogen across the ruminal wall 30

4.9 Absorption of ammonia from the rumen 31
4.9.1 The ruminal transport of ammonia: NH_3 or NH_4^+? 32
4.9.2 Open questions 33

4.10 Secretion of urea into the rumen 33
4.10.1 Open questions 34

4.11 Transport of chloride and bicarbonate 34
4.11.1 Diffusional uptake of CO_2 34
4.11.2 Apical Cl^-/HCO_3^- exchanger 35
4.11.3 Open questions 36

4.12 Absorption of SCFA from the rumen 36
4.12.1 Production of SCFA 36
4.12.2 Uptake of SCFA occurs transcellularly 37
4.12.3 Apical uptake of SCFA 37
4.12.4 Metabolism of SCFA 39
4.12.5 Basolateral efflux of SCFA 39
4.12.6 Open questions 40

4.13 Transport of anions across the omasum 40
4.13.1 Open questions 41

5 METHODS 41

5.1 Calculation of the upper limit for paracellular transport from the partial conductance equation 41

5.2 Isolation of cells from the rumen 42

5.3 Establishment of a method for the isolation of cells from the omasum 43

5.4 Confocal laser scanning microscopy and immunohistochemistry 44
5.4.1 HE staining and staining for cytokeratin and vimentin 45
5.4.2 Staining for tight junction proteins 46

5.5 Patch-clamp measurements 47
5.5.1 Electrophysiology 48
5.5.2 Perfusion of the bath chamber 52
5.5.3 Solutions and chemicals 52
5.5.4 Whole cell currents 53
5.5.5 Reversal potentials and relative permeability ratio 54
5.5.6 Single-channel conductances 55

5.6 Microelectrode experiments 56
5.6.1 Experimental set-up 56
5.6.2 Fabrication of double-barreled pH-sensitive microelectrodes 57
5.6.3 Measurements 59

5.7 Statistics 59

6 RESULTS 59

6.1 Identifying the proteins of the paracellular pathway 59

6.2 Apical microclimate 63

6.3 Electrogenic uptake of Na^+, Ca^{2+}, and Mg^{2+} by the rumen: the non-selective cation channel 65
6.3.1 Electrogenic conductance for sodium: interaction with Mg^{2+} 66
6.3.2 Permeability to Ca^{2+} and Mg^{2+} 68
6.3.3 Magnesium and the voltage dependence of the ruminal sodium conductance. 69
6.3.4 Interactions of the non-selective cation channel with SCFA 71
6.3.5 Interactions of the non-selective cation channel with cAMP 71
6.3.6 The basolateral efflux of Mg^{2+} 72
6.3.7 Interaction of the non-selective cation channel(s) with blockers 72

6.4 Conductance for potassium 73
6.4.1 Inwardly rectifying potassium conductance 73
6.4.2 Blocker sensitivity 74
6.4.3 Outwardly rectifying potassium conductance 74
6.4.4 A model for ruminal potassium transport 75

6.5 The conductance of the rumen for ammonium 76
6.5.1 Permeability of the intact rumen to NH_3 and NH_4^+ 77
6.5.2 Isolated cells of the ruminal epithelium express channels permeable to NH_4^+ 77
6.5.3 Interaction of NH_3/NH_4^+ transport with ruminal sodium transport 78
6.5.4 The basolateral efflux of NH_4^+ 79

6.6 The secretion of urea by the rumen 81
6.6.1 Transport of urea is mediated by a transport protein 81
6.6.2 Urea recycling and pH homeostasis 82

6.7 Apical uptake of SCFA 82

6.8 Distribution theory across epithelia or why lipid diffusion cannot work 84

6.9 Basolateral efflux of chloride and SCFA: the maxi-anion channel 87
6.9.1 The large-conductance anion channel of the rumen 87
6.9.2 Sensitivity to blockers 89
6.9.3 Potential dependence and the three state gating model 89
6.9.4 Halide selectivity sequence 91
6.9.5 Permeability of the ruminal anion channel to the anions of SCFA 93
6.9.6 Interactions of SCFA with the non-selective cation channel of the rumen 94
6.9.7 The large-conductance anion channel of the omasum 95
6.9.8 A model for the efflux of SCFA from the forestomachs 96

7 DISCUSSION 99

7.1 The apical non-selective cation conductance of the ruminal epithelium 99
7.1.1 Sodium, magnesium, and the potassium homeostasis of the ruminant 99

7.2 Urea, ammonia and pH homeostasis 102
7.2.1 The non-selective cation channel as a pathway for the apical uptake of NH_4^+ 103
7.2.2 The basolateral K^+ channel as a pathway for the efflux of NH_4^+ 103
7.2.3 The interactions between ammonia and ruminal Na^+ and H^+ transport 104
7.2.4 Urea, ammonia, and pH homeostasis 105

7.3 SCFA and the basolateral anion channel 107
7.3.1 Saliva is needed for ruminal buffering 107
7.3.2 The coupled transport of $SCFA^-$ and Na^+ 108
7.3.3 Basolateral efflux of SCFA from forestomach epithelia through a maxi anion channel 109
7.3.4 Multiple pathways mediate the efflux of SCFA from the rumen 111

8 SUMMARY 113

9 REFERENCES 115

10 ABBREVIATIONS 136

11 ACKNOWLEDGMENTS 138

12 APPENDIX 139

The general struggle for existence of animate beings is not a struggle for raw materials – these, for organisms, are air, water and soil, all abundantly available – nor for energy which exists in plenty in any body in the form of heat, but a struggle for [negative] entropy, which becomes available through the transition of energy from the hot sun to the cold earth. (Ludwig Boltzmann)

1 Introduction

The unique efficiency of ruminants in utilizing grass to meet their nutritional requirements is related to the development of a forestomach system in which fermentational processes break down ingested material before entry into the stomach and small intestine occurs. Because of this anatomical arrangement, ruminants have an outstanding ability to extract energy from low-grade raw materials such as cellulose. The microbial protein that is generated in the fermentational process not just from proteins, but also from non-protein nitrogen can be fully reclaimed by the lower parts of the digestive tract, leading to a nutritional efficiency that greatly exceeds that of hind gut fermenters on a grass diet.

The stratified squamous epithelia lining the forestomachs (133, 142) are probably of esophageal origin (243) and have evolved to function as a tight barrier protecting the animal from an uncontrolled efflux of substrate from the forestomachs into the blood, while selectively absorbing and secreting ions and molecules in order to maintain the homeostasis necessary for the survival of the microbial populations that ferment ingested material and to prevent damage to the forestomachs and the abomasum. In the process, the transport of ions across forestomach epithelia reaches quantities that exceed those of the ruminant kidney.

Thus, large quantities of Na^+ are absorbed from the rumen; this is essential for the maintanance of salivary flow. Conversely, the efflux of K^+ from the rumen has to be regulated to prevent problems with potassium homeostasis. Ammonia has to be absorbed from the rumen if its concentration exceeds the requirements optimal for microbial growth. Urea has to be supplied if ruminal nitrogen levels are too low. Bicarbonate has to be secreted when pH falls and absorbed when pH rises. Throughout this process, the absorption of short chain fatty acids (SCFA) has to keep up with their level of production to prevent dangerous rises in ruminal osmolarity. The transport of all of these substrates has to occur in a manner that integrates the

needs of the epithelium with those of the microbial populations living within in a manner that does not endanger plasma homeostasis.

In striking contrast to the impressive body of literature that supplies information on the impact of various feeding conditions on the ruminant *in vivo*, our current knowledge about the underlying transport processes across the rumen is surprisingly incomplete. At the time when this study commenced, no attempt had been made to identify the ionic conductances underlying transport across the rumen and the omasum. Filling this gap appears vital in developing a scientific approach toward ruminant nutrition and understanding the pathologies of ruminal function. Finally, analogies between the rumen and the colon in their function as an active barrier while permitting the uptake of energy-rich substrates may be of general interest for those interested in epithelial transport.

2 Open questions

When this study commenced, a number of pressing questions were open that are discussed in Chapter 4 (Literature). These questions were resolved by the publications listed below, which form the backbone of this study. The findings will be summarized in Chapter 6 (Results) and discussed in terms of their relevance for ruminal transport and the animal *in toto* in Chapter 7.

Microclimate

Do forestomach epithelia express a microclimate?

> ***Abdoun K, Stumpff F, Rabbani I, and Martens H.*** *Modulation of urea transport across sheep rumen epithelium in vitro by SCFA and CO_2. Am J Physiol 298: G190-202, 2010.*

Electroneutral sodium transport

What is the counter-anion for electroneutral sodium transport?

> ***Stumpff F, Martens H, Bilk S, Aschenbach JR, and Gäbel G.*** *Cultured ruminal epithelial cells express a large-conductance channel permeable to chloride, bicarbonate, and acetate. Pflugers Arch 457: 1003-1022, 2009.*

Electrogenic sodium transport

What is the pathway for the electrogenic efflux of sodium across the ruminal epithelium? How can its regulation by voltage be explained? Is it identical to the non-selective cation conductance that is blocked by Ca^{2+} and Mg^{2+}? What is its role in the homeostasis of the rumen?

Leonhard-Marek S, Stumpff F, Brinkmann I, Breves G, and Martens H. *Basolateral Mg^{2+}/Na^{+} exchange regulates apical nonselective cation channel in sheep rumen epithelium via cytosolic Mg^{2+}. Am J Physiol 288: G630-645, 2005.*

Stumpff F, Brinkmann I, Schweigel M, and Martens H. *High potassium diet, sodium and magnesium in ruminants: the story is not over. In: Production diseases in farm animals, edited by Joshi NP and Herdt TH, 2004, p. 284-285.*

Stumpff F and Martens H. *A role for magnesium in the regulation of ruminal sodium transport. In: Focus on signal transduction research, edited by McAlpine G. New York: New Nova Science Publishers, Inc. (ISBN 13 978-1-60021-376-2), 2006, p. 37-66.*

Transport of magnesium and calcium

Is there evidence for an apical Mg^{2+} channel? Can Ca^{2+} pass through this channel?

Stumpff F and Martens H. *A role for magnesium in the regulation of ruminal sodium transport. In: Focus on signal transduction research, edited by McAlpine G. New York: New Nova Science Publishers, Inc. (ISBN 13 978-1-60021-376-2), 2006, p. 37-66.*

Potassium transport

Does the ruminal epithelium express ion channels permeable to K^{+}? Why is the epithelium depolarized by K^{+}, if apical efflux of K^{+} is so low? What role might the stimulation of ruminal Na^{+} transport by high K^{+} solution play for the electrolyte balance of the rumen and of the animal?

Abdoun K, Stumpff F, Wolf K, and Martens H. *Modulation of electroneutral Na transport in sheep rumen epithelium by luminal ammonia. Am J Physiol 289: G508-520, 2005.*

Stumpff F and Martens H. *The rumen and potassium homeostasis: a model. Journal of Animal and Feed Sciences 16: 436-441, 2007.*

Transport of ammonium

Do isolated cells of the ruminal epithelium express ion channels with a conductance for the ammonium ion? What interactions occur between ruminal ammonia and ruminal sodium transport? How does basolateral efflux occur? How might SCFA affect the absorption of ammonia?

Abdoun K, Stumpff F, Wolf K, and Martens H. *Modulation of electroneutral Na transport in sheep rumen epithelium by luminal ammonia. Am J Physiol 289: G508-520, 2005.*

Abdoun K, Stumpff F, and Martens H. *Ammonia and urea transport across the rumen epithelium: a review. Anim Health Res Rev 7: 43-59, 2006.*

Transport of urea

Can the flux of urea into the rumen be explained by "lipid diffusion", or is a protein-mediated pathway mandatory? What physiological role might the transport of urea and the reuptake as ammonia have for ruminal acid-base equilibrium?

> ***Abdoun K, Stumpff F, and Martens H.*** *Ammonia and urea transport across the rumen epithelium: a review. Anim Health Res Rev 7: 43-59, 2006.*
> ***Abdoun K, Stumpff F, Rabbani I, and Martens H.*** *Modulation of urea transport across sheep rumen epithelium in vitro by SCFA and CO_2. Am J Physiol 298: G190-202, 2010.*
> ***Aschenbach JR, Penner GB, Stumpff F, and Gäbel G.*** *Role of fermentation acid absorption in the regulation of ruminal pH. J Anim Sci (submitted), 2010.*

Transport of chloride

What is the basolateral efflux pathway for chloride?

> ***Stumpff F, Martens H, Bilk S, Aschenbach JR, and Gäbel G.*** *Cultured ruminal epithelial cells express a large-conductance channel permeable to chloride, bicarbonate, and acetate. Pflugers Arch 457: 1003-1022, 2009.*

Transport of SCFA across the rumen

Do SCFA acidify the epithelium?

> ***Abdoun K, Stumpff F, Rabbani I, and Martens H.*** *Modulation of urea transport across sheep rumen epithelium in vitro by SCFA and CO_2. Am J Physiol 298: G190-202, 2010.*
> ***Aschenbach JR, Bilk S, Tadesse G, Stumpff F, and Gäbel G.*** *Bicarbonate-dependent and bicarbonate-independent mechanisms contribute to nondiffusive uptake of acetate in the ruminal epithelium of sheep. Am J Physiol 296: 1098-1107, 2009.*

How does ruminal SCFA transport occur if protons are buffered in the rumen by saliva? Do ruminal epithelial cells express a conductance for anions of the SCFA?

> ***Stumpff F, Martens H, Bilk S, Aschenbach JR, and Gäbel G.*** *Cultured ruminal epithelial cells express a large-conductance channel permeable to chloride, bicarbonate, and acetate. Pflugers Arch 457: 1003-1022, 2009.*

Transport of SCFA across the omasum

Is it possible to establish a method for the isolation of epithelial cells from the omasum? Do these cells express anion channels permeable to chloride and the anions of SCFA?

> ***Leonhard-Marek S, Stumpff F, and Martens H.*** *Transport of cations and anions across forestomach epithelia: conclusions from in vitro studies. Animal 4: 1037-1056, 2010.*

Paracellular pathway

What proteins maintain the barrier function of forestomach epithelia?

> *(manuscript in preparation)*

3 The Forestomach System: an Overview

To those not familiar with the physiology of the ruminant, the notion that absorptive processes across a stratified squamous epithelium occur and are physiologically necessary before the ingesta reach the duodenum must appear very peculiar. An understanding of the transport processes across the forestomachs requires an understanding of the physiological context within which these processes takes place. This overview will attempt to give a brief outline that will hopefully enable readers from outside the field to understand what follows.

3.1.1 Histology and organogenesis of the forestomachs

In ruminants, the glandular stomach, or abomasum, is preceeded by the three forestomachs. Fermentation of ingested matter occurs in the rumen by resident microbial populations, whereas the omasum can be seen as a "gate-keeper" regulating the flow of substrate from the rumen to the abomasum and filtering out particles and absorbing ions that lead to disturbances of abomasal function. Localized at the junction between the esophagus, the rumen, and the omasum, the reticulum might have several functions, one of which clearly is to return insufficiently degraded matter to the mouth for remastication.

All three forestomachs are covered with a non-glandular stratified squamous epithelium with histological similarities to that of the skin and the esophagus and clear distinctions from the gastric mucosa. Studies of organogenesis in ruminant embryos show that the forestomach system probably develops from an extension of the primordial proper esophagus to the dorsal side of the primordial stomach, which is subsequently separated from the proper esophagus by constriction (243). However, clear morphological differences from other stratified squamous epithelia abound.

Thus, the surface area of the rumen is enlarged by leaf-like papillae that are impressively large and dense, in particular when taken from animals on a diet rich in readily fermentable carbohydrates (100, 201, 328, 401). In cows, their length can reach 10 to 15 mm. Conversely, the papillae of the omasum are more discrete, but they also clearly serve to enlarge the surface area for absorptive functions (8, 129,

143, 371). In line with this, the ingesta to be found between the multiple leaflets of the omasum are densely packed and contain very little water.

The histology of the ruminal epithelium has been studied in some detail (82, 133) and shows a typical stratified squamous epithelium with stratum corneum, granulosum, spinosum, and basale; tight junctions (claudin-1 and ZO1) and gap junctions (connexin-43) make this epithelium a functional syncitium in which the cytosolic compartment of all cells is interconnected. Toward the basal membrane of this multilayered epithelium, increasing levels of the α subunit of Na^+/K^+-ATPase can be observed (133, 301). A copious fine network of capillaries underlies the epithelium (82). Our own results suggest that, in addition to claudin-1, both the rumen and the omasum express occludin and claudins 4 and 7.

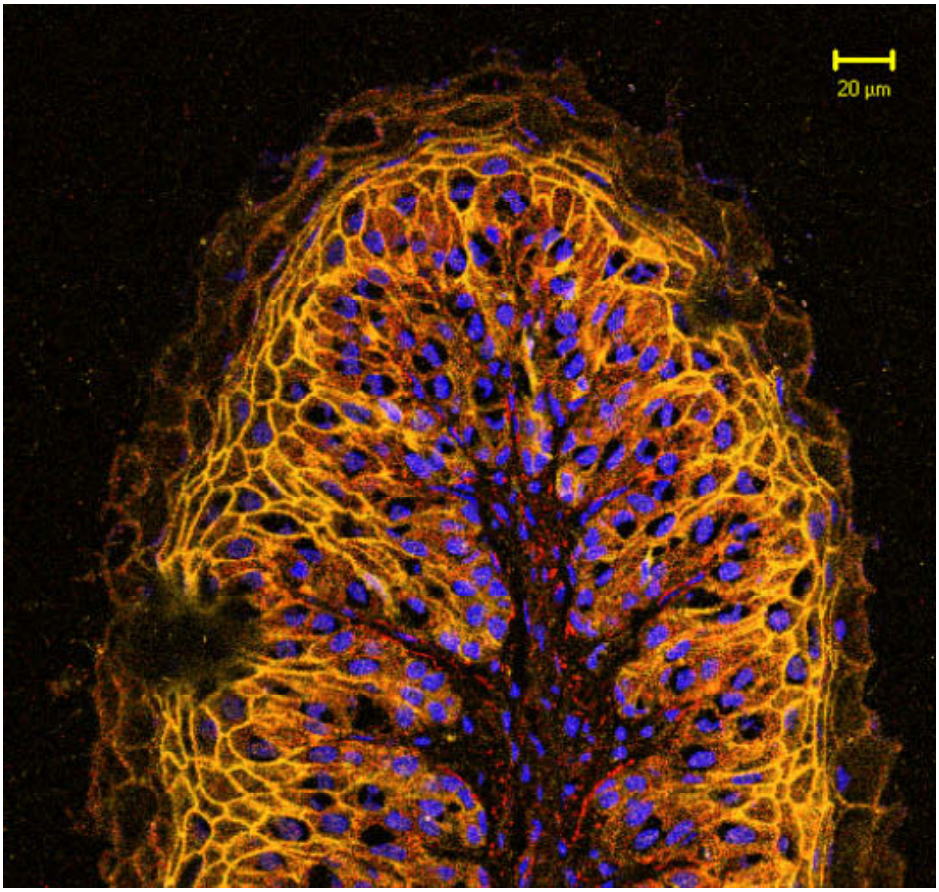

Figure 1: Cross section through a papilla of the omasum. The figure shows the multilayered stratified squamous epithelium separating the lumen side from the capillary bed. Cellular junctions were stained with antibodies against occludin (red) and claudin-1 (yellow). Cellular nuclei are shown in blue. (confocal laser scanning microscopy, cooperation with Dorothee Günzel, Institute for Clinical Physiology, Charité CBF, FU and HU Berlin.)

Our own attempts at cultivating epithelial cells from the rumen and the omasum confirm that, as in other stratified squamous epithelia, only the cells of the stratum basale have a regenerative function; these cells have to be isolated in order to obtain a viable cell culture that can then differentiate to express both apical and basolateral proteins (4, 199, 312, 314, 353).

3.1.2 Saliva

A major function of salivary secretion in the ruminant is to enable ruminal fermentation by buffering ruminal content. Accordingly, saliva contains large amounts of HCO_3^- (~120 mmol·l^{-1}) and PO_4^- (~30 mmol·l^{-1}), with a total secretion of $NaHCO_3$ of ~38 mol/day and of Na_2HPO_4 of ~7 mol/day in cows (98). The buffers contained in feed (~9 mol/day) are thought to play a minor role. Conversely, the influx of saliva cannot restore osmolarity after hypertonic challenges since the saliva of the ruminant is usually isotonic or very slightly hypotonic to blood (18-20, 59, 161, 162). The restoration of osmolarity after an osmotic challenge thus has to occur via absorption across the ruminal epithelium.

Salivary flow can amount to about 6-16 l/d in sheep (162, 191) and can reach 310 l/d in lactating cows (42, 53, 98, 330). This amount is 10 to 15 times as high as the plasma volume of the animal (279, 394). The saliva of ruminants is normally high in Na^+ (~160 -180 mmol·l^{-1}) and low in chloride (~22 mmol·l^{-1}) (20, 331). Secretion of Na^+ with saliva can exceed 50 mol/d (or more than 1 kg/d (98)) and is thus more than twice as high as the total amount found in the body (331). After feeding, the flow rate, but not the composition, of saliva increases and can be so massive that the ADH and renin-angiotensin mechanism is activated (330).

Likewise, salivary secretion of HCO_3 exceeds that found in plasma by a factor of 6-8 and thus reaches levels that can lead to acidaemia when salivary flow is high, as after a meal (266, 267, 316, 331). If experimentally obtained saliva is not returned to the rumen, the flow rate of saliva decreases to 50% of the initial value within two hours (33). This decrease can be prevented by the administration of $NaHCO_3$-containing solution to the rumen (30) and indicates the importance of the rapid reabsorption of salivary components by forestomach epithelia (75, 95, 97, 217).

3.1.3 Release of cations and anions into the rumen by fermentational processes

Both salivary secretion and fermentational processes lead to an accumulation of anions and cations in the ruminal fluid; these ions have to be absorbed for the osmolarity of the ruminal fluid to be restored. Quantitatively, short chain fatty acids (SCFA; frequently also referred to as volatile fatty acids or VFA) are the most important substrates formed and satisfy over 70% of the energy needs of the ruminant. Depending on the amount utilized by microbial populations, the amount of SCFA anions released into the rumen of cows ranges from 50 – 100 mol/day (9). Intraruminal concentrations of SCFA can reach 60 -150 $mmol \cdot l^{-1}$ (26), with roughly 70% in the form of acetate, 20% in the form of propionate, and 10% butyrate. Absorption of SCFA by the forestomachs is near total, so that the concentration of SCFA found in ingesta in the abomasum is usually below 10 $mmol \cdot l^{-1}$(229).

With the formation of SCFA, an almost equimolar amount of cations is released into the rumen, with protons (H^+) being the most abundant. As mentioned above, a major fraction of these protons are buffered by HCO_3^- entering the rumen with saliva (9), forming CO_2 that is removed from the rumen via ructus or transruminal absorption. At a ruminal pH of around 6.0, ruminal concentrations of HCO_3^- will drop below 10 $mmol \cdot l^{-1}$ (176) since the rumen is an open system with continuous removal of CO_2. The removal of protons from the rumen via this mechanism will thus be considerable.

Under most feeding conditions, the most abundant cation in the rumen is Na^+. The release of sodium from the diet only contributes about 4 mol/day in cows (225) wherease up to 50 mol/day of Na^+ are secreted with saliva. Conversely, the salivary concentration of K^+ is usually low, although it may rise when animals are sodium-depleted. The intake of K^+ with the diet shows great variation (3-24 mol/day in cows) and rises with the amount of forage ingested (135, 168). The K^+ contained in forage is completely released into the ruminal fluid (96). As potassium in the rumen rises to values that can attain 100 $mmol \cdot l^{-1}$, the sodium concentration falls, so that the osmolarity within the rumen remains constant. The inverse regulation of both ions (so that [Na] + [K] ≈ 130 $mmol \cdot l^{-1}$) seems to be a constant factor under many different feeding regimes (66, 136, 156, 159, 215, 238, 271, 317, 318, 324, 363, 385, 386).

One of the primary goals of this study has been to understand more about the mechanism behind this response.

Intake of magnesium with the fodder is around 2 mol/day or more (225) and is readily released from fodder, with additional amounts entering via saliva. When the rumen is bypassed, decreased plasma Mg^{2+} concentrations, decreased urinary Mg^{2+} excretion, and increased fecal Mg^{2+} excretion is observed. This negative magnesium balance cannot be compensated for by post-ruminal infusion of Mg^{2+} (369). The main site for the absorption of magnesium in the ruminant has thus been established to be the forestomach (260). Interestingly, a high intake of K^+ with accumulation of the element in the rumen can lead to hypomagnesemia in animals on low Mg^{2+} intake (215, 219, 221, 222, 225, 302).

Intake of Ca^{2+} lies between 3 and 5 mol/day and this element can also be absorbed across the ruminal epithelium (303, 304). However, the mineral appears to be tightly bound to plant cell walls and is thus only gradually released (96), so that the amount available for ruminal absorption will generally be low, unless the diet is supplemented.

Ammonium from dietary and endogenous sources rises to levels of around 20-30 $mmol \cdot l^{-1}$ postprandially with a total daily production that can reach 30 mol/day in dairy cows (1, 64, 65, 140, 164, 211, 230). After the initial postprandial rise, the ruminal concentration of ammonia rapidly drops via ruminal absorption (230, 309, 377).

The amount of inorganic anions released tends to be lower, with an intake of total phosporus for the formation of phosphates of below 4 mol/day, although the phosphates secreted with saliva can reach five times this amount (153). Release of sulfur is below 2 mol/day, and that of chloride around 1 mol/day, so that SCFA are the most abundant anions found in the rumen.

The release of these cations and anions and of other substrates such as sugars and starches from ingested material typically leads to a postprandial rise in ruminal osmolarity from values of below 290 mosmol/l to values that can approach 400 mosmol/l under certain feeding conditions (72, 275).

Efflux into the abomasum increases in animals on high energy diets but remains limited and tightly regulated. This allows completion of the fermentational processes and prevents an influx of buffers such as $SCFA^-$ and HCO_3^- into the abomasum. Extensive ruminal absorptive processes are thus necessary to maintain ruminal osmolarity.

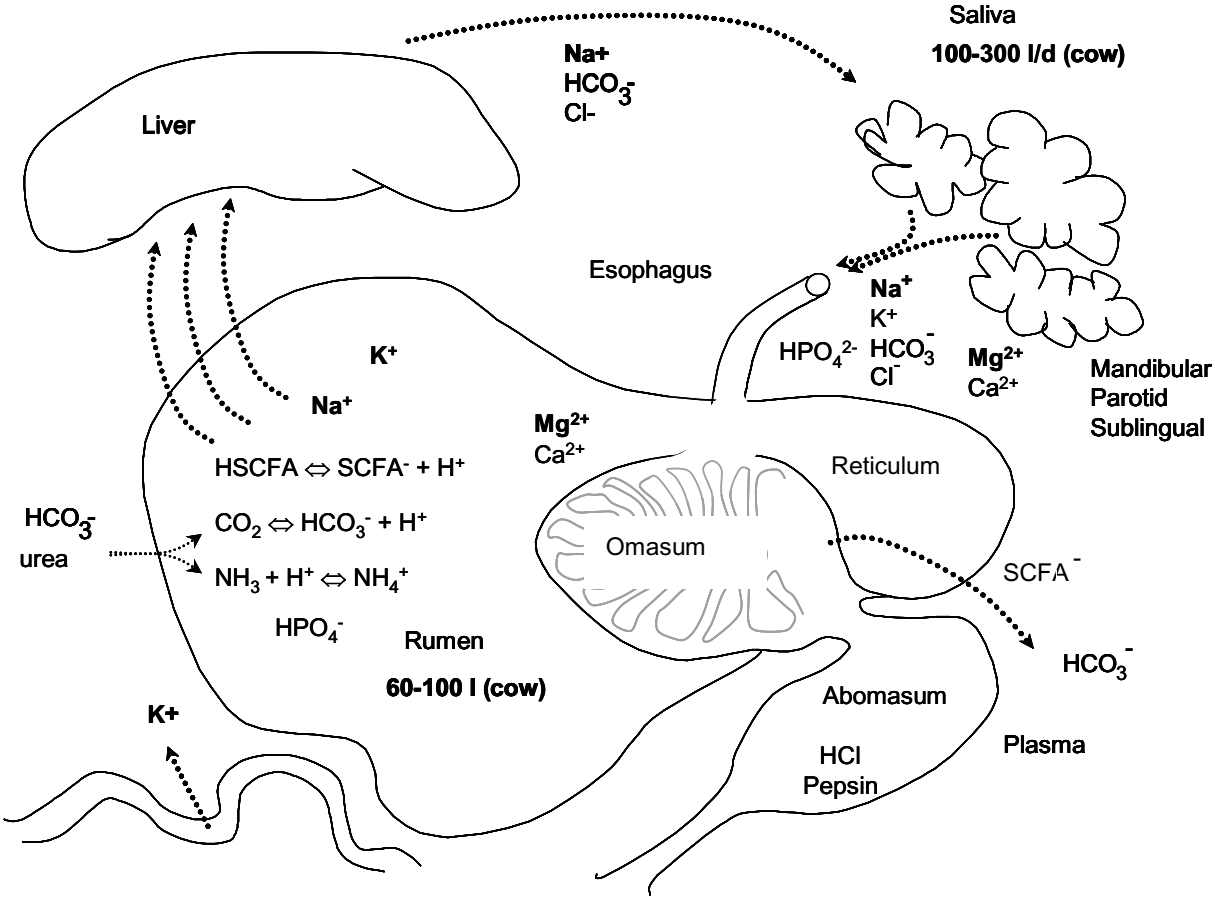

Figure 2: Schematic representation of the forestomachs. The forestomachs have evolved from parts of the esophagus and allow the fermentation of ingested material by microorganisms living within. Fermentational processes of organic matter release large quantities of short chain fatty acids (HSCFA), ammonia (NH_3) and CO_2, with an impact on ruminal pH. In addition, large quantities of inorganic cations are released, the most abundant of which is K^+. The survival of the microorganisms needed for ongoing fermentation requires the tight control of ruminal osmolarity, nitrogen levels, and pH. The maintainance of ruminal pH requires the secretion of large quantities of $NaHCO_3$ with saliva, whereas the maintanance of osmolarity requires extensive absorption across the ruminal wall. In addition, pH and nitrogen levels can be adjusted by transruminal secretion of HCO_3^- and of urea into the rumen. Before entry into the abomasum, residual buffering substances such as SCFA and HCO_3^- are removed from the ingesta by absorption across the omasal wall to allow speedy acidification with a minimal secretion of HCl and formation of gas.

3.1.4 Clinical importance of maintaining ruminal homeostasis

For optimal ruminal fermentation and fiber digestion, ruminal pH should lie between 6.0 and 6.4, whereas osmolarity should be slightly hypotonic to serum (~ 290 $mmol \cdot l^{-1}$). Both values will deviate from these levels for short periods during the day following feeding. When pH falls below the optimum, animals will tend to reduce their feed intake in order to reduce the acid load in the rumen until ruminal pH is once again above 5.6, resulting in short-term losses in productivity associated with a condition known as “subacute ruminal acidosis” (SARA). SARA frequently occurs in high-producing dairy herds as farmers respond to demands for increased meat and milk production with higher grain/lower fiber diets (174, 179, 263).

More severe secondary symptoms may follow such episodes of SARA and include ruminal necrosis and scarring, laminitis, weight loss, and poor body condition despite adequate energy intake, combined with unexplained abscesses suggesting that ruminal barrier function has been impaired (174, 179, 263). When ruminal pH falls to values below 5, the bacterial populations producing SCFA are increasingly overwhelmed by bacteria producing lactate (109). Since lactate cannot cross the apical membrane of the rumen, catastrophic developments follow that have been reviewed elsewhere (73, 174, 244, 263).

SARA and ruminal acidosis can usually be prevented by feeding enough fibrous material to stimulate salivary flow, and by allowing sufficient time for an adaptational response of the animal to a diet high in sugars and starch. This response involves an increase in the absorptive surface area of the rumen by hypertrophy of the papillae, coupled to an increase in epithelial thickness (73). Both salivary secretion and ruminal transport are thus essential for the maintanance of ruminal homeostasis.

3.1.5 Clinical importance of omasal absorption

With the introduction of modern dairy farming techniques, the incidence of abomasal displacement has been rising. In herds of dairy cows, typically 3% to 5% of the animals will suffer from this frequently fatal condition, and rates of up to 20 % have been reported in individual herds (83). A major contributing factor may be that, in animals on high energy diets, ruminal volume and osmolarity increase greatly with a

subsequent inability of the forestomachs to absorb sufficient amounts of HCO_3^- and $SCFA^-$, which will therefore flow on into the abomasum (214).

If HCO_3^- enters the acidic environment of the abomasum, CO_2 gas will form. Since the peculiar (and protective) properties of the gastric mucosa prevent absorption of CO_2 (41, 344, 380), gas (including CH_4) accumulates, the abomasum enlarges, motility drops, and ultimately, the abomasum will rise upward between the rumen and the abdominal wall or even twist in what is known as an abomasal volvolus (83, 214).

An insufficient removal of buffering SCFA from the ingesta will require the secretion of a larger amount of HCl by the abomasum to achieve the acidification necessary for the activation of gastric enzymes. Passage times, abomasal volume, and gas production by surviving microbial populations can be expected to increase and lead to abomasal distention. There is reason to believe that both distention and the direct effects of SCFA contribute to the inhibition of abomasal motility that is observed prior to abomasal displacement (364). In addition, the influx of SCFA may damage the abomasal epithelium (35). The mechanisms behind the transport of complex anions such as HCO_3^- and $SCFA^-$ across the omasal wall thus appear to be of considerable relevance.

3.1.6 Importance of developing transport models across forestomach epithelia

The great advances in modern human medicine during the last century are intricately linked to the progress made in understanding transport physiology. The discovery that the intestinal transport of Na^+ is linked to the transport of glucose has led to the introduction of simple and inexpensive solutions for rehydration that have arguably saved more lives world-wide than any other discovery in the medical field, not to mention the immeasureable impact that advances in our knowledge on the proteins that mediate the transport of substrates across cellular membranes has had on fields such as intensive care medicine, nephrology, cardiology, or pharmacology.

From the start, the ruminal epithelium has been an important model tissue in the study of epithelial transport in general. Thus, the notion that SCFA are an important metabolic product that can be transported across epithelia was first established in a study of the rumen (261). Ruminal physiologists have likewise led the way in

discoveries concerning the transport of chloride (337), urea (63, 139), and magnesium (221, 260). The cross-talk between physiologists studying various types of epithelia is likely to continue to contribute to general knowledge about transport processes.

In the ruminant, transport processes across forestomach epithelia are of essential importance not only for the maintanance of ruminal homeostasis as a precondition for an efficient fermentational process, but also for the health of the epithelia lining the forestomachs, for the prevention of damage to the abomasum, and for the acid-base and electrolyte balance of the animal *in toto*. Thus, an application of the knowledge derived from the transport physiological laboratory to the barn has led to the formulation of simple equations for determining the digestibility of magnesium in diets with differing K^+ content (302, 388). Further breakthroughs of this nature are likely to follow.

4 Literature

4.1 Paracellular pathway

The major part of this study is concerned with transport processes across the transcellular pathway that is formed by the functional syncitium of forestomach epithelia. Before these processes are discussed, an understanding of the degree to which substances are transported through the paracellular pathway between the cells is required.

In general, forestomach epithelia have to be extremely tight to maintain a protective barrier between the ingesta and the blood. However, in crises situations, ruminal homeostasis can often only be restored by the influx of water from the blood into the rumen (80, 114, 205, 310, 316, 386). In severe cases, loss of water into the rumen is so large that animals can become dangerously dehydrated (332).

This influx of water is usually coupled to an efflux of solutes out of the rumen (81), which has been suggested to occur across the paracellular pathway. Possibly, a breakdown of cellular volume regulation with the shrinking of cells leads to an increase in paracellular permeability (310). Interestingly, *in vitro* studies indicate that

the opening of this paracellular pathway is temporary, and that if the osmotic stimulus does not last for too long, the barrier function of the tissue can be restored (310). This route may thus respresent a physiological response to an acute emergency.

However, whereas this mechanism apparently helps to restore ruminal homeostasis and ensures the survival of the epithelium, the concomittant efflux of large organic molecules from the ruminal cavity as observed both *in vitro* (310) and *in vivo* (81) may have serious consequences. The efflux of endotoxins and other immunologically challenging stimuli is thought to underlie the systemic complications seen in acute and subacute ruminal acidosis (SARA) (52, 253) and may be the consequence of a corresponding breakdown in barrier function in response to a serious challenge of cellular homeostasis.

Since paracellular fluxes are passive and should strictly follow the electrochemical gradient, the upper limit of ion flow via the paracellar pathway can be calculated by using the partial conductance equation (150, 203, 308) according to which, at 310 K, the flux of an ion (in $mequ \cdot cm^{-2} \cdot h^{-1}$) is numerically related to the partial conductance (in $mS \cdot cm^{-2}$) (see methods, Chapter 5.1, for a derivation of the relationship). In doing so, we have to bear in mind that the conductance measured across the tissue almost certainly contains large contributions of transcellular charge flows (205).

4.1.1 Transport of chloride across forestomach epithelia: a transcellular process

In a study of chloride flux across sheep rumen, less than 20 % of the serosal to mucosal flux rate under standard Ussing chamber conditions could be stimulated by the application of an 80 mV potential gradient across the tissue (192), whereas in a study of cow rumen, no significant effect of the potential on the mucosal to serosal flux of chloride could be observed (322). Accordingly, a major part of serosal to mucosal chloride flux is influenced by the removal of HCO_3^- and by the application of diisothiocyanato-stilbene-2,2'-disulfonic acid (DIDS) (178, 218), suggesting a transcellular transport mechanism via anion exchange. These *in vitro* observations are supported by the observation that, *in vivo*, the upper limit of the ruminal chloride concentration is determined by the concentration of the anion in the saliva (10 – 40 $mmol \cdot l^{-1}$) (18-20). In the hours following the intake of feed, ruminal chloride

concentrations will generally fall, demonstrating that the rumen can absorb chloride against an extremely large electrochemical gradient, and that any reflux of the element down the chemical gradient from plasma into the rumen is small.

Interestingly, the replacement of chloride by gluconate leads to a sizable reduction of tissue conductance (218), whereas short-circuit current remains unaffected. The lack of an effect on short-circuit current again suggests that any paracellular efflux is small[1], whereas the impact on G_t can be explained on the basis of the contribution of a basolateral anion conductance (360) to total tissue conductance. Since the total transcellular resistance is the sum of the apical and the basolateral resistances, the closing of an additional pathway for the transfer of charge across the basolateral membrane by the removal of chloride can be expected to reduce tissue conductance. Conversely, the conductances for sodium and potassium (and not chloride) appear to be responsible for the transfer of charge across the apical membrane (189, 198, 199).

4.1.2 Paracellular transport: the rumen

Although the tissue appears to be relatively tight to anions under physiological conditions, a certain amount of sodium has been suggested to pass paracellularly (310), in particular when tissues are exposed to stressors such as hyperosmolarity.

Using the method of Frömter and Gebler (108) on the ruminal epithelium, Lang (189) has calculated a paracellular resistance of 1.3 $mS \cdot cm^{-2}$ for this tissue. It can be argued that the transcellular resistance is modulated by varying the apical concentration of Ca^{2+} and Mg^{2+} in these experiments; this might have had some effect on tight junction proteins. However, a paracellular resistance of similar magnitude emerges from other approaches. Analysis of the potential dependent component of *mucosal to serosal* sodium flux according to (107) suggests that a maximum of ~ 1.7 $\mu equ \cdot cm^{-2} \cdot h^{-1}$ of Na^+ ions pass through the tissue via an electrogenic pathway (188, 189, 205, 322) under standard Ussing chamber conditions without a gradient. Since the electrogenic transcellular transport of

[1] Since the mobilities of chloride (1.04) and gluconate (0.33) differ by 70%, a sizable change in Isc should result, even if the paracellular pathway had no selectivity filter!

sodium as measured by the short-circuit current (I_{sc}) is ~ 1 μequ·cm^{-2}·h^{-1}, and since the total tissue conductance is ~ 2 - 3 mS·cm^{-2} (4, 218), we can conclude that the bidirectional paracellular flux of sodium will be lower than ~ 2 μequ·cm^{-2}·h^{-1}; unidirectional fluxes should be half this size. This estimate is approximately equal to the value that emerges when the potential dependent *serosal to mucosal* sodium flux is analyzed by using the method of Frizzell and Schultz (107). The value obtained (of ~ 1 μequ·cm^{-2}·h^{-1}) remains remarkably constant when tissues are exposed to various osmotic pressures (205). Since the total serosal to mucosal flux of sodium is again significantly higher (~ 1.5 to 2 μequ·cm^{-2}·h^{-1}), a substantial part of J_{sm}(Na) must occur transcellularly. Accordingly, the application of amiloride significantly reduces the serosal to mucosal flux of sodium (218) (at constant G_t), as does the application of ammonia to the tissue (4).

As an aside, tissue conductance can double (to ~ 6 mS·cm^{-2} at 450 mmol·l^{-1}) under hyperosmolar conditions; this cannot be explained by an increase in the flux of sodium across the paracellular pathway. A substantial contribution of transcellular pathways has been suggested (205) and is supported by the effects of osmotic stress on the conductances of isolated cells of the ruminal epithelium (354).

4.1.3 Paracellular transport: the omasum

Tissues of the omasum typically display a similar conductance to that of the rumen (~ 2 - 3 mS·cm^{-2}), but a higher short-circuit current (of 1.7 μeq·cm^{-2}·h^{-1}(8, 307)). The strikingly high serosal to mucosal chloride fluxes (of ~ 8 μeq·cm^{-2}·h^{-1}(8, 217) must occur transcellularly, as must a significant proportion of the serosal to mucosal flux rate for sodium, which frequently reaches levels of over 6 μeq·cm^{-2}·h^{-1}(217). This assumption has been tested by replacing 85 mmol·l^{-1} of serosal Na^+ with N-methyl-D-glucamine (NMDG). Since the mobility of sodium (0.68) is twice as high as the mobility of NMDG (0.33), a significant increase in short-circuit current should occur, which is not the case. Instead, J_{ms}(Na) drops slightly, despite the increase in driving force. As in the rumen, both J_{sm}(Na) and J_{ms}(Na) can be inhibited by amiloride (7, 8), and no significant correlation has been observed between the G_t and the J_{sm}(Na). Similarly, the application of a serosal to mucosal gradient for chloride (mobility: 1.04) by apical substitution with the less mobile gluconate anion (0.33) does not result in

an increase in short-circuit current across the tissue (7, 8). In summary, these experiments suggest that the paracellular conductance of the omasum for sodium and chloride is at best marginal, in line with the extensive absorption of water seen across the tissue *in vivo* (94, 143, 335). The absorption of water depends on an effective barrier function to prevent a paracellular reflux of chloride and sodium ions from the plasma into the omasum.

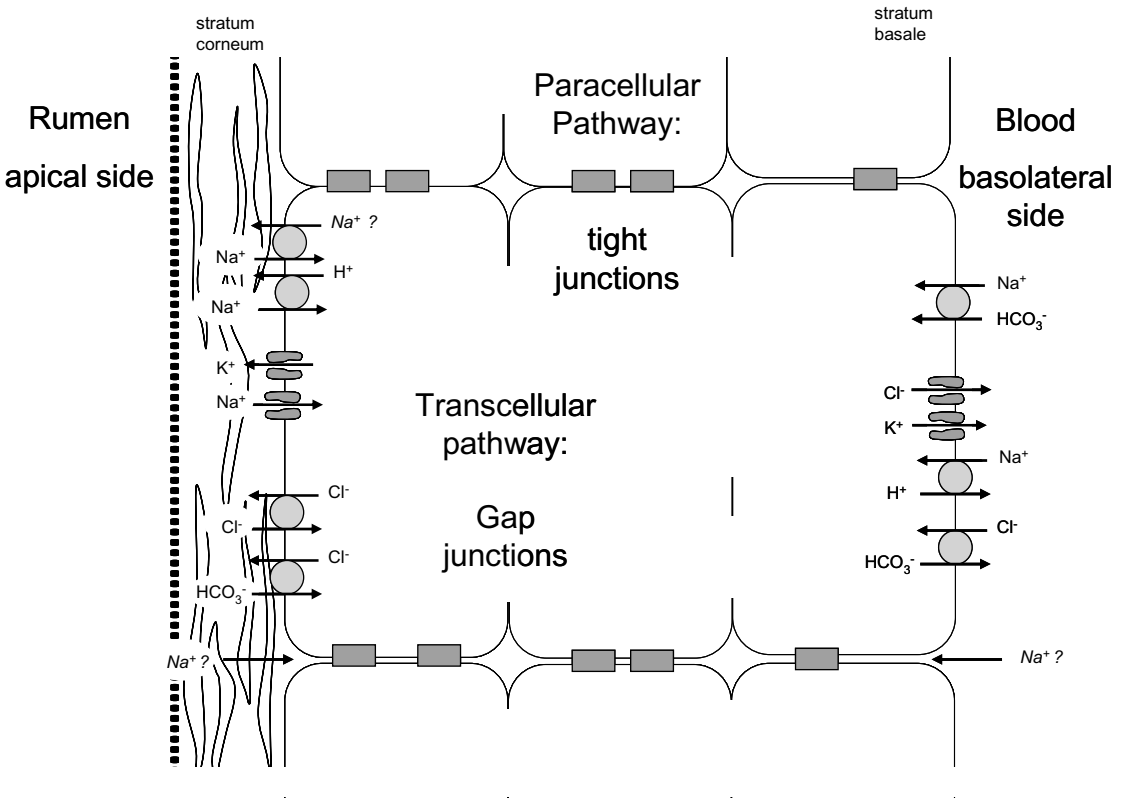

Figure 3: Representation of the epithelium lining the forestomachs. The forestomachs are lined with a functional syncitium of cells that resemble the stratified squamous epithelia of the skin or esophagus. Cells are connected by tight junction proteins that form an efficient functional barrier against the efflux of ions. Most transport processes occur across the tightly regulated transcellular pathway. Note that the tissue conductance will always include the contributions of apical and basolateral channels and thus cannot be equated with the paracellular conductance. Likewise, serosal to mucosal flux rates will contain considerable contributions of exchangers, the transport direction of which will be determined by the ion gradients present.

4.1.4 Paracellular transport: the reticulum

The most striking discrepancy between bidirectional flux rates and tissue conductance can be seen in the reticulum (115). Under *in vitro* conditions with no electrochemical driving force, fluxes of sodium and chloride in both directions are substantially higher than the G_t (of ~ 4 $mS \cdot cm^{-2}$), reaching levels of ~ 11 $\mu eq \cdot cm^{-2} \cdot h^{-1}$

for chloride and an amazing ~ 20 µeq·cm^{-2}·h^{-1} for sodium, with J_{sm}(Cl) at ~ 7 µeq·cm^{-2}·h^{-1} and J_{sm}(Na) at ~ 10 µeq·cm^{-2}·h^{-1}. Net flux rates and the short-circuit current are comparable with those seen in other forestomach epithelia. The application of ouabain reduces the flux rates for sodium in both directions, with the residual flux rate for sodium corresponding to the G_t. Amiloride inhibits not just the serosal to mucosal flux rate, but also the serosal to mucosal fluxes of sodium at constant G_t. Sodium fluxes have also been measured at various transepithelial potential levels, from which the potential dependent fraction of the total conductance can be calculated. These experiments suggest that, in the reticulum, the paracellular transport of sodium accounts for less than ~ 3 µeq·cm^{-2}·h^{-1}.

In summary, paracellular transport of chloride across forestomach epithelia is marginal. An upper limit for the paracellular transport of sodium can be calculated from the difference between the conductance and the short-circuit current of the preparation, bearing in mind that apical conductances for sodium and potassium and basolateral conductances for chloride and potassium will also contribute substantially to total tissue conductance.

4.1.5 Open questions

What proteins maintain the barrier function of forestomach epithelia?

In contrast to the wealth of observations concerning the tightness of forestomach epithelia, knowledge of the way that the cells are interconnected with each other is meager. The rumen expresses claudin-1 and ZO-1 (133). Prior to this study, nothing was known about the paracellular pathway of the omasum.

4.2 The stratum corneum and the apical microclimate

4.2.1 The functional significance of the apical microclimate

Like other stratified squamous epithelia, the forestomachs are covered with several layers of loosely adjoined cornified cells, the stratum corneum. This layer of cells probably does not have transporting properties, but serves to protect the underlying transporting epithelium. This might be one of several mechanisms protecting the rumen not just from mechanical impairment, but also from damage by toxins (348).

Functional pH microclimates are observed in a large number of epithelia (24, 56, 124, 208) or cells (242) and play an important, if somewhat underappreciated, role in acid-base metabolism. In the ruminal epithelium, evidence for such a microclimate has been obtained with the aid of a fluorescent microprobe inserted into the outer layers of the rumen epithelium in bicarbonate-containing solution (196). When the luminal Cl^- concentration is increased, an increase in surface pH can be observed, in line with a secretion of HCO_3^- in exchange for Cl^- absorption.

Little is currently known about the functional significance of this microclimate. Nevertheless, some speculation is possible. Current models of ammonia and SCFA transport assume that a major part of the uptake occurs via lipid diffusion of the uncharged form. The presence of a microclimate opens the possibility of limiting the influx of these substrates by altering apical pH and, thus, the concentration of the substrate available for transport via lipid diffusion. At low ruminal pH, bicarbonate extrusion into this microclimate should therefore limit the amount of HSCFA available for influx into the cell and hence contribute to cellular homeostasis.

4.2.2 Open questions

Can the existance of the microclimate be confirmed by direct measurement of surface pH?
Where is the microclimate localized?
Does it preceed the transporting cell layer?
Does the omasum express a microclimate?

Data obtained by using a fluorescent dye support previous hypotheses concerning the ruminal pH microclimate (196). In the present study, this microclimate was confirmed using an alternate method (ion-selective microelectrodes) to directly measure surface pH. The measurements clearly show that the microclimate preceeds the transporting layer of cells. The existance of a microclimate in the omasal epithelium could also be demonstrated using this method.

4.3 Basolateral extrusion of Na^+ via the Na^+/K^+-ATPase

As in other mammalian epithelia, the driving force for the active transport of sodium across the forestomachs is generated by the Na^+/K^+-ATPase. Immunohistochemical staining for the α-subunit of this protein is most prominent at the basolateral membrane of cells within the stratum basale with a decrease in staining intensity toward the stratum spinosum and granulosum (133, 301). Functionally, blocking the Na^+/K^+-ATPase by the basolateral addition of ouabain abolishes net Na^+ absorption across reticulum, rumen, and omasum (116, 142, 217). The secretion of K^+ by the ruminal epithelium is discrete (142, 198), and potassium is mostly recirculated basolaterally. Thus, the basolateral efflux of Na^+ is largely electrogenic, which means that it occurs coupled to a net transfer of a positive charge across the basolateral membrane.

4.4 Apical uptake of sodium via Na^+/H^+- exchange (NHE)

Quantitavely, the primary pathway for the efflux of sodium from the rumen is via an electroneutral pathway that is mediated by apical amiloride-sensitive sodium-proton-exchange (NHE) (4, 99, 112, 116, 118, 132, 223, 310, 341). Conversely, no indications have been found for Na-K-Cl cotransport in the rumen. In particular, bumetanide and furosemide have no effect on Na^+ transport across the intact ruminal epithelium (218, 223).

Transporters from the NHE family are ubiquitous and utilize the energy from the influx of Na^+ to drive the efflux of H^+ on a 1:1 basis, allosterically regulated so that the extrusion of protons stops when the cytosolic pH reaches the set point optimal for cellular function (14, 85, 381). In most mammalian transporting epithelia, the isoform NHE1 is found basolaterally, whereas the NHE3 form expressed by these tissues is localized apically and is involved in the transepithelial absorption of Na^+ (170), coupled to the absorption of chloride in exchange for bicarbonate via an anion exchanger. The activity of this anion exchanger is generally found to be closely linked to the activity of NHE, either functionally via pH, or physically via scaffolding proteins (85, 323).

To date, nine isoforms of NHE have been identified in various tissues (170, 400), at least two of which are functionally expressed by the ruminal epithelium. Thus, experiments with isolated epithelial cells from sheep rumen have shown that the specific inhibitors HOE 694 and S3226 inhibit an acid-induced pH_i recovery in these cells, corresponding to the presence of the mRNA of NHE3 and NHE1 (132, 310). Whereas immunohistochemical staining suggests a higher expression of NHE1-related proteins at the apical side of the tissue (132), functional studies with the specific blockers S3226 (NHE3) and HOE 694 (NHE1) confirm a pattern typical of transporting epithelia, with NHE3 being localized apically, while NHE1 is basolaterally expressed (84, 265). Correspondingly, manipulations that elevate cAMP in the tissue reduce mucosal to serosal electroneutral sodium transport (110, 393); this argues against a functional expression of NHE1 in the apical uptake pathway.

Inhibition by cAMP is a characteristic feature of NHE3, involving a linkage of the protein to the apical membrane via a signaling complex that involves the scaffolding proteins NHERF1 or NHERF2 and ezrin, which serves as a protein kinase A anchoring protein (AKAP) (400). Conversely, NHE1 is known to be stimulated by cAMP. Interestingly, the mRNA of two further isoforms (NHE2 and NHE8) has been detected in tissue from the rumen (132), both of which are normally apically expressed. Again, a functional significance of NHE2 appears unlikely, since it is stimulated and not inhibited by cAMP (32). The function and regulation of NHE8 is generally poorly understood (13, 32), and a functional role in the rumen has yet to be shown.

4.4.1 Stimulation of NHE by CO_2 and short chain fatty acids (SCFA)

As in the colon of monogastric animals (85), the end products of ruminal fermentation have a pronounced stimulatory effect on amiloride-sensitive Na^+ absorption via NHE (4, 109, 116, 217, 218, 322). Most likely, the signaling pathway is simple and involves an uptake of protons by the influx of CO_2 or HSCFA into the cells, or an efflux of bicarbonate via anion exchange; thus, the NHE is stimulated in order to maintain intracellular pH (286) as a prerequisite for the maintenance of enzymatic function.

The rapid apical extrusion of protons has to be seen as essential for the maintenance of epithelial viability. The concomittant uptake of sodium can be considered as advantageous for the production of $NaHCO_3$ for excretion with saliva; this is essential for the neutralization of acidic equivalents produced in the fermentational process. Accordingly, epithelia from animals adapted to a high ruminal SCFA concentration attributable to a high energy diet will generally show a marked increase in sodium uptake via NHE (205, 372).

4.4.2 Open questions

What is the counter-anion for electroneutral sodium transport?

Although the apical uptake of Na^+ via NHE is electroneutral and occurs in exchange for a proton, the basolateral efflux of Na^+ via the Na^+/K^+-ATPase is coupled to the transfer of a charge across the basolateral membrane. A model in which charges leave the epithelium, but no charges enter it, is clearly not workable, and thus, a counter-anion must accompany the efflux of Na^+ across the basolateral membrane in a manner that restores electroneutrality.

Under *in vitro* conditions, Cl^- functions as an important counter-anion for electroneutral sodium transport. Stimulation of electroneutral sodium transport by CO_2 results in a stimulation of Cl^- transport, resulting in the functionally coupled, electrically silent transport of Na^+ and Cl^- across the epithelium (217, 218). Apically, Cl^- is taken up in exchange for the HCO_3^- that is formed intracellularly from CO_2 via an anion exchanger (54, 115, 218, 367). In support of this, isolated rumenal epithelial cells show functional Cl^-/HCO_3^- transport and express mRNA for the anion transporters PAT, DRA, and AE2 (27, 154).

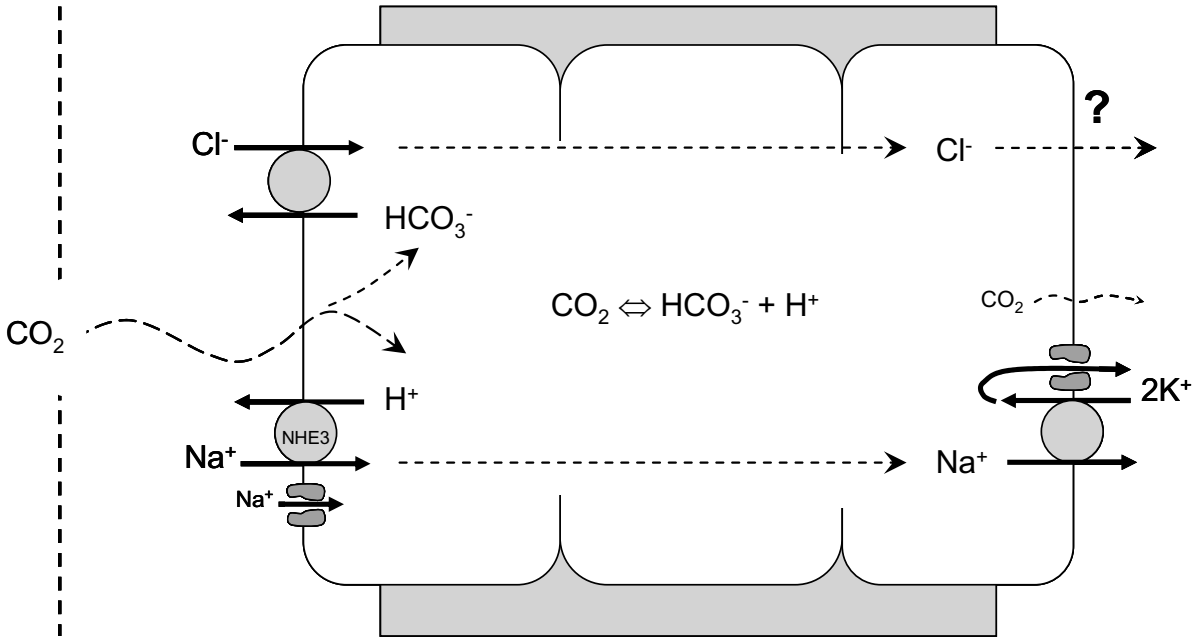

Figure 4: Model for the electroneutral uptake of sodium and chloride by the ruminal epithelium. If sodium and chloride both enter the epithelium via electroneutral mechanisms, the efflux of these ions also has to occur in a manner that does not involve a net transfer of charge across the tissue. Since potassium is basolaterally recirculated, the efflux of sodium via the pump will be electrogenic. To balance the charge and regain electroneutrality, the efflux of chloride also has to occur electrogenically.
Conversely, sodium entering electrogenically through an apical channel will also leave electrogenically. This will generate a measureable potential across the epithelium.

At the time when this study commenced, no data existed concerning the nature of the basolateral efflux pathway for Cl^-, and no hypothesis had been proposed concerning a potential counter-anion for that part of electroneutral sodium transport induced by SCFA.

4.5 Electrogenic Na^+ conductance of the rumen

Following Skou's landmark discovery of the Na^+/K^+-ATPase (336), a corresponding potential of some 30 mV was discovered across the ruminal wall *in vivo* (75, 318) and *in vitro* (101). This potential is sensitive both to the basolateral application of ouabain (142) and to the apical removal of sodium (101). Whereas energetically, this potential is generated by the activity of the basolateral Na^+/K^+-ATPase, its size is determined by the current flowing across the apical membrane.

In most mammalian transporting epithelia such as the lung, gut, and kidney (22, 186, 288), the conductance of sodium across the apical membrane is mediated by a well-

characterized channel known as the "epithelial sodium channel" or ENaC. Characteristic features include the blocking properties of low doses of amiloride in the micromolar range, its stimulation by aldosterone, and its lack of voltage dependence (although a slightly higher open probability after *hyperpolarization* of the cell has been observed (287)).

In addition to this classical pathway for the electrogenic entry of sodium into transporting epithelia, evidence has been presented for the existance of epithelia in which the electrogenic uptake of Na^+ occurs through non-selective cation channels (163, 247, 376). In the rumen, amiloride given at a dose as high as 1 $mmol \cdot l^{-1}$ only marginally affects PD_t and short-circuit current, although Na^+ transport via NHE is significantly reduced. In addition, extensive *in vivo* (220) and *in vitro* experiments (unpublished results and (307)) by our group have failed to show any regulation of sodium transport across forestomach epithelia by aldosterone, and *in vivo*, adrenalectomy does not affect the PD_t of the ruminal epithelium (318). Thus, the electrogenic Na^+ conductance of the ruminal epithelium is clearly distinct from that of the members of the ENaC group and may, instead, resemble the amiloride-insensitive cation channels found in esophageal epithelia (17) or in the lung (163).

4.5.1 Interactions of Na^+ conductance with Ca^{2+} and Mg^{2+}

Ussing chamber experiments have shown that the removal of mucosal Ca^{2+} and Mg^{2+}, singly or together, increases PD_t and short-circuit current across the omasal (307) and ruminal epithelium (194). In microelectrode experiments, the removal of mucosal divalent cations leads to a depolarization of the apical membrane (189), whereas paracellular conductance is not affected.

These experiments were performed in the absence of an electrochemical gradient for sodium and thus cannot be explained by the opening of a paracellular shunt pathway attributable to the removal of divalent cations. Similar divalent-sensitive currents can also be carried by other monovalent ions such as Li^+, K^+, Rb^+, and Cs^+ (194, 307), but whether these currents, which occur passively down the electrochemical gradient, reflect the same conductance or occur via a paracellular pathway opened by the removal of divalent cations, remains unclear.

At physiological concentrations of both divalent cations, the conductance saturates at a Na^+ concentration of about 30 $mmol \cdot l^{-1}$ (290). In light of the great physiological variability of ruminal Na^+ content (which varies from 25 $mmol \cdot l^{-1}$ to > 100 $mmol \cdot l^{-1}$), this property is essential for maintaining sodium conductance at low levels of Na^+, while preventing a massive influx of Na^+ into the tissue at higher concentrations, an occurrence that would endanger cell homeostasis.

4.5.2 Effects of voltage on electrogenic Na^+ transport

In further experiments, *depolarization* of the apical membrane was found to increase the conductance of the ruminal epithelium for sodium and to decrease the fractional apical resistance (189, 310). At the time of the first publication, a voltage-dependent conductance for sodium in an epithelial tissue had not previously been reported and had to be seen as most unusual.

From the perspective of ruminant physiology, the significance of such a pathway for the uptake of sodium is clear. A marked increase in sodium transport is observed *in vivo* when ruminal potassium concentrations rise and plays an important role in the maintanance of ruminal osmolarity (156, 317, 324, 339, 386). This effect cannot be attributed to a rise in osmotic pressure, since the effects of urea or mannitol on sodium absorption are discrete (386). A high increase in osmotic pressure due to the administration of non-ionic osmotic agents can even reduce Na^+ absorption and induce water influx into the rumen (114, 205, 310). Conversely, potassium stimulates the absorption of sodium, even in the absence of an osmotic gradient (220).

Given the depolarizing effects of potassium on the ruminal epithelium *in vivo* (324) (49, 215) and *in vitro* (101, 102, 198), the increase in sodium transport across the rumen in response to an elevation of ruminal potassium may thus be related to a depolarization of the epithelium with a subsequent impact on a voltage-dependent conductance for Na^+, but prior to this study, the nature of this pathway remained a mystery.

4.5.3 Open questions

What is the pathway for the electrogenic efflux of sodium across the ruminal epithelium?
How can its regulation by voltage be explained?
Is it identical to the non-selective cation conductance that is blocked by Ca^{2+} and Mg^{2+}?
What is its role in the homeostasis of the rumen?

In light of the importance of ruminal sodium conductance for ruminal osmoregulation and its highly unusual characteristics in terms of what was classically established knowledge about epithelial sodium transport, the identification and characterization of this conductance in isolated cells of the ruminal epithelium via the patch clamp technique was considered a top priority at the commencement of this study.

4.6 Transport of magnesium

Interest in the uptake of magnesium by the ruminant extends back many years and is related to the surge of cases of an affliction known as “grass tetany”, which led to widespread losses of cattle in the last century (225). Following their sudden transfer from normal winter rations to young spring grass, the animals became excitable and were afflicted with excess salivation, ataxia, recumbency, and tetanic muscle spasms (333, 334). Despite the normal magnesium content of the fodder, the animals were apparently unable to absorb this mineral and thus suffered from hypomagnesemia. Sjollema’s hypothesis that the surge in frequency was related to the introduction of fertilizers containing “potash” (or potassium) has since been confirmed by a solid body of evidence, which has been reviewed elsewhere (88, 225). In modern approaches to ruminant nutrition, the potassium concentration of the diet is taken into account in order to be able to predict magnesium digestibility in cows quantitatively (302, 388)[2].

Absorption of magnesium from the rumen has been studied extensively at the level of the animal, the tissue, and the cell, and the main site for the absorption of magnesium in the ruminant has been established as being the forestomach (260).

[2] Mg digestibility (% of intake) = 31.6 (±6.3) – 0.75 (±0.35) x dietary K (g/ kg of DM)

Any negative interactions between K^+ and the absorption of Mg^{2+} occur in the rumen (198, 219). Notably, a number of other factors are known to contribute to the malabsorption of magnesium; these include sodium deficiency (220, 297) and high protein content of the diet with subsequent high levels of ruminal ammonia (111).

4.6.1 Apical uptake of magnesium

The apical uptake of Mg^{2+} has been shown to depend in part on the electrochemical driving force for Mg^{2+} across the apical membrane. Depolarization of this membrane by potassium has been found to reduce the transport of Mg^{2+} across the rumen *in vivo* by using various approaches (50, 111, 136, 220, 223, 224, 232, 396). Experiments carried out across isolated ruminal epithelium in the Ussing chamber have established that the potential difference, and not the potassium concentration, are central to the reduction in the uptake of Mg^{2+} (198, 219). Likewise, the exposure of isolated cells of the ruminal epithelium in culture to high potassium solution results in a reduced uptake of Mg^{2+} (312, 313), a procedure that depolarizes the isolated cells of the ruminal epithelium (4). In contrast, plasma magnesium concentration has no influence on the rate of Mg^{2+} absorption (226), and the effects of K^+ on Mg^{2+} absorption are not attributable to high levels of absorbed K^+, but rather to the concentration of K^+ present in the rumen (271).

Interestingly, Mg^{2+} transport across the rumen is also inhibited by ammonia (49, 224). The influx of NH_4^+ into the epithelium via a conductance for potassium has been postulated and should depolarize the epithelium (34, 38). The negative effect of a sudden increase of ruminal ammonia concentration on Mg^{2+} absorption disappears within 3 – 4 days, indicating mechanism(s) of adaptation (111, 225). Observations concerning the interaction of ammonia with Na^+ uptake in adapted animals (6) suggest that the adaptational resonse results in shifts in the relative permeability of the apical membrane of the ruminal epithelium to NH_3 and NH_4^+, respectively.

In addition to this pathway, evidence has been presented for a second transporting process that is not potential dependent and that facilitates the uptake of magnesium into depolarized cells at higher ruminal potassium concentrations (159, 198, 313). Thus, a number of factors are known to stimulate the absorption of magnesium from the rumen, including a rise in bicarbonate, SCFA, and a low but physiological pH of

around 6.4 (225); this has led to the model of an uptake via a $Mg^{2+}/2H^{+}$ antiport (197) or by Mg^{2+}- anion – cotransport (313).

4.6.2 Basolateral efflux of Mg^{2+}

Given that the serosal side of the rumen is positive versus the mucosal side (30 mV), any paracellular transport will move Mg^{2+} from the blood into the rumen at low concentrations of ruminal Mg^{2+} (51). Transport must thus be transcellular and active and was first demonstrated by Martens and Harmeyer in 1978 (221). The same study revealed that the transport is ouabain-sensitive and saturable.

4.6.3 Open questions

Is there evidence for an apical Mg^{2+} channel?

Prior to the beginning of these studies, some hypotheses suggested that Mg^{2+} influx could occur via an electrodiffusive pathway, but no concrete evidence had been presented with regard to the nature of this pathway. Although an active transport mechanism for basolateral efflux had been proposed, its nature was speculative.

4.7 Transport of potassium

Potassium enters the rumen both with the diet (3.8 mmol/kg·d to 20 mmol/kg·d (270, 319)) and with saliva (5 $mmol \cdot l^{-1}$ to 100 $mmol \cdot l^{-1}$)(30, 318). Secretion of potassium via a transcellular pathway under experimental conditions with extremely low ruminal potassium concentrations was first noted by Sperber and Hyden (337); this finding has been confirmed many times (89, 156, 215, 317, 386). Likewise, an increase in ruminal potassium leads to an increase in the potential across the ruminal wall *in vivo* and *in vitro* (101, 102, 324), and a high mucosal concentration of potassium has been found to depolarize the apical membrane of the ruminal epithelium and to decrease the fractional apical resistance (198). All three observations suggest that the rumen expresses conductances permeable to K^{+}. However, a paracellular efflux of potassium has also been suggested (235, 342).

4.7.1 Potassium conductances of the rumen

From the apical side, the K^+ conductance of the ruminal epithelium can be blocked by quinidine or verapamil, whereas basolaterally, the conductance is sensitive to inhibition by barium (34, 198). These observations argue against an efflux via tight junction proteins, which are not sensitive to these blockers and do not show a pronounced selectivity for K^+ over Na^+ (Dorothee Günzel, personal communication). Efflux of potassium from the rumen thus occurs primarily via a transcellular pathway. The existence of apical and basolateral K^+ channels with a differential pharmacological profile has been postulated (34, 142, 198). Conversely, no indications for Na-K-Cl cotransport have been found in the rumen (218, 223).

4.7.2 The inverse regulation of ruminal Na^+ and K^+ concentration

When sheep are transferred from a low potassium diet of hay and concentrate to a diet of high potassium grass from a heavily fertilized meadow, ruminal potassium concentrations can rise from levels of about 30 $mmol \cdot l^{-1}$ to peaks of 100 $mmol \cdot l^{-1}$ (324). Concomitantly, the concentration of sodium falls from levels as high as 100 $mmol \cdot l^{-1}$ to values of 25 $mmol \cdot l^{-1}$. The elevation of the ruminal K^+ concentration thus leads to an increase in the uptake of Na^+. The inverse regulation of both ions within the rumen seems to be a constant factor under many different feeding regimes (66, 136, 156, 159, 215, 235, 238, 271, 317, 318, 324, 363, 385, 386).

4.7.3 Open questions

Does the ruminal epithelium express ion channels permeable to K^+?
Why is the epithelium depolarized by K^+, if apical efflux of K^+ is so low?
What role might the stimulation of ruminal Na^+ transport by high K^+ solution play for the electrolyte balance of the rumen and of the animal?

Although the observation that high potassium depolarizes the ruminal epithelium *in vivo* and *in vitro* is extremely well-documented, the conventional model, which assumes that this depolarization occurs via an efflux of K^+ through apical and basolateral potassium channels, fails to clarify a number of observations. Thus, the apical efflux of K^+ is less than a third as large as the corresponding electrogenic

sodium conductance (142, 198, 393) under standard Ussing chamber conditions. In a static model, an increase in apical Na^+ concentration should thus have a greater impact on potential than an increase in apical K^+. Instead, the opposite has been observed (101, 102, 324): the increase in K^+ concentration has a higher impact on transepithelial potential than a corresponding increase in Na^+ concentration. Importantly and paradoxically, the transport of Na^+ across the tissue *increases* with rising levels of K^+, despite the fact that the absorption of Na^+ from the rumen has to occur against an electrochemical gradient.

As mentioned, the development of a model of epithelial transport that might clarify this confusing and counter-intuitive situation has been one of the top priorities of this study and has required a detailed understanding of the regulation of the conductances involved. When this study commenced, no previous attempt had been made to discuss the inverse regulation of ruminal Na^+ and K^+ concentration in terms of its importance for the animal *in toto*.

4.8 Transport of nitrogen across the ruminal wall

In ruminants, the intake of nitrogen is important not only to meet the requirements of the protein metabolism of the organism *in toto*, but also to serve the needs of the microbial populations that ferment ingested matter. Since in the natural habitats of the ruminant the dietary intake of nitrogen tends to be low, ruminal nitrogen is supplemented by endogenous secretion, mostly as urea (140, 190, 204, 213). It has been calculated that in ruminants, between 50% and 80% of intestinal nitrogen is endogenously secreted (140, 190, 204, 213). In absolute terms, 300 to 800 mmol/day of urea reach the rumen of sheep (57, 137, 152, 164, 276), whereas up to 10 mol/day of urea reach the rumen of bovines (130, 140, 155, 277). The ruminal wall is the main locus of urea secretion into the gastrointestinal tract of the ruminant (~70%), with secretion into the colon being around 25%, whereas secretion with saliva is usually below 5% (140, 213), although values of up to 30% have been reported (278).

Nitrogenous compounds not utilized by ruminal microorganisms are set free as ammonia[3]. The production of ammonia in the rumen can reach peak levels of 4 mol/day in sheep and 30 mol/day in dairy cows (64, 65). Ruminal concentrations can rise from some 2 to 4 $mmol \cdot l^{-1}$ to over 30 $mmol \cdot l^{-1}$ in the three-hour period following a meal (1, 105, 274, 276, 365)(for review: see (1)). Peak values are thus much higher than the ~ 3.5 $mmol \cdot l^{-1}$ to 5 $mmol \cdot l^{-1}$ required for optimal bacterial growth (230, 298, 309, 377). Following the postprandial rise in concentration, ammonia is rapidly reabsorbed into the portal blood across the ruminal wall, whereas the efflux into the omasum only accounts for ~ 10% of the ammonia produced. In the liver, NH_3 is converted into the non-toxic urea, so that from 26% to 72% of plasma urea is formed in the liver from ruminal ammonia (165). The secretion of urea and the absorption of ammonia thus form a cycle, the speed of which will ultimately set the pace for microbial growth and, thus, for the fermentation processes in the rumen.

However, another aspect requires closer inspection. As outlined above, a surprisingly large amount (35%-70%) of the ammonium released into the rumen is reabsorbed across the ruminal wall (1, 74, 230, 255, 262), converted to urea in the liver, and recycled back to the rumen. Further, somewhat smaller amounts are recycled to other parts of the gut, whereas in animals on high protein diets, considerable amounts leave via the kidney (2%-30%) (190, 273, 278, 389). Given that the formation of urea in the liver requires aspartate and ATP, urea recycling is energetically expensive, and it may be asked what purpose it serves.

4.9 Absorption of ammonia from the rumen

The transport of ammonia[3] across biological membranes is a key physiological process throughout all domains of life (167). Although it is highly toxic to animals, ammonia is the preferred source of nitrogen for most microorganisms, and a specific concentration of ammonia (3.5 $mmol \cdot l^{-1}$ to 5 $mmol \cdot l^{-1}$ (230, 298, 309, 377)) is essential for the maintanance of fermentational processes in the rumen.

The absorption of ammonium from the rumen of sheep can reach values of 300 mmol/day (74, 230) or even 1 mol/day (202). In cattle, portal flows of ammonium

[3] Here and in the following, the term „ammonia“ will be used to designate both forms (NH_3 and NH_4^+).

have been estimated to amount to 100 mmol per kg body weight(BW)$^{0.75}$(255), and recent studies of dairy cows on a high protein diet demonstrate even higher portal fluxes of ammonium of 25 mol/day (64, 65).

4.9.1 The ruminal transport of ammonia: NH_3 or NH_4^+?

Ammonia can occur in the form of NH_3 or NH_4^+, the relative proportions of which can be calculated from the pH and the pK value (~ 9.2) by using the Henderson-Hasselbalch equation. The passage of both forms across biological membranes is ubiquitous, and the form in which ammonia is taken up has dramatic consequences for pH regulation.

Uptake of ammonia from the rumen is stimulated by an alkaline pH (60, 151, 202), and an increased toxicity of ammonia can be observed at high ruminal pH (193), which suggests that large amounts pass across the ruminal wall as NH_3. Although ruminal concentrations of NH_3 will be low at physiological pH, the molecule is highly lipophillic (382) and may simply diffuse across the lipid bilayer, with efflux facilitated by the enormous surface area available for transport. In addition, uptake by specific transport proteins such as the aquaporins (241) or transporters of the Amt/MEP/Rh family (392) might take place. Amt/MEP/Rh proteins function as NH_3 scavangers and facilitate transport at extremely low concentrations of ammonia. Within the cytosol, NH_4^+ is formed and trapped since it does not permeate through the protein (167). It is thus essential for the function of these proteins that they are not permeable to ammonia in the form of NH_4^+.

Gärtner (120, 122, 123) first suggested that the disproportionately high rates of absorption at low NH_3 concentration were attributable to an additional uptake of the charged form (NH_4^+). Absorption of ammonia from the rumen is most rapid when fermentational processes lead to a sharp decline in ruminal pH, while ammonia concentrations peak (235, 275, 276). The discrepancy between ammonia efflux from the rumen and the concentration of the lipophillic form (NH_3) was confirmed in later studies (34-36, 38, 236, 329). In particular, it was noted that the ratio between ammonia and SCFA absorbed from the rumen did not change with ruminal pH, a finding not readily explicable on the assumption of a simple model of diffusive uptake of both substrates in the lipid permeable form (262). Intriguingly, the absolute

transport rates for NH_4^+ were found to rise with the concentration of SCFA and CO_2 (Bödeker *et al.*, 1992a; 1992b; Remond *et al.*, 1993b).

Subsequent *in vitro* experiments in the Ussing chamber showed that the uptake of NH_4^+ is quinidine-sensitive (34) and occurs with a corresponding increase in the short-circuit current, thus implying the passage of a charged positive ion through the tissue.

4.9.2 Open questions

Do isolated cells of the ruminal epithelium express ion channels with a conductance for the ammonium ion?
What interactions occur between ruminal ammonia and ruminal sodium transport?
How does basolateral efflux occur?
How might SCFA affect the absorption of ammonia?

4.10 Secretion of urea into the rumen

As mentioned above, large amounts of urea are transferred from the plasma into the gut of mammalian species, with the quantities being particularly high in ruminants. In camels, famously, the transfer rate is so high that no excretion of urea into the urine is observed (273).

In the ruminant, urea primarily enters the gastrointestinal tract via the rumen (~70%), while secretion into the colon rarely exceeds 25%. Secretion with saliva is usually below 5% (140, 213), although values of up to 30% have been reported (278). The fraction of urea transferred into the gut or excreted in the urine shows little relationship to plasma urea levels but is regulated by dietary intake. Secretion of urea can be negligible in animals on a high protein diet, whereas a low protein, high carbohydrate diet has maximal stimulatory effects on the flux of urea into the rumen (64, 140, 164, 190, 245, 248, 249, 251, 274, 278, 300, 389). In response to an increase in the fermentational production of CO_2, the urea flux into the rumen can thus increase significantly in as little as 15 minutes (276, 366), with flux rates rapidly returning to baseline after stimulation. Similar effects are seen after an exposure to SCFA.

4.10.1 Open questions

Can the flux of urea into the rumen be explained by "lipid diffusion", or is a protein-mediated pathway mandatory?
What physiological role might the transport of urea and the reuptake as ammonia have for ruminal acid-base equilibrium?

Since ruminal tissues express the urea transporter UT-B (210, 283, 296, 345), this protein might represent a pathway for the influx of urea into the rumen, with the concentration gradient serving as a driving force. However, the paracellular passage of urea and its diffusive influx through the lipid membrane are alternatives that have to be ruled out before a protein-mediated influx pathway can be postulated, the short-term and long-term regulation of which then has to be explored.

4.11 Transport of chloride and bicarbonate

The salivary production of HCO_3^- is considerable and can exceed 40 mol/day (9, 20, 98). In addition, the ability of the rumen to secrete bicarbonate (HCO_3^-) contributes to an optimally buffered environment within the reticulorumen, in general, and in the microclimate adjacent to the transporting layer of cells, in particular, and might play a major role in ruminal buffering in situations in which salivary flow is insufficient (15, 109). Part of this bicarbonate is converted to CO_2 in the course of acid buffering and is exhaled by ructus in the animals.

In practice, the transport of bicarbonate can occur in the form of CO_2, which dissociates to form H^+ and HCO_3^-, and as the anion (HCO_3^-) in exchange for chloride, with the gradients present determining the direction of the exchange.

4.11.1 Diffusional uptake of CO_2

Like most tissues (with the notable exception of the gastric mucosa (41)), the membranes of forestomach epithelia are highly permeable to CO_2 (7, 8, 27, 116). At the neutral pH of the cytosol, roughly half of the CO_2 taken up will dissociate (176). The protons are apically extruded in exchange for Na^+ via NHE, leading to a formidable stimulation of electroneutral sodium transport in both the rumen and the

omasum when the tissues are exposed to CO_2 (109, 116). In isolated cells, a corresponding acidification (with subsequent recovery) can be observed directly (27).

Transport studies *in vitro* show that, in the rumen, considerable amounts of CO_2 dissociate within the cytosol into H^+ and HCO_3^-, which are apically extruded in exchange for Na^+ and Cl^-, respectively, resulting in a net coupled uptake of Na^+ and Cl^- (116).

4.11.2 Apical Cl^-/HCO_3^- exchanger

The discovery that chloride ions can pass through the rumen *in vivo* against an electrochemical gradient (75, 77, 78, 337) has to be seen as one of the major break-throughs in transport physiology, following Hans Ussing's discovery of active Na^+ transport through toad skin one year earlier (373). At this point, an extremely solid data base supports the apical uptake of chloride via Cl^-/HCO_3^- exchangers functionally coupled to Na^+/H^+ exchange via intracellular pH in analogy to other absorptive epithelia of the gastrointestinal tract (54, 115, 218, 367).

Proteins mediating functional Cl^-/HCO_3^- exchange are structurally diverse but are expressed almost ubiquitously (144, 175, 284, 370). Isolated cells of the ruminal epithelium express PAT, DRA, and AE2 (27, 154), all of which are prime candidates for the apical uptake of chloride by the rumen. The current model of ruminal transport suggests that ruminal secretion of HCO_3^- via this anion exchanger is of great importance for ruminal buffering. *In vivo*, the apical chloride concentration will usually be below 40 $mmol \cdot l^{-1}$ (18-20). However, the exchanger also accepts anions of SCFA (15). In addition, the high partial pressure of CO_2 within the rumen of 0.5-0.7 atm (176, 235) can lead to high cytosolic concentrations of HCO_3^- within the (near neutral) cytosol to serve as a driving force.

In the omasum, conversely, the exchanger has been discussed in terms of bicarbonate absorption. Because of tissue- and organ-specific differences (such as the apical expression of an apical NaCl cotransporter and the lower concentration of SCFA), the exchanger operates in the reverse mode and thus absorbs HCO_3^-, thus acidifying the ingesta and preventing the entry of HCO_3^- into the abomasum, an event

that would lead to the production of CO_2 gas. Gas formation may be one of the primary causes for abomasal displacement (83, 214).

Taken together, these exchanges of bicarbonate across the ruminant forestomach system play a decisive role in the acid-base metabolism of the ruminant, one that may exceed even that of the kidney.

4.11.3 Open questions

What is the basolateral efflux pathway for chloride?

The need for an electrogenic efflux pathway for chloride has previously been discussed in the context of electroneutral Na transport (3.4.3, Figure 4). Since both chloride and sodium are taken up in an electroneutral process, while sodium leaves electrogenically via the pump, the basolateral efflux of chloride must occur in an electrogenic manner.

4.12 Absorption of SCFA from the rumen

The ruminal epithelium was the first epithelium in which the transepithelial transport of SCFA was studied, undoubtedly because of the high quantities that are physiologically absorbed. The mechanism by which SCFA cross the forestomach epithelia is decisive in determining both the impact that a rise in intraruminal production and absorption of SCFA will have on intraruminal pH, and the impact that ruminal pH will have on SCFA absorption (109).

A model of SCFA absorption that might serve as a satisfactory guide to the nutritionist has to take into account the finding that, whereas a lowering of ruminal pH stimulates the absorption of SCFA, the protons appear to be left behind and require further buffering by saliva.

4.12.1 Production of SCFA

Fermentational processes in the rumen release between 55 and 100 mol/day of SCFA into the forestomach of cattle (9, 25, 109), with acetate representing ~ 70% of

the total amount, followed by propionate (~ 20%) and butyrate (~ 10%). To meet the energy demands of the animal, a major proportion of these SCFA have to be absorbed and enter the portal blood unmetabolized (21, 109, 181).

The absorption of SCFA must occur rapidly at the site of production in order to maintain osmolarity (43, 109, 119, 174, 179, 180, 244, 257, 263, 340, 346). In the course of the fermentational process, SCFA frequently rise to a concentration of over 100 $mmol \cdot l^{-1}$ in the rumen. Assuming a production rate of 80 mol/day (258), a ruminal volume of 100 l, and a liquid turnover rate of 2 – 3 times per day (327), we can estimate that ~ 50 mol/day of SCFA , or 60% to 80% of the SCFA produced (206), are absorbed by the ruminal epithelium. A large fraction of the remainder are absorbed by the omasum (8, 21, 92-94, 160, 228, 261, 292, 397), so that the amounts of SCFA found in the abomasum are marginal (261, 292). As mentioned, some evidence suggests that the entry of SCFA into the abomasum is associated with damage to the abomasal epithelium (35) and abomasal displacement (83, 364).

4.12.2 Uptake of SCFA occurs transcellularly

At the beginning of the investigations into the epithelial tranpsort of SCFA, the suggestion was made that $SCFA^-$ anions can pass out of the rumen through intercellular water-filled pores (62), accompanied by Na^+ as a counter-ion. However, the application of a transepithelial potential did not lead to a sizable effect on the transport of either chloride (Sehested, 1996) or SCFA across the ruminal epithelium (321, 343) or other tissues of the digestive tract (12, 28, 46, 325), so that this hypothesis has had to be abandoned. SCFA cross the epithelium primarily via a transcellular pathway [4].

4.12.3 Apical uptake of SCFA

The apical uptake of SCFA by epithelia is thought to occur both via lipid diffusion (104, 233, 252, 383) and via anion exchange (15, 28, 178, 227, 378). Both influx of

[4] Note that a paracellular pathway open for the transfer of $SCFA^-$ anions would show an even greater permeability to the smaller and more mobile anions of Cl^-, so that the influx of Cl^- from the blood into the rumen would predictably exceed any efflux of $SCFA^-$ anions out of the rumen. Osmolarity would rise and not decrease.

HSCFA with subsequent dissociation into H^+ and $SCFA^-$, and efflux of HCO_3^- with subsequent dissociation of H_2CO_3 ($\leftrightarrow H^+ + HCO_3^-$) should lead to a net transfer of protons into the cytosolic space of the epithelium. Conversely, a sizable involvement of monocarboxylate transporters (91, 264) in the apical uptake of SCFA from the rumen can be ruled out, since the permeability of the tissue to lactate is so low (15).

A solid body of evidence from numerous gastrointestinal tissues shows that under most circumstances, protons taken up with SCFA are returned to the mucosal side via NHE, apparently to maintain cytosolic pH at constant levels. This leads to a functionally coupled uptake of Na^+ and $SCFA^-$ anions into the tissue (11, 46, 109, 113, 145, 157, 291, 320-322, 325, 347). Thus, the estimated daily SCFA absorption from the human colon *in vivo* is roughly equivalent to colonic Na^+ absorption (325), and SCFA are generally regarded as a major force driving the absorption of Na^+ from the colon (28, 61, 325). A similar close correlation between the transport rates of Na^+ and $SCFA^-$ across the ruminal epithelium can be found both *in vitro* (62, 116, 320) and *in vivo* (235).

Unlike the almost universal stimulation of sodium absorption by SCFA *in vitro* and *in vivo*, the effects of a removal of mucosal sodium on SCFA transport appear to be variable, even when observed in the same study (326). In forestomach epithelia, certain effects of the removal of Na^+ on SCFA transport have been observed in bovine rumen (321), but not in sheep rumen (178). Blocking NHE by amiloride, which should reduce the uptake of Na^+ into the tissue, has been shown to have effects on SCFA transport across sheep omasum (8) but not across sheep rumen (178, 321). The coupling of ruminal SCFA and sodium transport is thus clearly functional, rather than being fixed in the manner of a co-transport.

There can be no doubt that both *in vivo* and *in vitro*, the uptake of SCFA from the mucosal side of the rumen continues even after NHE breaks down. The NHE will only be able to maintain an apical pH gradient as large as the Na^+ gradient of ~ 10:1; if ruminal pH drops below 6, cytosolic pH will become acidic, unless other regulatory mechanisms exist (313). This will not slow down the uptake of SCFA into the tissue; it will merely prevent the removal of protons from the tissue. *In vitro*, the cytosol will become increasingly acidic and facilitate the basolateral efflux of the undissociated

form (HSCFA). However, transport of SCFA in this manner can hardly be considered physiological; accordingly, the short-circuit current measured *in vitro* will tend to decline if the pH regulatory function of NHE is suppressed, suggesting epithelial damage. *In vivo*, prolonged periods of ruminal acidosis (pH <6) initially result in high transport rates of SCFA across the tissue, but also in the swelling of the epithelial cells followed by subsequent keratinization (parakeratosis) (149). Possibly, this response serves to protect the epithelium from more far-reaching damage with loss of barrier function.

In summary, the coupling of SCFA transport to Na^+ transport is functional rather than fixed and probably serves to limit the concentration of protons within the epithelium. *In vitro* and *in vivo* evidence suggests that the majority of protons taken up with SCFA are apically returned via pH regulatory mechanisms such as NHE. In the absence of such mechanisms, the transport of SCFA will continue. However, there is reason to believe that the capacity of the tissue to transport protons is limited. Salivary secretion of buffers (such as $NaHCO_3^-$) is thus essential to minimize the amount of protons that have to be transported across the epithelium. In addition, adaptational responses of the tissue are necessary to prevent epithelial damage if diets high in energy are fed (109).

4.12.4 Metabolism of SCFA

From the start of the investigations into SCFA transport across the forestomachs, it was noted that whereas the rate at which SCFA were absorbed from the rumen appeared to rise with molecular weight, the order of their appearance in blood showed an inverse correlation to chain length (21, 169, 229). Recent studies suggest that whereas butyrate is extensively metabolized, 95% of propionate passes through the tissue unmetabolized, and the recovery rate of acetate is complete (181-185).

4.12.5 Basolateral efflux of SCFA

Currently established models of SCFA transport suggest that SCFA leave the epithelium together with the protons taken up either via a diffusive route or via a transport protein such as monocarboxylate transporter 1 (MCT 1 (171)). Both models predict a coupled efflux of protons and SCFA from the rumen at a ratio of 1:1.

However, considerable amounts of protons are undoubtedly buffered in the rumen by saliva, and therefore, large amounts of SCFA anions must cross the epithelium without a proton. This clinical finding is not integrated into the current models of ruminal SCFA absorption; similar questions emerge when considering SCFA transport across other epithelia. A new model of SCFA transport across epithelia is therefore overdue.

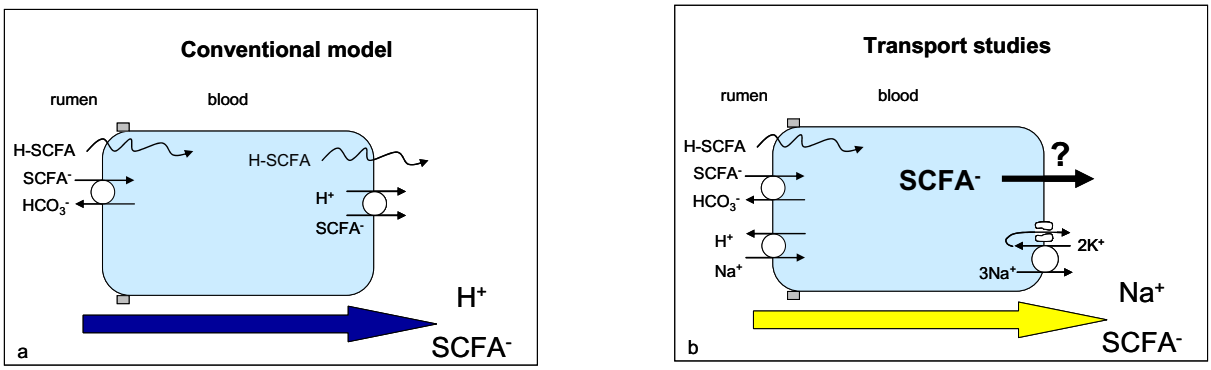

Figure 5: Models of ruminal SCFA transport. a) Conventional model of SCFA transport suggesting that the efflux of SCFA anions occurs in symport with protons via diffusion or mediated by a basolateral monocarboxylate transporter. Large quantities of protons have to be transported across the epithelium. b) Conversely, clinical experience and transport studies suggest that large quantities of SCFA are transported functionally coupled to sodium or other cations, whereas the protons set free from fermentational processes are buffered within the rumen.

4.12.6 Open questions

Do SCFA acidify the epithelium?

Do ruminal epithelial cells express a conductance for anions of SCFA?

How does ruminal SCFA transport occur if protons are buffered in the rumen by saliva?

4.13 Transport of anions across the omasum

In vitro investigations with high mucosal Cl^- have demonstrated a net electroneutral absorption of Na^+ and Cl^- across the omasum; this absorption essentially resembles that found in the rumen (217). Apical uptake occurs by functionally coupled Na^+/H^+ exchange linked via cytosolic pH to Cl^-/HCO_3^- exchange. Basolateral efflux of Na^+ is ouabain-sensitive and occurs via Na^+/K^+ exchange, with K^+ mostly recirculating basolaterally. As in the rumen, the basolateral efflux of Cl^- thus has to occur electrogenically, with a channel being the most likely candidate.

SCFA transport, too, closely resembles that of the rumen (8), with the uptake of SCFA occurring together with protons that are apically extruded via NHE. Since the protons have largely been removed from the ingesta entering the omasum, the argument against the absorption of SCFA with protons is even more pertinent than in the case of the rumen. A model for the functional efflux of the SCFA anions with cations other than protons is lacking and requires a basolateral efflux pathway for the SCFA anion.

4.13.1 Open questions

Is it possible to establish a method for the isolation of epithelial cells from the omasum?
Does the omasum express anion channels permeable to chloride and the anions of SCFA?

5 Methods

5.1 Calculation of the upper limit for paracellular transport from the partial conductance equation

As is standard knowledge among electrophysiologists, the flux of an ion is numerically related to the partial conductance. However, an (understandable) derivation of the underlying equation is difficult to find in the literature, and therefore, the origin of this relationship will be briefly discussed. Related to the surface of the tissue, the flux Φ of the ions (in $A \cdot cm^{-2}$) can be calculated from the more commonly used molar flux J (given in $\mu eq \cdot cm^{-2} \cdot h^{-1}$ (as in (4, 8, 110, 218)) by using Faraday's constant (= 96 485 $A \cdot s \cdot mol^{-1}$)

$$\Phi = 96\,485\ A \cdot s \cdot mol^{-1} \cdot J\ \mu eq \cdot cm^{-2} \cdot h^{-1} / (3600\ s \cdot h^{-1}) \cdot 10^{-6}\ mol/\ \mu eq = J \cdot 26.8\ \mu A \cdot cm^{-2}$$

The partial conductance equation of Nernst-Planck diffusion theory (150, 203, 308) states that, in the absence of an electrochemical driving force, the conductance of a

tissue (G) is proportional to the sum of the unidirectional fluxes of the ions (Φ, in amperes) through a transepithelial electrogenic pathway[5]:

$$G = F/(R \cdot T) \cdot \Sigma \Phi_i \cdot z_i = \Sigma \Phi \cdot z_i / 26.7mV$$

where R, z, and F have their usual meanings (see Appendix), and T = 310K in our example, so that, at this temperature (37 ºC) and by coincidence, the numerical value of the sum of the unidirectional fluxes of the various ions multiplied by their valency $\Sigma J_i \cdot z_i$ (in $\mu eq \cdot cm^{-2} \cdot h^{-1}$) is almost exactly equal to the conductance G in $mS \cdot cm^{-2}$.

$$G \cong \Sigma J_i \cdot z_i \; mS \cdot cm^{-2}$$

A tissue conductance of 1 $mS \cdot cm^{-2}$ thus reflects an ion flow of $\cong$ 1 $\mu eq \cdot cm^{-2} \cdot h^{-1}$. This represents one of many approaches that allow an estimation of the flux via an electrogenic pathway, which may, however, be either transcellular or paracellular. The conductance thus represents an upper limit for the paracellular flux of ions.

5.2 Isolation of cells from the rumen

The rumen was removed immediately after slaughter of the sheep, and isolation of cells was performed according to established methods by fractional trypsinization (117, 312). Briefly, the papillae were manually dissected and incubated in a trypsin-containing DPBS buffer solution (Dulbecco's PBS + 4% of a 10 000 U/ml/10 000 μg/ml penicillin/streptomycin solution, Biochrom AG, Berlin, Germany) in order to lyse the apical cell layers from the epithelium. The supernatant was repeatedly removed until cells from the stratum basale were obtained, which could then be plated in cell culture dishes and cultured according to established methods (117, 312).

After about one week in culture, cells were reseeded. For immunostaining, cells were grown until confluent. For patch-clamping, cells were reseeded onto glass coverslips and cultured for another 2-4 days before being used in experiments. The remaining

[5] This equation can be derived from the current equation of Goldman-Hodgkin-Katz theory((146) equation 14.5). The external and internal concentrations are taken as the apical and basolateral concentrations, which are equal ($[S_i] = [S_o]$).

cells were reseeded. Only single cells with no attachments to other cells were used for patch-clamping. After a maximum of 3 passages, cells were discarded.

5.3 Establishment of a method for the isolation of cells from the omasum

Research on the omasum has been limited because of the lack of a cell culture model. In the course of this study, a new method for the isolation of cells from forestomach epithelia was developed in which the tissue from the omasum or the rumen was placed in a purpose-built Ussing-chamber-style device with the apical side facing upward (2, 127). After placement in a glass beaker, the basolateral side of the tissue was immersed in Ca^{2+}- and Mg^{2+}-free DPBS buffer solution (Dulbecco's PBS + 4% penicillin/streptomycin (10 000 $U \cdot ml^{-1}$ and 10 000 $\mu g \cdot ml^{-1}$) (Biochrom AG, Berlin, Germany), whereas a DPBS-EDTA buffer with 1.25 % trypsin-EDTA solution (Sigma-Aldrich, St. Louis, Mo., USA) was applied apically. Subsequently, the tissue was incubated at 37 ºC in a shaking warm water bath. The supernatant with the enzymatically dissected cells was harvested roughly every 30 minutes and replaced with fresh trypsin buffer. The supernatant was centrifuged, and cellular material was plated into cell culture dishes coated with collagen A and covered with M199 cell culture medium containing fetal calf serum (150 $ml \cdot l^{-1}$), L-glutamine (6.8 $mmol \cdot l^{-1}$), HEPES (20 $mmol \cdot l^{-1}$), nystatin ($2.4 \cdot 10^5$ $U \cdot l^{-1}$), gentamycin (50 $mg \cdot l^{-1}$), and kanamycin (100 $mg \cdot l^{-1}$) (Biochrom AG, Berlin, Germany or Sigma-Aldrich, St. Louis, Mo., USA). Typically, the first fractions obtained by this proceedure only showed cellular detritus from the stratum corneum. Depending on the thickness of the overlying epithelium, the isolation of viable cells from the stratum basale required a trypsinization time from 1 ½ to 3 ½ hours. After reaching confluence, cells were trypsinized (0.25% trypsin/0.02% EDTA in PBS, Biochrom AG) and reseeded in DMEM medium (Pan Biotech GmbH, Eidenbach, Germany; with 4.5 $g \cdot l^{-1}$ glucose, 3.7 $g \cdot l^{-1}$ $NaHCO_3$, and L-glutamine) to which fetal calf serum (10%), HEPES (2%) and penicillin/streptomycin (1%) were added. Cells were passaged for a maximum of 3 times.

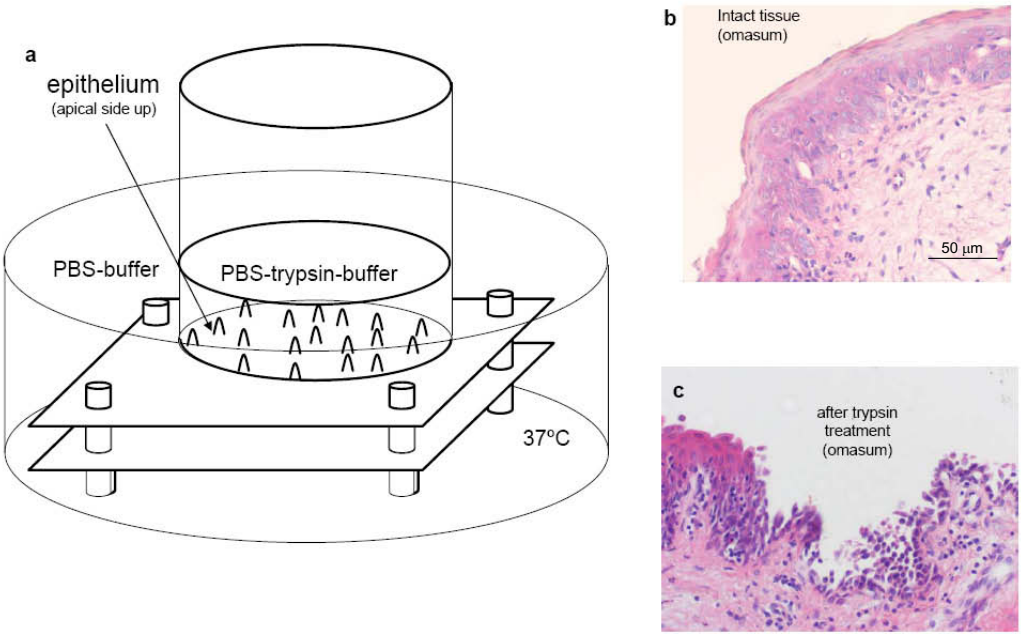

Figure 6: An improved method for the isolation of cells from forestomach epithelia. a) Representation of the device used for the incubation of the tissue. The apical buffer was strictly separate from the basolateral buffer, thus allowing the harvesting of trypsinized cells from the apical side of the tissue without contamination from basolateral layers. b) Hematoxylin/eosin (HE) staining of intact tissue of the omasum, showing the stratum corneum and the various layers underneath. c) Tissue after treatment with trypsin. The cells from the stratum basale are set free and can be harvested from the supernatant[6]. Incubation times varied depending on the thickness of the stratum corneum.

Cells were otherwise treated as previously described (117). After one day in culture, cell detritus was carefully removed by repeated washing with Ca^{2+}-free PBS buffer solution. If necessary, this treatment was repeated on the second day in culture. The first fraction of cells to show growth was used in further experiments. After 1 ½ to 2 weeks, the cell layer reached confluence.

5.4 Confocal laser scanning microscopy and immunohistochemistry

Cells of epithelial origin typically express cytokeratin and tight junction proteins such as occludin and the members of the claudin family. To confirm the epithelial origin of the ruminal and omasal cells, and to gain a better understanding of the tight junction proteins that limit paracellular flux across the forestomachs, both the tissue and the cells were stained for cytokeratin and for various tight junction proteins.

[6] Here and in the following, the generous help of Dr. L. Mundhenk, Institute for Veterinary Pathology, FU Berlin, with the staining of tissues and cells by HE and for cytokeratin and vimentin is gratefully acknowledged.

5.4.1 HE staining and staining for cytokeratin and vimentin

Staining with HE and for vimentin and cytokeratin was carried out with the kind help of Lars Mundhenk, Institute of Veterinary Pathology, FU Berlin, according to established methods. For vimentin and cytokeratin staining, cells were washed three times in PBS buffer, fixed with 4% paraformaldehyde for 15 minutes, washed, permeabilized with 0.1% Triton X, washed again, and blocked with a goat-serum-containing blocking buffer. Subsequently, cells were incubated for 1 hour in a PBS buffer containing 2% bovine serum albumin without (controls) or with specific antibodies for staining. Controls and antibody-treated cells were incubated with a fluorescently tagged secondary antibody. Vimentin and cytokeratin antibodies (mouse) were obtained from Dako Cytomation, Denmark (Clone V9) and ZyMED; S. San Francisco, Calif., USA, respectively. The secondary antibody was obtained from Dianova GmbH (Hamburg), and all other reagents were either from Carl Roth GmbH (Karlsruhe) or from Sigma Aldrich (Mo., USA).

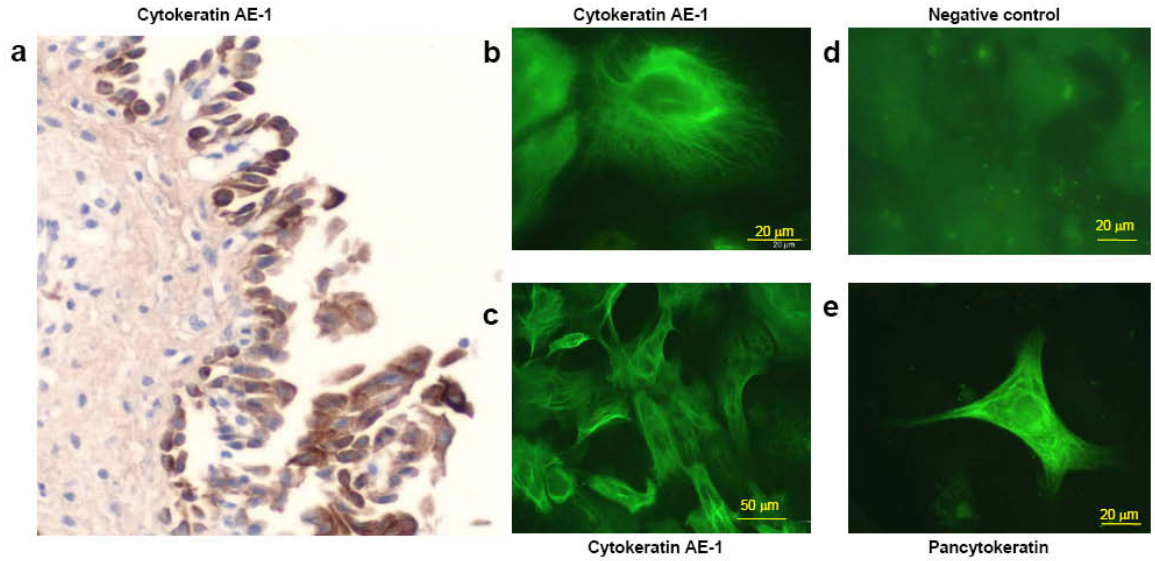

Figure 7: Staining for cytokeratins. a) Omasal tissue after the trypsinization process. The stratum basale is exposed and shows staining for cytokeratin AE-1. b to e) Immunofluorescent imaging of cultured cells from the omasum, showing staining for cytokeratin AE-1 (b and c), the corresponding negative control (d), and pancytokeratin (e)[6].

5.4.2 Staining for tight junction proteins

Staining for tight junction proteins was performed with the kind help of Dorothee Günzel, Institute for Clinical Physiology, Charité CBF, FU and HU Berlin. After reaching confluence, the cells were seeded onto microfilters (pore size 0.4 μm, 0.6 cm^2, Millicell-PCF, Millipore, Schwalbach, Germany). Subsequently, cells were washed with DPBS, fixed with methanol, permeabilized with 0.5% Trition X-100 solution and blocked with 2% goat-serum in PBS. For costaining of different proteins, primary antibodies from different species (mouse and rabbit) were used (Zymed, San Francisco, USA). Anti-body marked cells and controls were subsequently exposed to the secondary antibodies (Alexa Fluor 488 goat anti-mouse and Alexa Flour 594 goat anti-rabbit) (Eugene, OR, USA). Cellular nuclei were stained using DAPI (4*, 6-diamidino-2-phenylindole dihydrochloride). The images were obtained using a confocal laser microscope (Zeiss LSM510, Carl Zeiss, Jena, Germany) at 543 nm, 488 nm and 405 nm.

The presence of occludin and claudins 1, 4, and 7 could be demonstrated both in the cells and in the native tissue of the rumen and the omasum (Figures: see “Results”). The expression of these proteins could also be demonstrated by using Western blot and polymerase chain reaction (PCR) techniques using standard protocolls.

In cell cultures, a few isolated cells showed staining for claudin-3; this tended to be localized intracellularly. In the intact tissue, claudin-3 was absent from the epithelial layers and was expressed by cells of the capillary endothelium instead. A potential contamination of the cultures with small numbers of cells from the endothelium could thus not be ruled out. Conversely, the expression of occludin was robust and suggested that any fibroblasts present in the primarily isolated cells did not proliferate, a result that was possibly related to the selective culture media used (117).

In these studies, it also emerged that a robust staining for vimentin could be observed in a substantial number of cells. In native tissues, the expression of vimentin is frequently associated with the proliferation of fibroblasts. However, vimentin expression cannot be taken as a characteristic feature of fibroblast growth,

as it is also routinely observed in cultured keratinocytes (368) and might be related to the adaptation of cells to in vitro growth conditions (280) or more generally signify an active proliferative state of the cells (138, 272). Thus, the coexpression of vimentin and cytokeratin can also be observed in native epithelia in response to inflammation (375).

To clarify the issue, we stained cells for vimentin and tight junction proteins. Expression of tight junction proteins has to be seen as a highly characteristic feature of epithelial cells. Costaining for both vimentin and occludin by the same cells could be observed not just in cultured cells of ruminal and omasal origin, but also in cells of a well-established epithelial cell line (MDCK). As this example shows, expression of vimentin thus clearly does not argue against an epithelial origin of the cells.

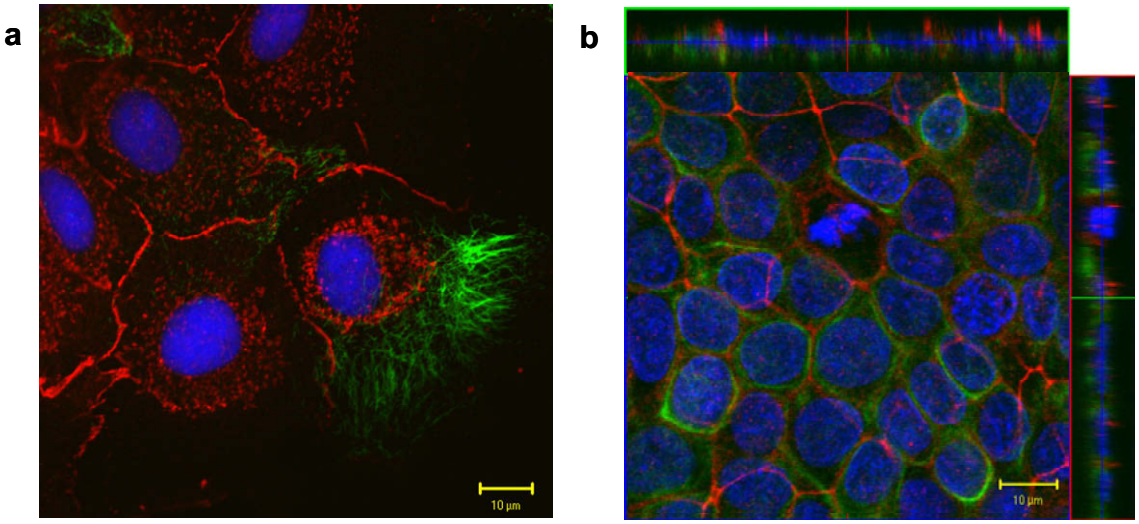

Figure 8 Costaining for vimentin and occludin: Costaining for vimentin (green) and the tight junction protein occludin (red) could be demonstrated in various preparations. a) ruminal epithelial cells b) epithelial cell line MDCK [7].

5.5 Patch-clamp measurements

Whereas transport studies on intact tissues have led to the conclusion that ions pass through pores or channels driven by the electrochemical gradient, the multiple possible interactions of various conductances in a tissue cannot lead to a clear identification of these conductances or their regulation. The patch-clamp technique continues to be the only method that allows a direct demonstration of the functional

[7] Here and in the following, the help of Dorothee Günzel, Institute for Clinical Physiology, Charité CBF, FU and HU Berlin is gratefully acknowledged for help in connection with the demonstration of tight junction proteins.

expression of ion channels by a tissue. The method allows the precise control of intra- and extracellular ion concentrations and of the potential. A determination can therefore be made as to which ion is being conducted through the cell membrane, and the regulation of the conductance can be directly studied.

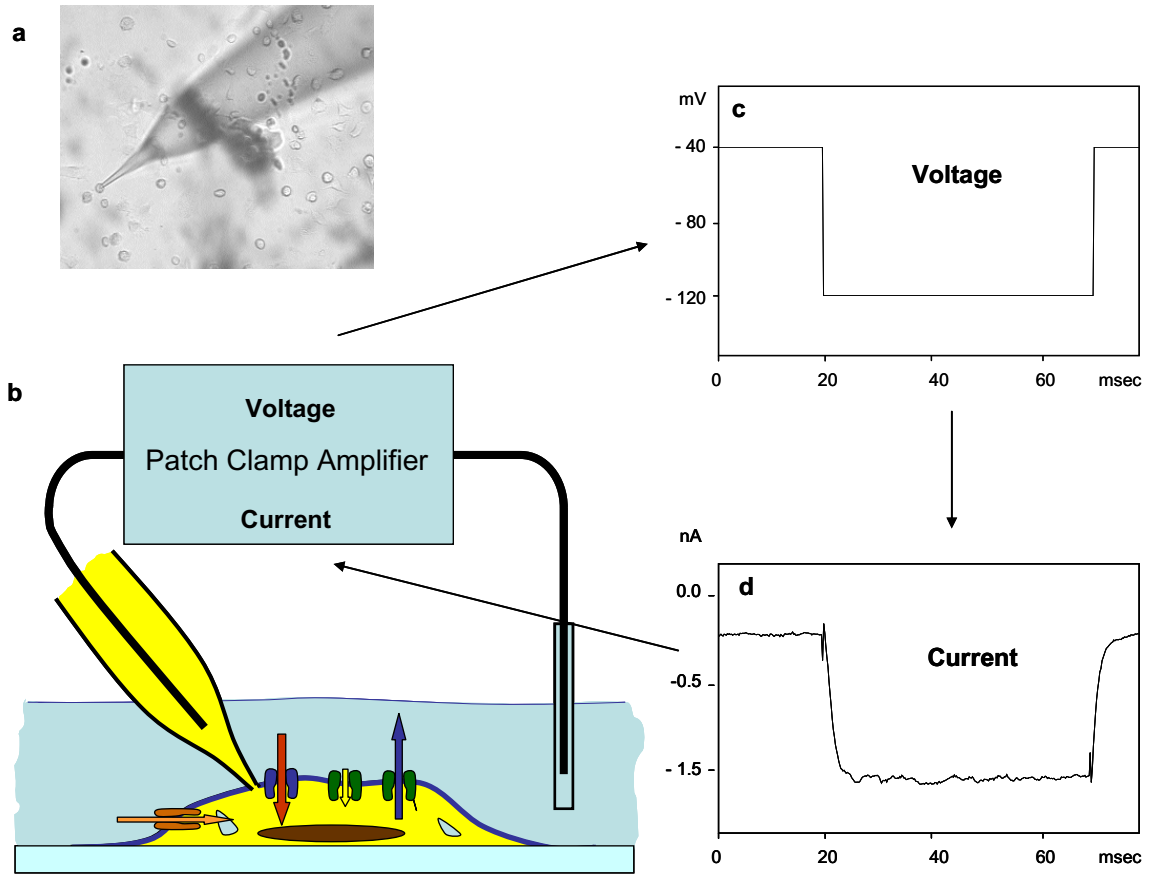

Figure 9: Patch pipette with ruminal epithelial cell in the whole cell configuration. a) Photographic image showing a ruminal epithelial cell in the whole cell configuration. b) Schematic representation. The pipette is lowered onto the cell until the (lipophillic) glass forms a seal with the cellular membrane. Subsequently, the membrane patch under the pipette is ruptured by gentle suction, and after one to two minutes, the pipette solution has diffused into the cell. c) The voltage between the inside of the cell and the outside bath can be automatically clamped to different potentials using the patch-clamp amplifier. d) The potential generates a current through the ion channels in the cellular membrane that can be measured with the patch-clamp amplifier. The negative current measured in “d” can mean that cations are flowing from the bath through ion channels into the pipette. Alternately, anions may be flowing out of the pipette and through the cell membrane into the bath.

5.5.1 Electrophysiology

All patch-clamp experiments were performed essentially as in previous studies (5, 195, 348). In short, cells were seeded onto glass coverslips and placed in a perfused bath chamber on the inverted stage of a microscope. All pipette potentials were referenced to the bath solution via a silver chloride wire in a small KCl-Agar bridge.

Currents between the patch pipette and an electrode placed in the perfusion chamber were recorded by using an EPC 9 patch-clamp amplifier (HEKA Elektronic, Lambrecht, Germany). Pulse generation, data collection, and analysis were performed with commercially available software (TIDA for Windows, HEKA Elektronic, Lambrecht, Germany) and filtered with a 2.9 kHz Bessel filter. Records were corrected for capacitance via TIDA software. Positive ions flowing into the pipette correspond to a negative current and are depicted in the figures as moving downward. Conversely, negative ions flowing from the bath across the cell membrane into the pipette generate a current that is depicted as passing upward in the figures.

For whole cell experiments, two types of pulse protocols were applied. Conventional voltage pulse protocols were used that recorded data at a sampling rate of 5 kHz ("pulse protocol I"). Voltage was increased from –120 mV to 100 mV in steps of 10 mV, returning to a holding potential of -40 mV between each step.

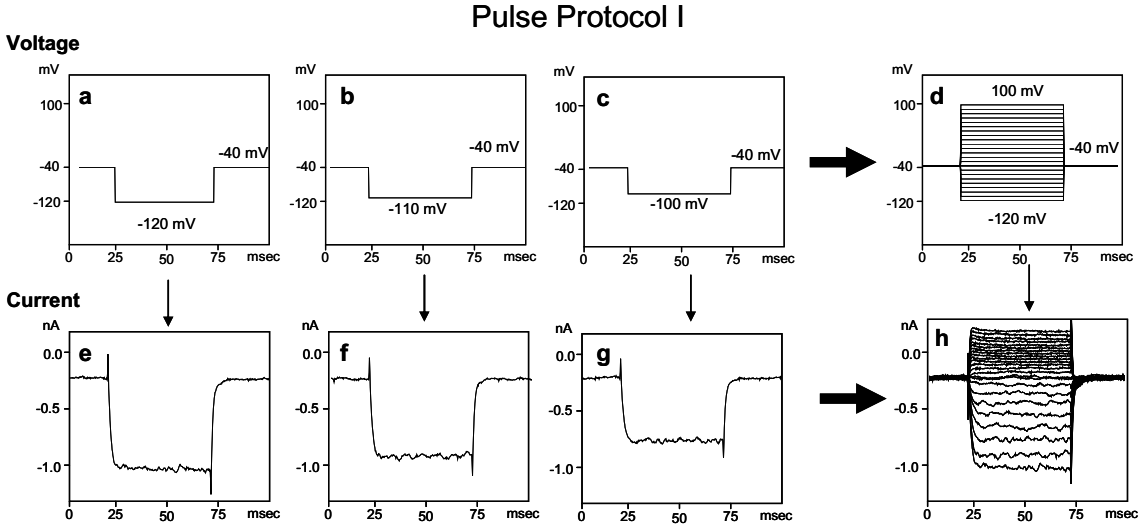

Figure 10: Conventional pulse protocol ("pulse protocol I"). The voltage was stepped from -40 mV to various voltages and back (a,b,c), and the current reponse to each voltage step was measured at a high frequency (5kHz) and stored (e,f,g). Subsequently, all traces obtained were overlaid to give one figure with all of the current responses (h). This type of voltage protocol gives a good overview of the activation and inactivation of a current in response to the voltages applied. The trace in "h" shows the activation of currents at negative potential, corresponding to an influx of cations through ion channels in the membrane into the pipette or to an efflux of anions from the pipette solution through the membrane into the bath. The voltage dependence of the current ("rectification") argues against a non-specific leak, but further information is necessary in order to determine whether a cation or an anion is being transported.

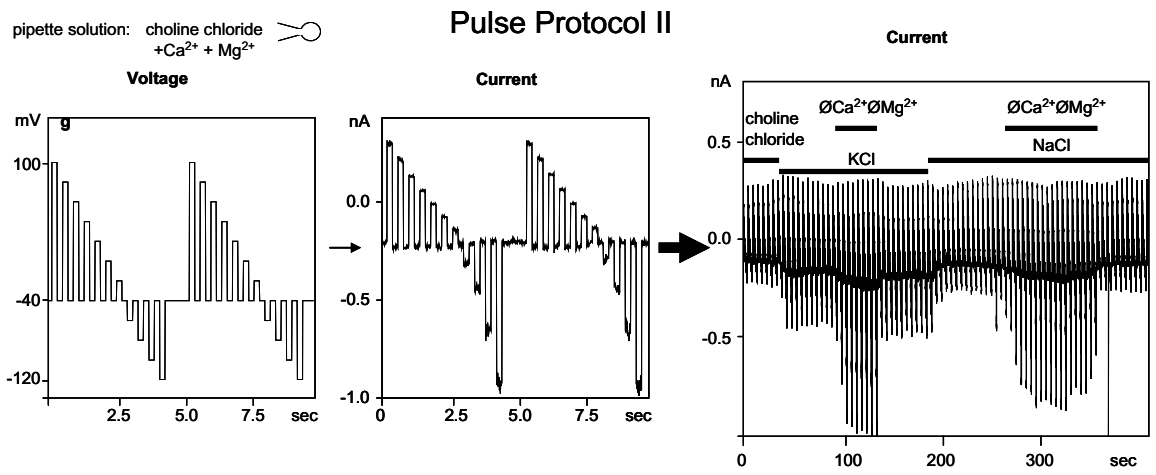

Figure 11: Continuous pulse protocol ("pulse protocol II"). As before, the voltage was stepped to various voltages between -120 and +100 mV from a resting potential of -40 mV. This sequence was reiterated many times. Current responses were continuously monitored at low frequency (100 Hz) and depicted in sequence as measured. This type of protocol gives a good overview of the activation or inactivation of currents in response to the application of various solutions. (The trace shown is an original recording of a ruminal epithelial cell filled with choline chloride solution. The bath solution was consecutively changed to various solutions as indicated by the bars over the trace. The current at negative potential changed in response to these solution changes, demonstrating an influx of cations through the cell membrane into the pipette.)

Alternately, current responses were recorded at 100 Hz by using a protocol that generated steps of 200 ms duration to voltages between –120 mV and 100 mV in 20 mV steps, returning to a holding potential of – 40 mV for 200 ms between each step (“pulse protocol II”). This protocol was repeated continuously to allow the monitoring of current responses of the cells to changes in external solution.

In all whole cell experiments, cells were allowed to equilibrate for at least 3 minutes after the whole cell configuration had been achieved. During this time, voltages were clamped in alteration with the pulse protocols I and II, and the current was monitored. Cells that did not reach stable current levels during this equilibration period were discarded. If the current-voltage relationship was linear with no signs of channel activation/inactivation and a reversal potential of 0 mV was measured, the seal was judged to be ruptured, and the measurement was discontinued.

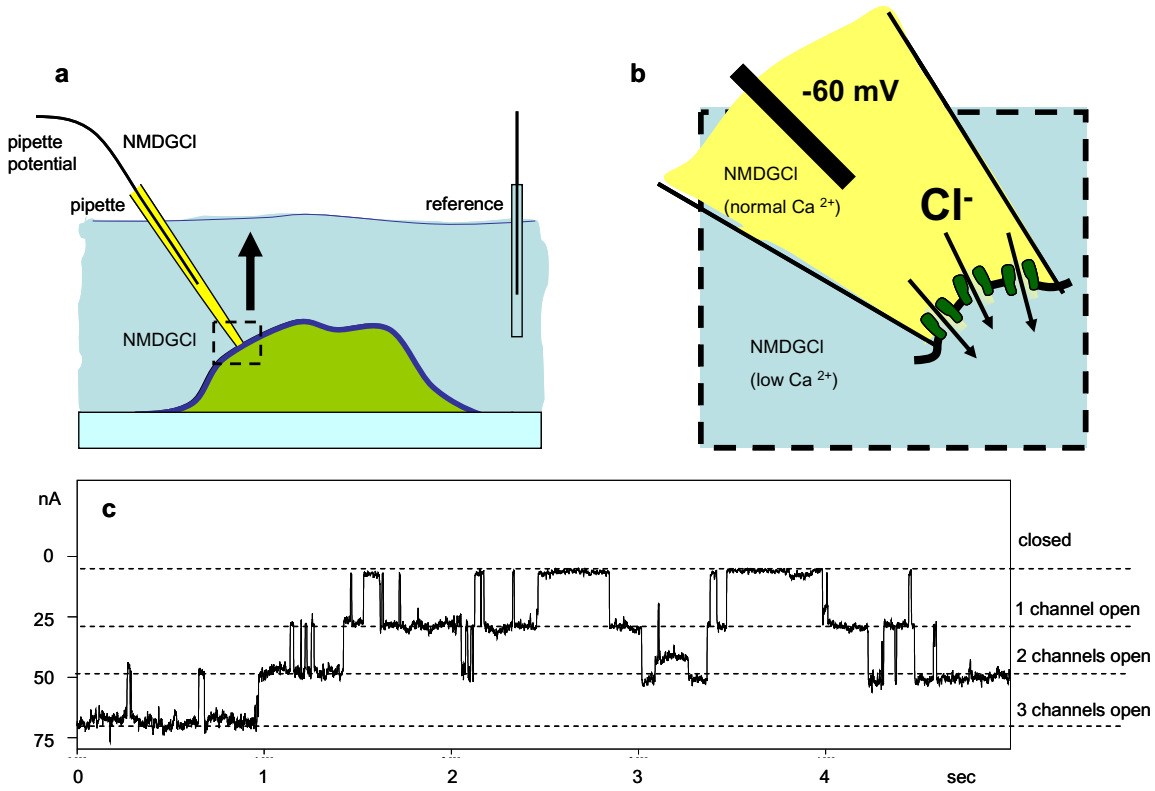

Figure 12: Single-channel configuration (inside-out). a) After the formation of the seal, the membrane under the pipette was not ruptured. Instead, the pipette was moved upward so that a piece of membrane was excised out of the cellular membrane, with the cytosolic side facing the bath solution. b) Potentials could be applied between the inside of the pipette and the bath solution, generating currents. c) The majority of patches were silent, showing no current across the membrane. In some patches, the current flickered back and forth, forming a pattern of steps. These current steps are generated by individual channels flickering between an open state and a closed state, with no "in between". In the trace in c) the patch has at least 3 channels; more channels might have been present but were not open during the recording shown. The nature of the current can be identified by varying the potential and by changing the bath solution. Here, chloride is flowing out of the pipette and through the channels into the bath solution, driven by the pipette potential of -60 mV. At + 60 mV, the current should change sign, if it is, indeed, generated by chloride. In some cases, the channel will be inactivated at this voltage, so that no channel events are visible. To make sure that NMDG is not being conducted, the bath solution can be switched to one containing gluconate as the major anion. Since gluconate is much larger and less mobile than chloride, this should greatly reduce the current amplitude at + 60 mV.

For inside-out single-channel experiments, membrane patches were excised into the bath solution directly after seal formation. Outside-out patches were obtained by removing the pipette from the cell after formation of the whole cell configuration had occurred. Data were sampled at 10 kHz and filtered with a 250 Hz low-pass Bessel filter after recording.

5.5.2 Perfusion of the bath chamber

All perfusion solutions were warmed to 37°C immediately before infusion into the 200 ml perfusion chamber via a perfusion cannula (PH01, multichannel systems, Reutlingen, Germany) connected to a temperature controller (TC01/2, multichannel systems, Reutlingen, Germany). The solutions were applied via two separate but identical pumps (MS/CA4/840, Ismatec, Glattbrugg-Zürich, Switzerland), both of which were equipped with four parallel lanes of high precision Tygon tubing (Ismatec) to ensure identical flow rates (4 $ml \cdot min^{-1}$). All eight lanes ended in a milli-manifold (ALA Scientific Instruments, Westbury, N.Y., USA) attached to the heating cannula (PH01) and leading into the perfusion chamber. Solutions from lanes not in immediate use for cell perfusion were recirculated into the storage containers (50 ml syringes, Heiland, Germany) via eight separate three-lane valves, ensuring constant mixing and constant pressure in all parts of the system at all times and preventing the backflow of the test solution into other parts of the system via the manifold.

5.5.3 Solutions and chemicals

For whole cell experiments, the pipette solution designated as “K-gluconate solution” contained (in $mmol \cdot l^{-1}$): 123 K-gluconate, 10 NaCl, 10 Hepes, 1 KH_2PO_4, 0.8 $CaCl_2$, 0.9 $MgCl_2$, 5 EGTA, adjusted to pH 7.2 with Tris. In the pipette solution designated as “choline chloride solution”, 123 $mmol \cdot l^{-1}$ K-gluconate was replaced by 123 $mmol \cdot l^{-1}$ choline chloride. Extracellular NaCl solution contained ($mmol \cdot l^{-1}$): 130 NaCl, 1 NaH_2PO_4, 5 KCl, 10 Hepes, 1.7 $CaCl_2$, 0.9 $MgCl_2$. The NaCl of this basic recipe was substituted by either KCl, choline chloride, NH_4Cl, Na-gluconate, or K-gluconate to give the solutions designated by these ions; these solutions were adjusted to 290 $mosmol \cdot l^{-1}$ with the dominant salt. Unless indicated otherwise, the pH was adjusted to 7.4 with Tris. All other experiments (i.e., whole cell experiments with Na-gluconate pipette solution and the single-channel experiments) were performed with solutions that contained 138 $mmol \cdot l^{-1}$ Na^+, 130 $mmol \cdot l^{-1}$ of which were replaced by NMDG as indicated. In addition, the solutions contained 130 $mmol \cdot l^{-1}$ of the anion as indicated, and 0.9 Mg^{2+}, 1.7 Ca^{2+}, 5 $mmol \cdot l^{-1}$ K^+, 1 $mmol \cdot l^{-1}$ $H_2PO_4^-$, 18.2 $mmol \cdot l^{-1}$ Cl^-, and 10 $mmol \cdot l^{-1}$ Hepes. Solutions for use on the intracellular side of the cell membrane were buffered with 5 $mmol \cdot l^{-1}$ EGTA, and the pH was adjusted to 7.2 with Tris. Unless indicated otherwise, solutions for use on the extracellular side of the membrane were adjusted to pH 7.4 (Tris); subsequently, the osmolarity was raised to the (measured)

level of the intracellular solution with mannitol. Solutions were frozen in small aliquots (50 ml or 100 ml) to allow rapid thawing at 37°C when needed. The pH of the experimental solutions was monitored immediately before use.

All chemicals for making these solutions were obtained from Carl Roth GmbH (Karlsruhe, Germany) or Sigma Aldrich (St. Louis, Mo., USA). To ensure constant concentrations of calcium and magnesium, appropriate amounts of a commercially produced 1 $mol \cdot l^{-1}$ standard solution were added (Fluka, Switzerland). Commercially unavailable salts, such as NMDG-gluconate or NMDG-acetate, were produced by titrating N-Methyl-D-glucamine (Fluka) with gluconic acid (Sigma Aldrich) or acetic acid (Fluka) to a pH of 7.

All blockers used in the study were obtained from Sigma Aldrich or Fluka. Solutions containing blockers were protected from light throughout. Diisothiocyanato-stilbene-2,2'-disulfonic acid (DIDS) was either directly and slowly added to the prewarmed stirred solutions (37ºC) or used as a stock solution dissolved in dimethyl sulfoxide (DMSO). Stock solutions of DIDS, niflumic acid, flufenamic acid, or 5-nitro-2-(3-phenylpropyl-amino) benzoic acid (NPPB) were prepared by dissolving appropriate amounts of the substances in DMSO. These stock solutions were stored at -20ºC and added to the prewarmed test solution at a ratio of 1:1000 to yield the concentrations indicated.

The mercurial derivative *p*-chloromercuribenzoate (pCMB) was difficult to dissolve, both directly in aqueous solutions and in DMSO. In NaCl Ringer, the direct addition of pCMB resulted in a milky deposit, which was removed from the solution by filtration prior to experiments. However, when the powder was slowly sprinkled into prewarmed Na-acetate solution under continuous stirring, no visible precipitate formed, and the solution was used without prior filtration.

5.5.4 Whole cell currents

To compare whole cell data from the various cells with each other, currents were normalized to capacitance as measured by using TIDA software. Alternately, currents were allowed to stabilize in NaCl solution as indicated above. The current level at the 100 mV pipette potential was then assigned a value of 100%. All other currents were expressed as a percentage of this value obtained at the beginning of the experiment.

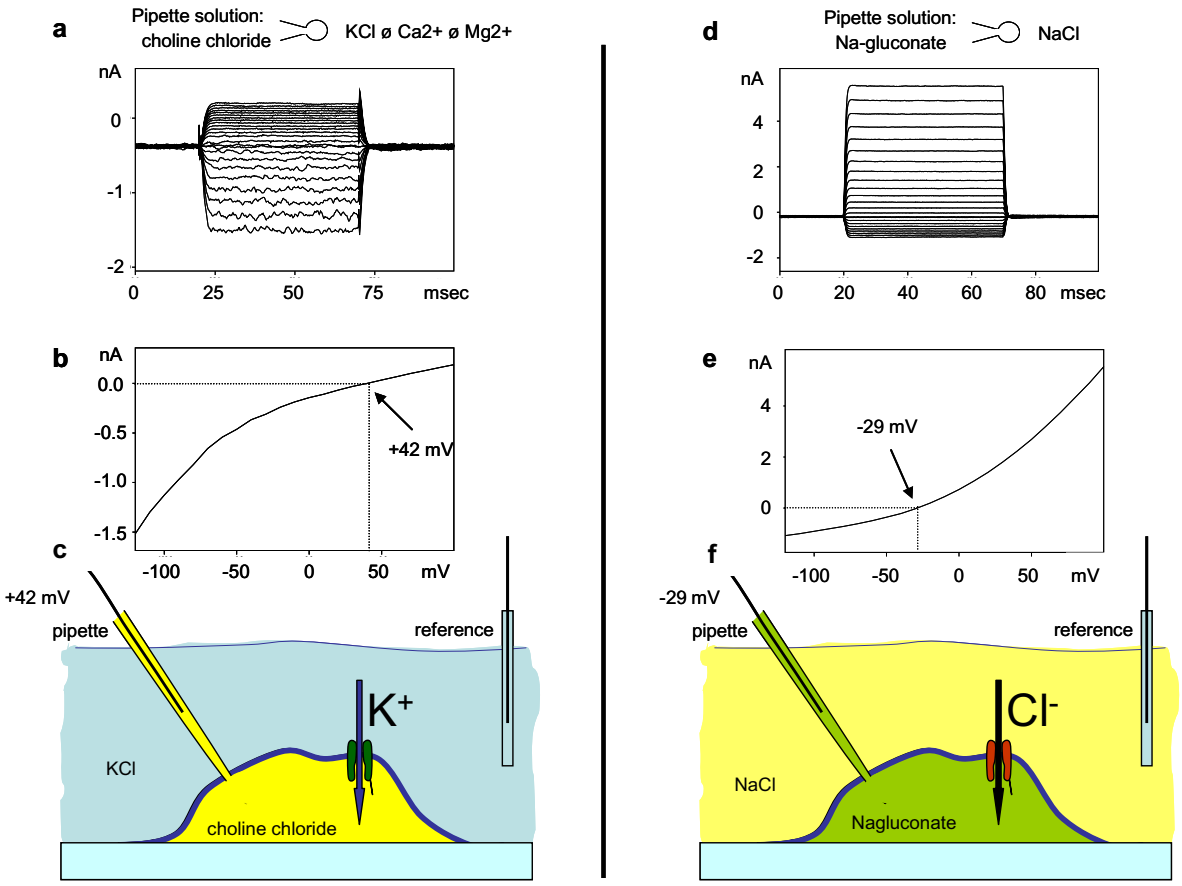

Figure 13: Determination of reversal potentials. a) Original recording of a ruminal epithelial cell in the whole cell configuration. The cell is filled with a choline chloride pipette solution; the bath solution is KCl (divalent-free). At negative pipette potential, a large negative current can be seen, which might reflect either Cl^- flowing out of the cell membrane into the bath, or K^+ flowing into the cell, or a combination of both. b) Current voltage relationship of the trace in a), showing that the current increases at negative potentials (inwardly rectifying). The current is zero (reverses direction) at + 42 mV. Since the chloride concentration is equal on both sides of the membrane (Nernst potential = 0 mV), this positive potential must reflect the influx of K^+ through the membrane. c) Schematic representation. A potential of +42 mV is necessary to clamp the current between the pipette and the reference electrode to zero. d) Original recording of a cell filled with Na-gluconate solution in NaCl bath. Currents increase at positive voltages (outwardly rectifying) and can reflect either an efflux of Na^+, or an influx of Cl^-, or both. e) Current voltage relationship of the current in d). The current reverses direction at -29 mV. Since Na^+ is equal on both sides of the membrane, this negative potential means that chloride must be flowing into the cell. It can be concluded that the cell expresses a conductance for chloride. Conversely, distinguishing between a genuine conductance for sodium and a nonspecific leak in this configuration is difficult, since the Na^+ concentration is equal on both sides of the membrane. f) Schematic representation. A potential of -29 mV is necessary to clamp the current between the pipette and the reference electrode to zero.

5.5.5 Reversal potentials and relative permeability ratio

In patch-clamping, the reversal potential is defined as the potential at which the current across the membrane is “zero” and thus reflects the potential that can be measured across the cellular membrane if the voltage is not clamped. Reversal potentials thus depend on the composition of the external and internal solution and on the ionic conductances of the cellular membrane. The usual sign convention has

been used, so that an influx of cations into the cell leads to a depolarization of the reversal potential. All reversal potentials were corrected for liquid junction potential according to established methods (23).

The relative permeability ratios for two ions a and b (P_b/P_a) were calculated by switching the major ion in the external solution and measuring the corresponding reversal potential. The relative permeability ratio could then be calculated from the difference in the reversal potentials by using Goldman-Hodgkin-Katz theory (146):
$E_{rev,b} - E_{rev,a} = RT/zF \cdot \ln(P_b[B]_o/(P_a[A]_o)$

5.5.6 Single-channel conductances

Assuming independence, single-channel conductances were fitted by using the current-voltage formulation of the Goldman-Hodgkin-Katz equation (146) and standard software (SigmaPlot for Windows, 8.02).

For K^+/NH_4^+ channels, the equation was:

$$(1)\ I=E\cdot F^2/(R\cdot T)\cdot(P_{NH4}[NH4]_i + P_K[K]_i - (P_{NH4}[NH_4]_o + P_K[K]_o) \cdot \exp(-E\cdot F/(R\cdot T)))/(1- \exp(-E\cdot F/(R\cdot T)))$$

For the anion channel, the equation was adapted to reflect the change in sign:

$$(2)\ I=E\cdot F^2/(R\cdot T)\cdot(P_{Cl}[Cl]_o + P_{Gl}[Gl]_o + P_{Ac}[Ac]_o - (P_{Cl}[Cl]_i + P_{Gl}[Gl]_i + P_{Ac}[Ac]_i)\cdot\exp(-E\cdot F/(R\cdot T)))/(1-\exp(-E\cdot F/(R\cdot T))).$$

In this equation, E designates the potential (calculated from the pipette potential by correcting for liquid junction potential (23)), R the gas constant, T the temperature, and F the Faraday constant. P_x designates the permeability for substance X; $[X]_i$ and $[X]_o$ are the concentrations of the substance X inside and outside of the pipette.
In symmetrical solution with just one ion ($[X]_i=[X]_o$), this equation can be simplified to:

$$(3)\ I=E\cdot F^2/(R\cdot T)\cdot P_X[X]$$

Using equation 3, the values for P resulting from the fit of currents in asymmetrical solutions were used to predict the conductance C in symmetrical 130 $mmol \cdot l^{-1}$ solution at a given concentration of the ion ([X]), assuming that the interaction of different ions in the pore was marginal:

(4) $C_X = I/E = F^2/(R \cdot T) \cdot P_X [X]$

5.6 Microelectrode experiments

5.6.1 *Experimental set-up*

Fresh ruminal epithelium was introduced into a small microelectrode chamber, apical side up. The apical and basolateral side of the chamber were continuously perfused (MS/CA4/840, Ismatec, Glattbrugg-Zürich, Switzerland) by a perfusion system that has been previously described (348, 360). Ringer solutions were used that were bicarbonate-free, buffered to the pH value indicated using MOPS, and warmed to 37ºC. Solutions were bubbled with O_2 throughout, and the pH was monitored at hourly intervals by using a conventional pH meter (Inolab pH 720, Weilheim, Germany) and adjusted if necessary. In solutions designated as SCFA free, gluconate was used to replace an equimolar amount of SCFA (see (2) for details).

The transepithelial voltage, resistance, and short-circuit current of the tissues were controlled via voltage clamp (Biomedical Instruments, Munich, Germany) (189). The potentials of the two barrels of the microelectrode were measured with an FDA223 Dual Electrometer (World Precision Instruments, Sarasota, Fl., USA) and referenced to the mucosal side of the bath via a KCl bridge. All parameters were recorded by using Chart 5 for Windows (Adinstruments, Bella Vista, NSW, Australia) and filtered with digital median filters. The fractional apical resistance $f(R_a)$ was calculated from the potential response (ΔVa) of the microelectrode to 10 mV transepithelial voltage pulses of 0.3 s duration (ΔV_t) (108), i.e., ($f(R_a)$ (%)= $\Delta V_a / \Delta V_t \cdot 100$).

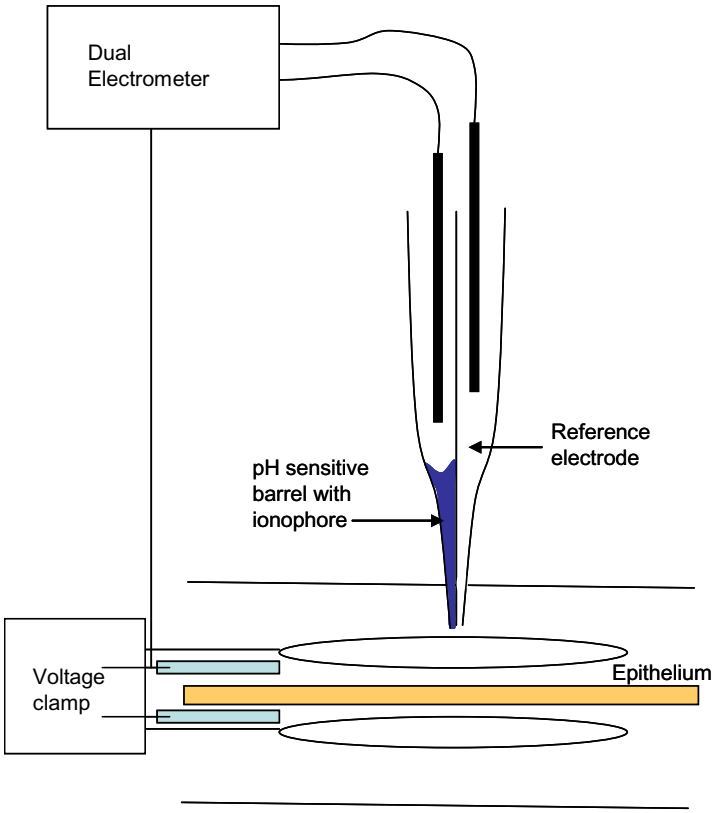

Figure 14: Representation of the microelectrode set-up. The epithelium was placed in a vertical voltage clamp set-up (Ussing chamber). The pH measurements were performed by using double-barreled pH-sensitive microelectrodes, with one barrel serving as a reference, whereas the other was filled with the pH-sensitive ionophore. The difference between the two was linearly correlated to the pH. All potential measurements were referenced to the mucosal bath solution via a 3 mol·l^{-1} KCl-Agar bridge.

5.6.2 *Fabrication of double-barreled pH-sensitive microelectrodes*

Piggy-back double-barreled microelectrodes were prepared from filamented GC120F 10 and GC150F 15 borosilicate glass tubing (Harvard Apparatus, Kent, UK). One end of the smaller diameter tubing (GC120F 10) was heated and gently bent at a small angle from the main shaft (67). Two core cable ends (4x10, 611889, Conrad Bauelemente, Conrad Elektronik, Hirschau, Germany) were pushed into tightly fitting shrink tubing (Deray-H-set 1/8″, DSG-Canusa, Meckenheim, Germany) and used to join this bent glass tube with the larger diameter tube, leaving the middle section free of tubing. After being baked (190ºC) until firmly adjoined, the piggy-back electrodes were pulled by using a programmable multipipette puller (PMP-107, Microdata Instrument Inc, South Plainfield, N.J., USA) to give a resistance of about 50 MΩ (measured with EPC 9, Heka Elektronik, Lambrecht, Germany).

For silanization, the bent ends were connected to a pressure source and perfused with dried air, whereas the straight ends were pushed into the rubber lid of a heated glass jar and exposed to the vapor formed by a drop (200 µl) of dichlorodimethylsilane (Sigma-Aldrich) for 30 minutes. Pipettes were then baked at 190ºC for two hours, after which time the silanized channel was immediately backfilled with 3 µl Hydrogen Ionophore I – Cocktail A (Sigma Aldrich) via a modified Hamilton Syringe (Type 7000.50C, 0.5 ml, MedChrom, Germany). In some experiments, Theta glass tubing (TGC150-7.5, Harvard Apparatus, Kent, UK) was used, but in this case, it proved more difficult to silanize one channel selectively.

The filled pipettes were placed tip downward in a jar containing a dehydrating agent at least overnight to allow the hydrogen ionophore to diffuse into the tip of the electrode. On the day before use, the hydrogen-sensitive barrel was back-filled with a solution containing 100 $mmol \cdot l^{-1}$ KCl, 20 $mmol \cdot l^{-1}$ Hepes, pH 7.4. The reference channel was filled with 0.5 $mmol \cdot l^{-1}$ KCl. Both solutions were degassed by being heated at 40ºC before use.

Electrodes were bevelled by using a beveller with an impedance meter (BV-10, Sutter Instrument Company, Novato, Calif., USA), which greatly facilitated the routine fabrication of functional microelectrodes with resistances of > 20 MΩ.

Electrodes were judged suitable for impalement if they showed a differential response of over 40 mV per pH unit ($mV \cdot pH^{-1}$) (pH 7.4 to pH 6.4) between the pH-selective and non-selective barrel immediately before the experiments commenced. This test pulse was used to calculate cytosolic pH via linear regression. The speed of pH change was calculated for each point by subtracting the pH level from the value measured 30 seconds previously by using Chart for Windows.

Care was taken to choose the sharpest electrodes from the 16 typically available on a given experimental day. Impalements were judged to be stable if the fractional apical resistance remained constant. The resistances of functional microelectrodes were checked after successful completion of the experiment and typically yielded values of over 2 but under 10 MΩ. These resistances were thus clearly lower than desirable, which might explain why the apical potentials measured with pH-sensitive microelectrodes tended to be less negative and less stable than those measured previously by using single-barreled electrodes (43).

5.6.3 Measurements

All tissues were allowed to settle in HCO_3^--free solution at pH 7.4 for 10 minutes before experiments commenced. Tissues were kept in the open circuit mode but briefly clamped from time to time to measure the short circuit current (0.63 ± 0.11μEq·cm^{-2}·h^{-1}) and tissue conductance (3.1 ± 0.5 mS·cm^{-2}). All microelectrodes were rechecked for function by briefly changing the apical perfusion solution to an identical solution buffered to pH 6.4 (figure 7) before the beginning of the actual experiment, yielding an average sensitivity of 53 ± 4 mV·pH^{-1} unit. The pH response of the pipettes to the change in external solution was rapid, reaching a maximal speed of 1.93 ± 0.05 pH·min^{-1}.

5.7 Statistics

Data were tested by using the Kolmogorov-Smirnov test for normality (SigmaStat 3.0). All data drawn from a normally distributed collective were tested for significance by using the paired or unpaired Student's t-test and standard software (SigmaStat 3.0). Data that were not normally distributed were tested by using the Wilcoxon Signed Rank Test (Sigmastat 3.0). Statistical comparison between multiple groups was made by using one way repeated measures ANOVA and the Holm-Sidak method for multiple pair-wise comparisons (SigmaStat 3.0). Curves were fitted with SigmaPlot 8.0.

6 Results

6.1 Identifying the proteins of the paracellular pathway

What proteins maintain the barrier function of forestomach epithelia?

Considerable evidence suggests that, under most physiological situations, the paracellular pathway of the forestomachs is able to maintain large gradients for chloride and sodium (usually blood > rumen) and for potassium, protons, or SCFA (usually rumen > blood). Osmotically active particles do not simply diffuse across the paracellular pathway, but are selectively absorbed via tightly regulated and highly selective transcellular pathways.

In the past, the rumen has been shown to express ZO-1, occludin, and claudin-1 (125, 133, 355, 362). In this study, we were able to confirm the expression of these tight junction proteins by the bovine rumen (355). In addition, we were able to demonstrate the expression of claudins 4 and 7.

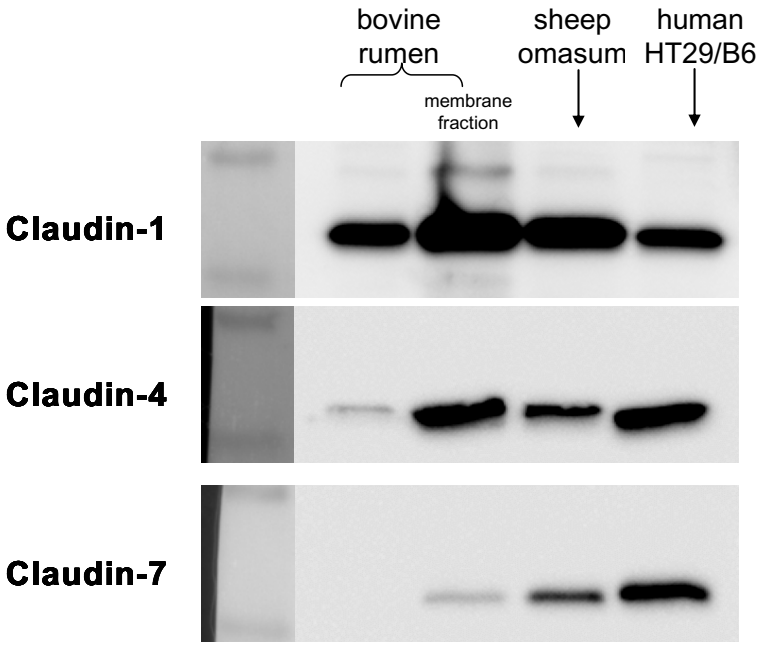

Figure 15: Western blot showing claudin expression by forestomach epithelia. Forestomach epithelia and cells derived from forestomach epithelia express claudins 1, 4, and 7. (last lane: control cell line expressing all three claudins)[7].

Staining for occludin and claudins 1, 4, and 7 could also be demonstrated in sheep rumen, in the sheep omasum, and in cell cultures from both sheep rumen and omasum. PCR and Western blot techniques confirmed the ample expression of these proteins both by the intact tissues and in cell cultures derived from them. In general, the staining for claudin-7 was slightly weaker than that for the other tight junction proteins.

Claudin-2 could be seen both in omasal tissue and cultures derived from the omasum, but it was not possible to reliably confirm the presence of this tight junction protein by PCR and Western blots. Claudins 2 and 7 are candidates for the paracellular cation-selective pathway that may be present in forestomach epithelia

(205, 310), whereas occludin and claudins 1 and 4 are thought to be relatively impermeable to both anions and cations. Conversely, claudins 5, 8, and 12 do not appear to be expressed by the rumen or the omasum of sheep in significant quantities.

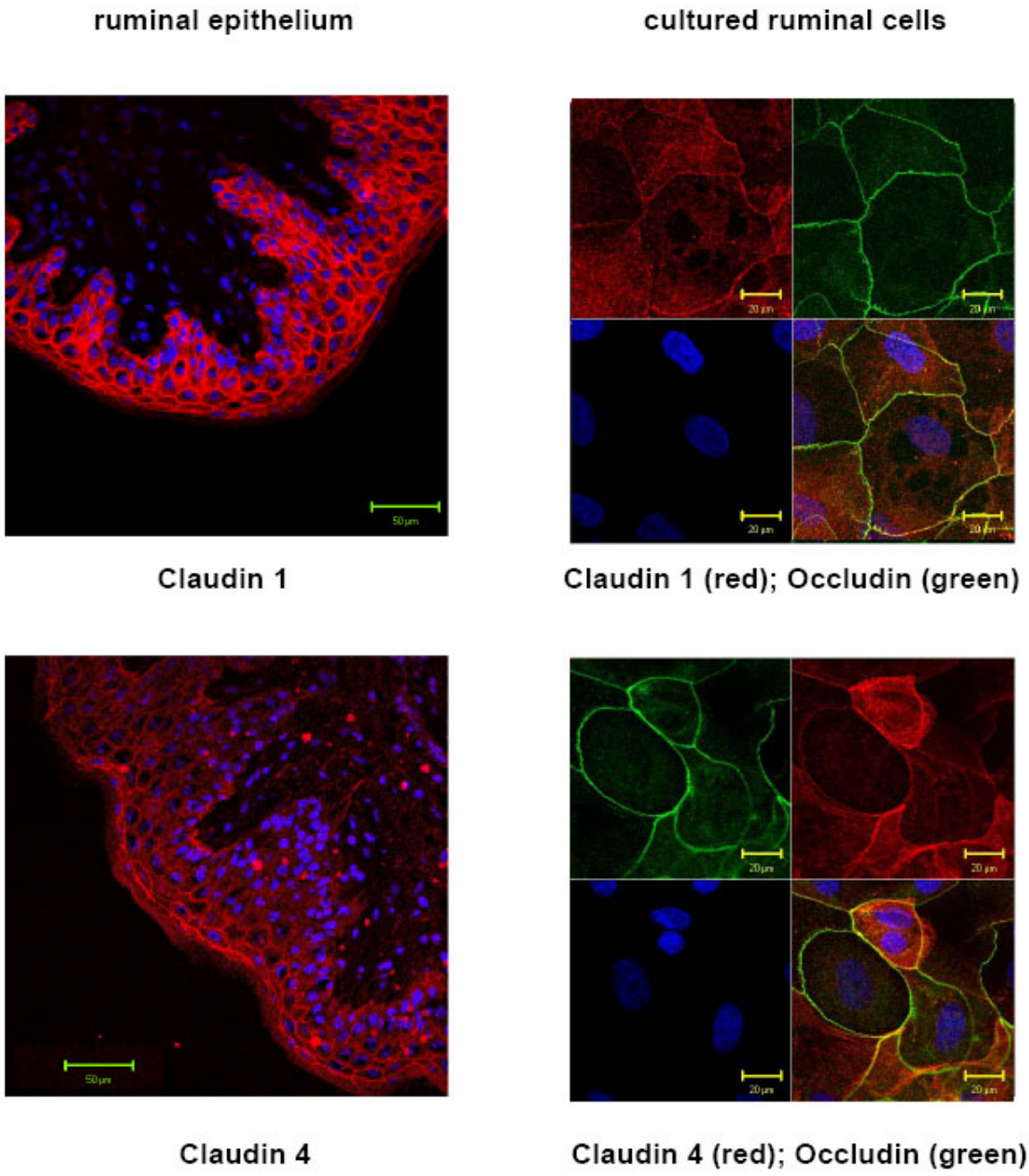

Figure 16: Staining for tight junction proteins: the rumen. The figure shows staining for claudins 1 and 4 in both the tissue and the cells. Note that the expression of both claudins appears to extend across all layers of the multilayered epithelium, although the staining intensity for claudin-4 decreases. The submucosal tissue exhibits no staining[7].

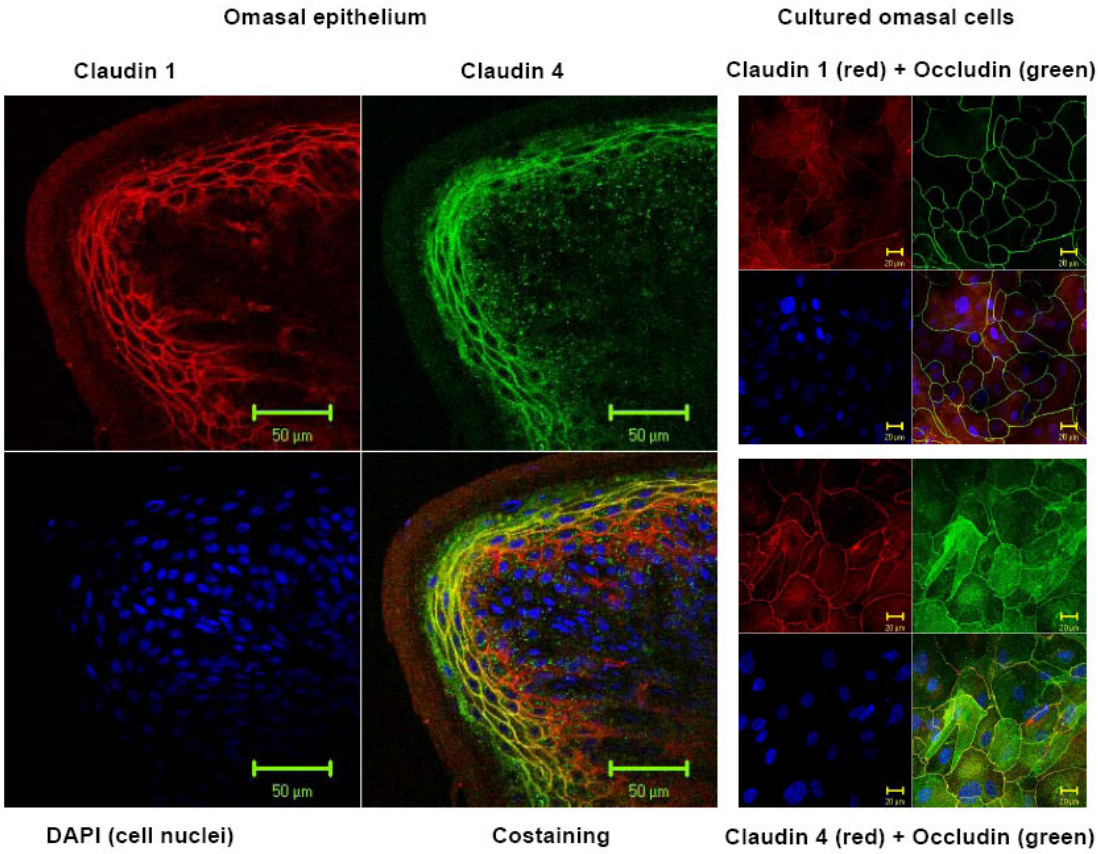

Figure 17: Staining for tight junction proteins: the omasum. The figure shows staining of the tissue and the cells for claudins 1 and 4 and occludin[7].

The nucleotide sequences for the mRNA of claudin-1 and claudin-4 were obtained for sheep omasum and showed strong homology with the bovine sequences. Claudin-1 from the sheep showed eight differences in the coding sequence versus the bovine species, whereas 17 differences were observed for claudin-4 (Genebank accession numbers: BankIt1343052 HM117762 BankIt1343054 HM117763). The help of Dorothee Günzel is again gratefully acknowledged.

In further experiments, tissues were incubated in Ussing chambers with fluorescently marked dyes at both the apical and the basolateral sides. The epithelium (*in toto*) was shown to form a functional barrier to an efflux of substrate, with the stratum corneum and the submucosal tissue apparently not contributing significantly. However, at higher incubation times, a highly discrete efflux of the markers into the

epithelial junctions could be observed. Interestingly, an overlap of these pathways could only be observed in one tissue out of a total of four studied.

In conclusion, these results suggest that the paracellular pathway of forestomach tissues is organized in a complex manner and forms a relatively tight barrier against the efflux of solutes, which thus occurs primarily across the transcellular pathway. However, further work is necessary in order to obtain more information about the physiological function and possible regulation of the different claudins lining the paracellular pathway of the forestomach epithelia.

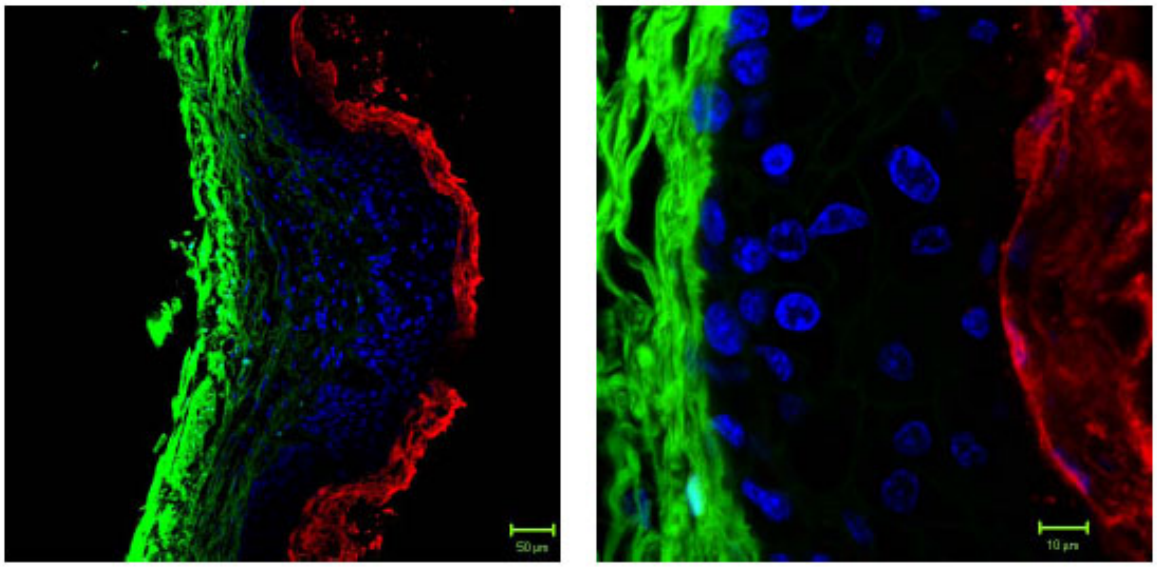

Figure 18: Barrier function of forestomach epithelia. A piece of omasal tissue was placed between the two chambers of a Ussing chamber and incubated with labeled dyes (green: flourescein, red: biotin). Microscopic inspection reveals that the stratum corneum and the submucosal tissue are highly permeable to the fluorescent dye, but that the paracellular pathway between the stratum granulosum and the stratum basale forms an efficient barrier[7].

6.2 Apical microclimate

Can the existance of the microclimate be confirmed by a direct measurement of surface pH?
Where is the microclimate localized?
Does it preceed the transporting cell layer?
Does the omasum express a microclimate?

Abdoun K, Stumpff F, Rabbani I, and Martens H. *Modulation of urea transport across sheep rumen epithelium in vitro by SCFA and CO_2. Am J Physiol 298: G190-202, 2010.*
Leonhard-Marek S, Stumpff F, and Martens H. *Transport of cations and anions across forestomach epithelia: conclusions from in vitro studies. Animal 4: 1037-1056, 2010.*

As outlined in the introduction, a pH microclimate has long been postulated in the rumen and the omasum (8) and is thought to play a role in modulating the transport of weak acids and bases across the epithelium.

We were able to demonstrate this microclimate directly in the rumen and in the omasum by using pH-sensitive microelectrodes. Following calibration, the pipette was lowered onto the epithelium with a micromanipulator. A drop in potential could be observed on the pH-selective electrode, corresponding to a shift in the apical pH. At this point of the measurement, the potential of the reference electrode did not change notably, and the response to transepithelial voltage pulses remained negligible. When the microelectrode was moved further down, a drop in potential across both the reference and the pH-selective electrode signaled an entry into the transporting syncitium, with a corresponding increase in the response of the electrode to transepithelial voltage pulses. The microclimate thus clearly preceeds the transporting layer of cells and is probably localized in the stratum corneum.

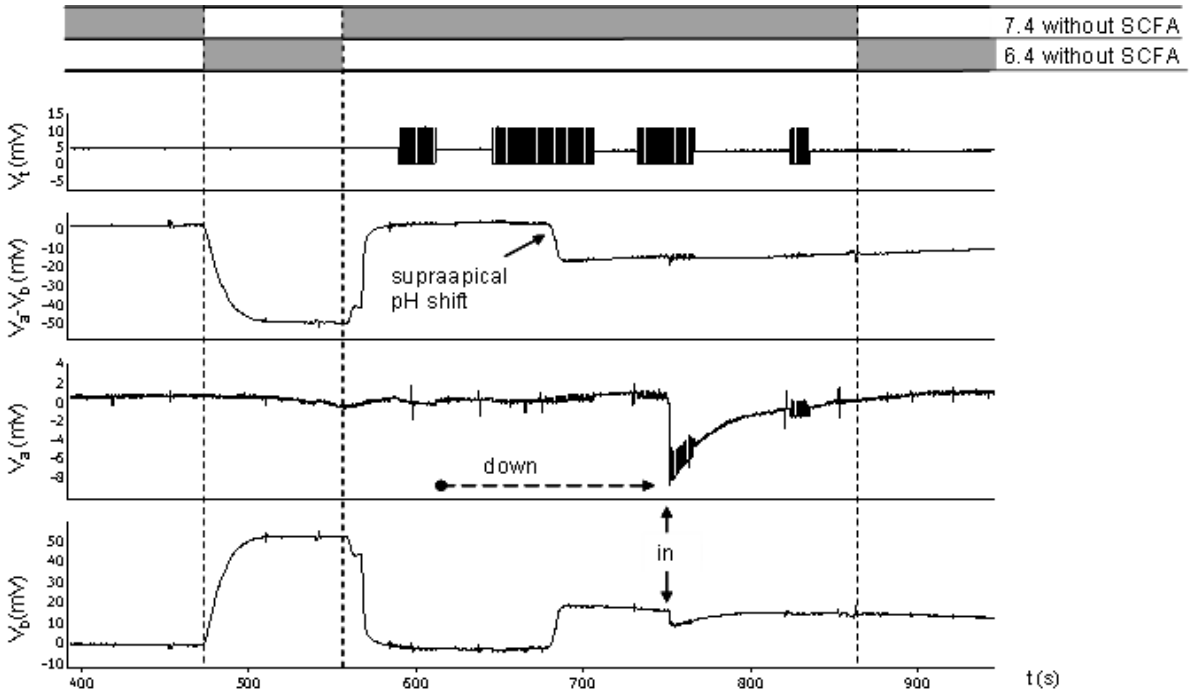

Figure 19: Microclimate of the ruminal epithelium. A pH microclimate can be detected over the ruminal epithelium by using ion selective microelectrodes. The figure shows an original recording of the transepithelial potential (V_t), the potential of the pH-insensitive electrode (V_a), the potential of the pH-sensitive electrode (V_b), and the difference between the two (V_a-V_b) over time. After calibration, the electrode was moved downward slowly. A pH shift toward a more acidic value ("supra-apical pH shift") could be seen before the electrode entered the epithelium ("in"). Note the drop in the potential of V_a and V_b and the rise in the fractional apical resistance as measured by the response of the electrode to transepithelial voltage pulses.

In the rumen, experiments were carried out in a solution containing SCFA, but no bicarbonate, so that the apical anion exchanger did not contribute to pH control. Under these conditions, the pH of the microclimate was found to be more acidic than that of the bulk solution (7.2 ± 0.05 (p = 0.05, n = 7, Holm-Sidak), reflecting the acidifying effects of the apical Na^+/H^+ exchanger (2).

Interestingly, a significantly acidic microclimate was also found in the omasum (7.28 ± 0.06 (p = 0.04, n = 4)) in the presence of both SCFA and CO_2/HCO_3^- (177).

6.3 Electrogenic uptake of Na^+, Ca^{2+}, and Mg^{2+} by the rumen: the non-selective cation channel

What is the pathway for the electrogenic efflux of sodium across the ruminal epithelium?
Is it identical to the non-selective cation conductance that is blocked by Ca^{2+} and Mg^{2+}?
Is there evidence for an apical Mg^{2+} channel?
Can Ca^{2+} pass through this channel?
How can its regulation by voltage be explained?
What is its role in the homeostasis of the rumen?

Leonhard-Marek S, Stumpff F, Brinkmann I, Breves G, and Martens H. *Basolateral Mg^{2+}/Na^+ exchange regulates apical nonselective cation channel in sheep rumen epithelium via cytosolic Mg^{2+}. Am J Physiol 288: G630-645, 2005.*
Stumpff F, Brinkmann I, Schweigel M, and Martens H. *High potassium diet, sodium and magnesium in ruminants: the story is not over. In: Production diseases in farm animals, edited by Joshi NP and Herdt TH, 2004, p. 284-285.*
Stumpff F and Martens H. *A role for magnesium in the regulation of ruminal sodium transport. In: Focus on signal transduction research, edited by McAlpine G. New York: New Nova Science Publishers, Inc. (ISBN 13 978-1-60021-376-2), 2006, p. 37-66.*
Leonhard-Marek S, Stumpff F, and Martens H. *Transport of cations and anions across forestomach epithelia: conclusions from in vitro studies. Animal 4: 1037-1056, 2010.*

The importance of ruminal sodium absorption for maintaining ruminal homeostasis and supplying sodium for resecretion with saliva has been mentioned in the Introduction. Quantitatively, the electroneutral pathway will usually play a larger role. The electrogenic pathway is of great importance for two reasons. Firstly, the electrogenic transport of sodium is not coupled to a secretion of protons into the rumen and, thus, allows a selective absorption of this osmolyte without leading to an acidification of the apical microclimate. Secondly, electrogenic sodium transport appears to be the decisive transport protein mediating the increase in the efflux of sodium that restores ruminal homeostasis when animals are switched to a diet high

in potassium (189, 324, 338, 386). As mentioned above, previous studies have shown that the protein is not regulated by aldosterone (318) and thus, appears to be destinct from the well-characterized ENaC channel.

6.3.1 Electrogenic conductance for sodium: interaction with Mg^{2+}

Initial attempts to identify a sodium conductance in isolated cells of the ruminal epithelium proved extremely frustrating (44). In whole cell experiments with conventional pipette solutions, the replacement of sodium with a large cation such as choline did not lead to the significant drop in inward current at negative potential that had been anticipated. However, Ussing chamber experiments had demonstrated that the electrogenic conductance of sodium across forestomach epithelia can be enhanced by the removal of divalent cations from the mucosal solution (194, 307).

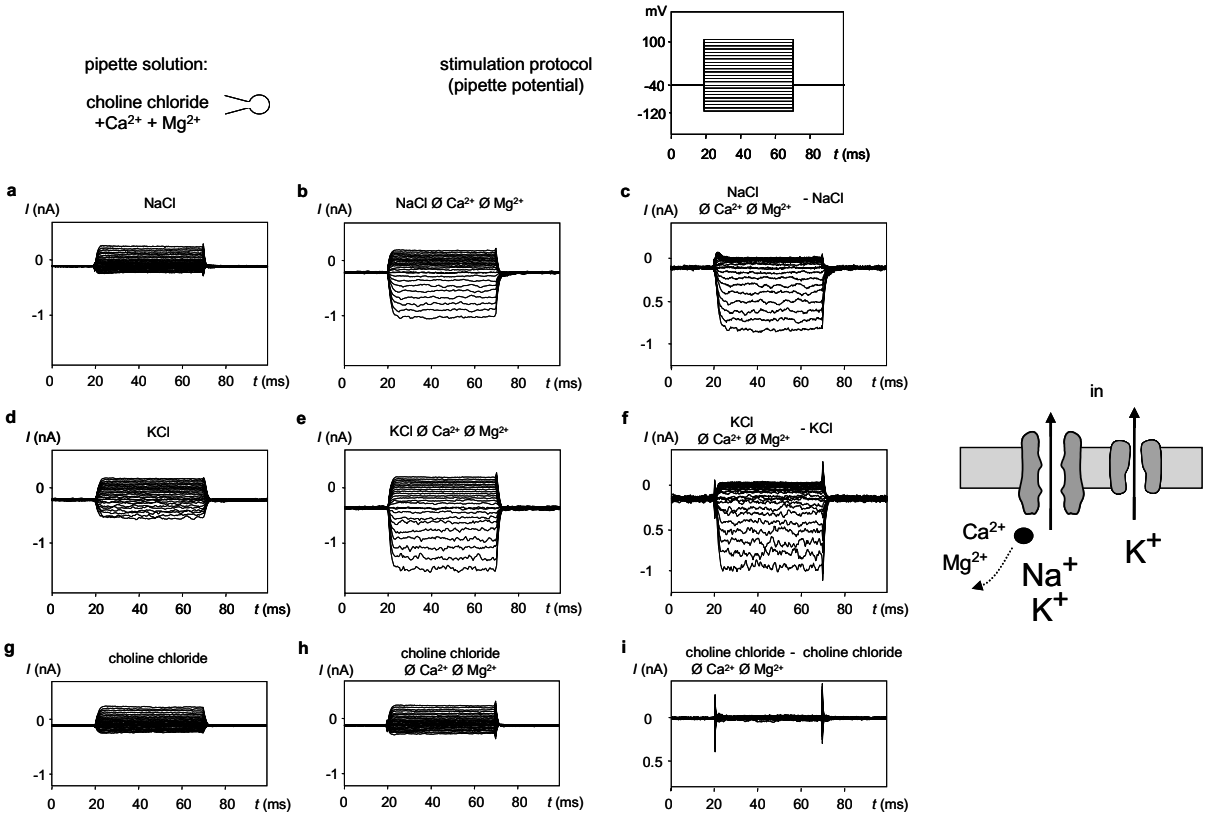

Figure 20: The non-selective cation channel of the ruminal epithelium (whole cell). Original traces from measurements performed on one isolated cell of the ruminal epithelium and filled with a choline chloride solution with 0.9 $mmol \cdot l^{-1}$ Mg^{2+} while Ca^{2+} was buffered by EGTA. a) cell in NaCl solution. b) After removal of divalent cations in the bath, a strong inward current at negative potential can be seen. c) Current carried by sodium (b minus a). d) Cell in KCl solution. At negative potential, a marked inward current can be seen that is enhanced by the removal of divalent cations (e). f) Current carried by potassium (e minus d). g) Current of the cell in choline chloride solution. The currents are not markedly different from those seen in the presence of sodium (a). h) Removal of divalent cations has no significant effect. i) The current carried by choline is negligible; the current in g and h must be carried by chloride.

When these experiments were repeated on isolated cells in the whole cell configuration, a marked increase in the sodium conductance of the cells could be observed (199, 351, 352). This divalent-cation-sensitive conductance was also shown to be permeable to potassium and caesium (Fig 17). The permeability sequence observed with $P_{Cs}>P_{Na}$ suggests a "large" or weak-field-strength pore, with permeability being limited primarily by the hydration energy rather than by cation size (146).

In these experiments, we also observed that the sodium conductance opened strongly when the potential was clamped to more negative voltages, or that it was "inwardly rectifying". The classical model for an inwardly rectifying conductance is the inward rectifier potassium channel (146). The voltage dependence of this channel has been extensively studied and is known reflect the voltage-dependent blocking effects of Mg^{2+} (or other large cations) on the internal mouth of the channel pore.

As before, no sodium currents could be convincingly demonstrated when divalent cations were present in physiological amounts. However, the uptake of Mg^{2+} into the ruminal epithelium is well known as being subject to changes *in vitro* and *in vivo*, and therefore, the cytosolic concentration of Mg^{2+} may be highly variable (198, 215, 312). An attempt was made to demonstrate a physiologically relevant conductance for sodium by reducing the concentration of Mg^{2+} in the pipette solution, which had been set to a relatively arbitrary 0.9 $mmol \cdot l^{-1}$ following standard recipes used on other cells. Following removal of magnesium from the solution, rectification was abolished, and a measureable sodium conductance now emerged in extracellular solutions containing physiological amounts of Ca^{2+} and Mg^{2+} (199, 351, 352, 359).

The non-selective cation channel has recently been reinvestigated at the single-channel level by using the inside-out technique, with membrane patches being excised into the bath solution (Stumpff, unpublished). The gating by cytosolic Mg^{2+} could again be clearly demonstrated.

These experiments also show that, at high applied potentials, the block by Mg^{2+} is relieved, and that Na^{+} can permeate the channel. Mg^{2+} can thus be considered to mediate the voltage dependency of the ruminal cation conductance as previously

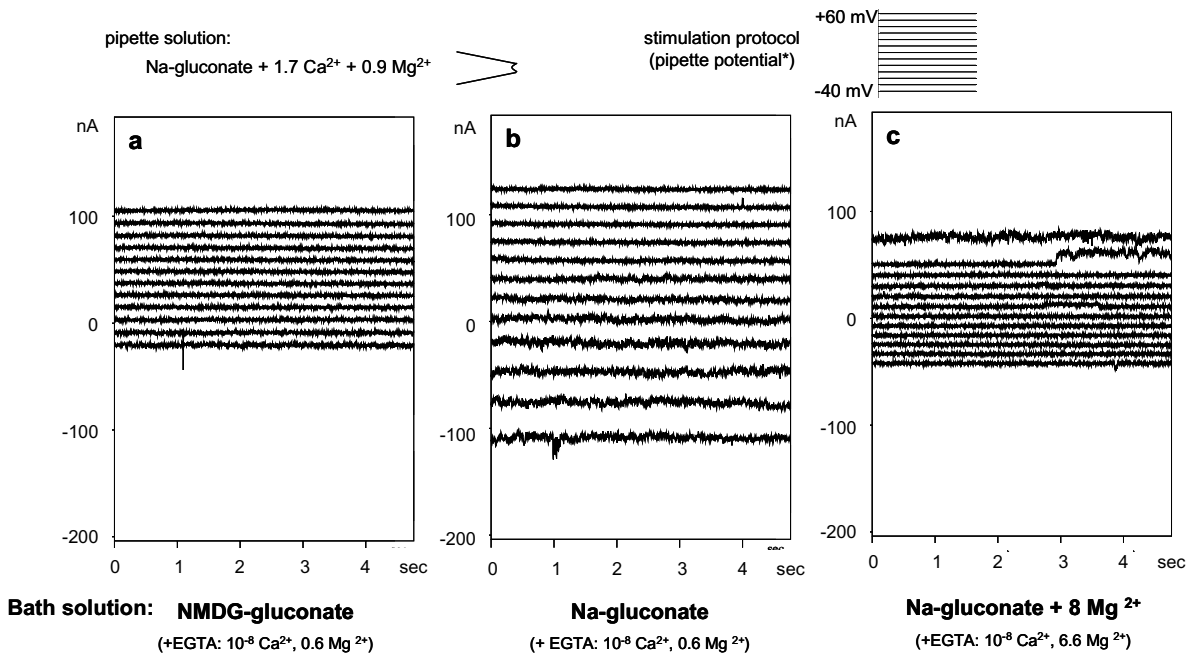

Figure 21: The non-selective cation channel of the rumen (single-channel, inside-out). Original traces from one patch. The pipette solution faced the external side of the cell membrane and contained physiological concentrations of Ca^{2+} and Mg^{2+}. The concentrations of Na^{+} and Mg^{2+} facing the cytosolic side (=bath) were varied. Voltage was stepped to the levels depicted in the figure. Recording of the currents began 10 seconds after each voltage jump to allow the stabilization of the current. a) Patch in NMDG-gluconate solution. Currents at positive pipette potentials were slightly higher than those at negative potentials, reflecting the efflux of Na^{+} from the pipette. b) When Na^{+} was added to the bath, the current at a negative pipette potential increased. Although Na^{+} was present on both sides of the membrane in equal concentrations, the inward and outward currents were clearly different. A negative pipette potential (= depolarization of the cell) relieved the block of Ca^{2+} ions on the external mouth of the pore. c) When Mg^{2+} was elevated on the cytosolic side, the Na^{+} mediated currents at negative potential were partially blocked. The Na^{+} current at positive potential was also blocked, but this block could be relieved if the driving force was high enough.

described (189). The relief of the block by high potentials suggests that the channel is permeable to Mg^{2+}(166). Classical unitary channel events were difficult to detect, suggesting that membrane patches contained clusters of large numbers of channels, making it difficult to resolve the single-channel conductance.

6.3.2 Permeability to Ca^{2+} and Mg^{2+}

The strong gating by cytosolic Mg^{2+} observed in ruminal epithelial cells greatly resembles that found in the non-selective cation channels TRPV5 and TRPV6 (379), and the expression of TRPV6 has since been demonstrated in the rumen (200, 390, 391), where it is thought to mediate the uptake of Ca^{2+} (305). TRPM7 is similarly regulated (166, 234) and has been found to be expressed by the ruminal epithelium (311) in which it undoubtedly represents a prime candidate for mediating the electrogenic uptake of Mg^{2+} (312).

In whole cell experiments, attempts to demonstrate significant currents carried by Mg^{2+} or Ca^{2+} were prevented by the strong interaction with the conductance for Na^{+}. Since the permeability sequence with $P_{Cs}>P_{Na}$ suggests a weak-field-strength pore (199), the permeability for other ions can be estimated from the energy necessary for removing the hydration shell from the ion. This requires -398 $kJ \cdot mol^{-1}$ for Na^{+}, -314 $kJ \cdot mol^{-1}$ for K^{+}, -293 $kJ \cdot mol^{-1}$ for NH_4^{+}, and -256 $kJ \cdot mol^{-1}$ for Cs^{+}, but -1577 $kJ \cdot mol^{-1}$ for Ca^{2+} and -1908 $kJ \cdot mol^{-1}$ for Mg^{2+}. The failure to observe currents conducted by Ca^{2+} or Mg^{2+} is thus unsurprising and does not argue against a slow permeation of these ions through the non-selective cation channels expressed by the ruminal epithelium. However, it should be mentioned that when cells were measured in otherwise symmetrical Na-gluconate solutions showing a gradient for Ca^{2+}, the reversal potentials were invariably slightly, but significantly, greater than zero (127, 360, 361). This may reflect an electrogenic influx of Ca^{2+} through what may well be TRPV6. (305). The gating kinetics of the ruminal cation conductance suggest that Mg^{2+} can permeate the channel if the driving force is high enough. This is typical of both TRPV6 (379) and TRPM7 (166, 234), both of which have been linked to the influx of Ca^{2+} and Mg^{2+} into cells.

Whereas the selectivity of channels from the TRP family for divalent cations varies, all members display a high permeability to sodium, which is modulated by divalent cations in a competetive manner (254). All TRP channels can thus also function as channels for the uptake of Na^{+}. Most likely, the ruminal epithelium apically expresses a plethora of different non-selective cation channels from this group.

6.3.3 Magnesium and the voltage dependence of the ruminal sodium conductance.

Patch-clamp experiments show that the voltage dependence of the ruminal sodium conductance is not related to the presence of a classical voltage sensor within the channel protein but is related to the presence of divalent cations on the apical side and within the cytosol. As the cytosol becomes depolarized, the blocking divalent cations (Ca^{2+} and Mg^{2+}) entering the pore from the external side of the membrane

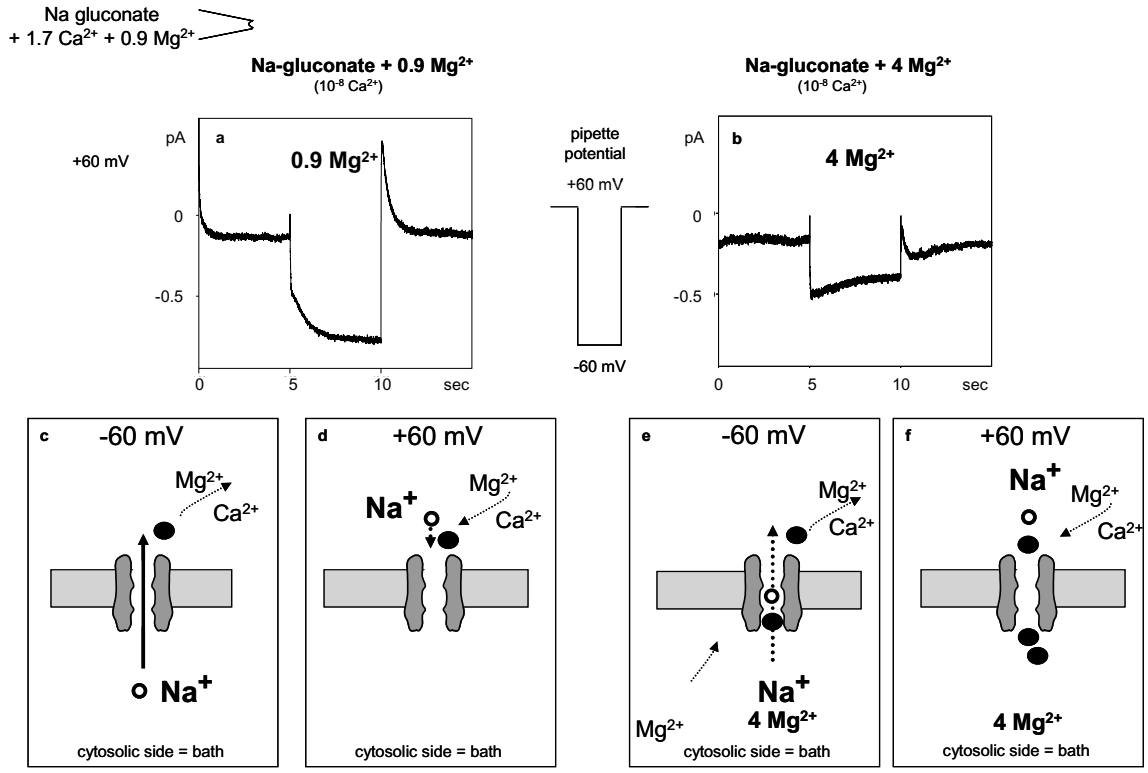

Figure 22: Voltage dependence of the non-selective cation channel of the ruminal epithelium (inside-out). After seal-formation and excision into the bath solution, patches of cellular membrane were exposed to the depicted voltage protocol. The pipette solution faced the external side of the membrane and contained Na-gluconate solution with physiological amounts of calcium and magnesium, whereas calcium on the cytosolic side (bath) was buffered to extremely low levels with EGTA.

a) Current trace*) from a membrane patch excised into a bath solution containing Na-gluconate and 0.9 Mg^{2+}. Hyperpolarization of the pipette potential to -60 mV (= depolarization of the cytosol) induced an influx of sodium into the pipette. The current increased with time. Depolarization of the pipette to +60 mV induced an outward current, the size of which rapidly declined. b) When 4 Mg^{2+} was added to the cytosolic side, hyperpolarization to -60 mV (= depolarization of the cytosol) induced a much smaller current, and the magnitude rapidly decreased with time. Depolarization to +60 mV only resulted in a transient outward current c) Model showing the non-selective cation channel. Hyperpolarization of the outside of the membrane to – 60 mV (corresponding to a depolarization of the cell) relieves the blocking effects of divalent cations, resulting in the increase of current amplitude with time as seen in the corresponding current trace depicted in (b). d) After depolarization of the pipette to + 60 mV (= hyperpolarization of the cytosol), the block by Ca^{2+} and Mg^{2+} from the outside is rapidly restored. e) After hyperpolarization of the pipette to -60 mV (depolarization of the cytosol) with a high concentration of cytosolic Mg^{2+}, blocking magnesium ions move into the internal mouth of the non-selective cation channels in the cellular membrane. The current amplitude is small and decreases with time. g) After repolarization of the pipette potential to + 60 mV (corresponding to a membrane potential of – 60 mV), the influx of Mg^{2+} into the pore prevents an efflux of Na^{+}.

*) The baseline current in NMDG-gluconate solution was subtracted from all currents depicted. Most likely, the currents depicted reflect the contribution of multiple low conductance channels found in a cluster on the membrane surface.

are pushed out by the positive potential, and the permeability of the channel for Na^{+} rises. The cytosolic concentration of Ca^{2+} is extremely low so that this cation will not be pushed into the channel pore from the inside. In addition, the influx of magnesium into the cell decreases (198, 312, 315), so that the cytosolic concentration of this large cation will also drop. This should further enhance the conductance of the channel for sodium (358).

Depolarization of the ruminal epithelium *in vitro* thus leads to an increase in the electrogenic conductance for sodium across the tissue (189). *In vivo*, the absorption of sodium across the ruminal wall rises with the concentration of ruminal potassium, thus contributing to ruminal osmoregulation ((216, 317, 384, 386); for reviews see (358, 359)).

6.3.4 Interactions of the non-selective cation channel with SCFA

In a minority of the cells studied, SCFA had a pronounced stimulatory effect on the sodium and potassium conductance of ruminal (360) and omasal epithelial cells. At this point, the signaling cascade has not been clarified in any detail. Most likely, the responding cells are insufficiently perfused by the patch pipette solution and are, thus, not buffered by HEPES. Exposure to SCFA can then be expected to lead to changes in cytosolic pH. Similar changes of cytosolic pH might underlie the increase in short-circuit current that is frequently observed when intact tissues are exposed to moderate concentrations of SCFA in the absence of buffering CO_2 (3, 116).

In emergency situations in which the ruminal pH drops to low levels and the driving force for the uptake of sodium via NHE breaks down, a shift toward an uptake of Na^+ via the non-selective cation channel, coupled to an extrusion of protons via the apical H^+-ATPase, may be an energetically expensive, but life-saving, alternative to the NHE (31, 158, 313). More work needs to be done to clarify this issue.

6.3.5 Interactions of the non-selective cation channel with cAMP

The ruminal epithelium shows an endogenous secretion of prostaglandins (110), which lead to the cytosolic formation of cAMP as a second messenger. Complex effects on ruminal sodium transport are observed that include a decrease in the electroneutral transport of Na^+ via NHE3, resulting in acidification and a drop in the activity of the Na^+/K^+-ATPase (110, 393). In the absence of divalent cations, however, cAMP had an enhancing effect on the short-circuit current measured across the epithelium, suggesting stimulatory effects of cAMP on the non-selective cation channel.

Because of the large number of possible actions of cAMP on the intact tissue, work on isolated cells of the ruminal epithelium was necessary in order to confirm that cAMP has effects on the non-selective cation channel of the ruminal epithelium (45, 199, 350, 357). Thus, cAMP was shown to increase the conductance of the non-selective cation channel of the ruminal epithelium for Na^+ in a manner partially, but not entirely, linked to a reduction of cytosolic Mg^{2+} concentration.

This finding is significant in terms of understanding the effects of prostaglandins and other tissue hormones that elevate cytosolic cAMP in the ruminal epithelium. These hormones might play an important role in decreasing the number of protons recirculated to the apical side and into the rumen via NHE, while partially maintaining the absorption of sodium by increasing the fraction of Na^+ taken up electrogenically. Cyclic AMP might thus act as a “switch” between these two uptake pathways for sodium, with dramatic consequences for intracellular and ruminal pH. Additional tissue hormones will probably be found that regulate ruminal sodium absorption.

6.3.6 The basolateral efflux of Mg^{2+}

Knowledge of the manner in which the apical non-selective cation channel is regulated has also played an important role in establishing that the basolateral efflux pathway for Mg^{2+} from the intact tissue occurs via Na^+/Mg^{2+} exchange (199). This finding has since been confirmed by using a cell culture model (314).

6.3.7 Interaction of the non-selective cation channel(s) with blockers

In whole cell experiments carried out in the absence of divalent cations, the non-selective cation channel could be blocked by the following agents: verapamil (100 $\mu mol \cdot l^{-1}$), quinidine (100 $\mu mol \cdot l^{-1}$), Ca^{2+} (1.7 $mmol \cdot l^{-1}$), Mg^{2+} (0.9 $mmol \cdot l^{-1}$), Ba^{2+} (5 $mmol \cdot l^{-1}$), und La^{2+} (100 $\mu mol \cdot l^{-1}$). The effects of amiloride (1 $mmol \cdot l^{-1}$) or flufenamic acid (10 $\mu mol \cdot l^{-1}$) did not reach significance levels. Glucose (20 $\mu mol \cdot l^{-1}$) had no effect.

6.4 Conductance for potassium

Does the ruminal epithelium express ion channels permeable to K^+?
Why is the epithelium depolarized by K^+, if the apical efflux of K^+ is so low?
What role might the stimulation of ruminal Na^+ transport by high K^+ solution play for the electrolyte balance of the rumen and of the animal?

> ***Abdoun K, Stumpff F, Wolf K, and Martens H.*** *Modulation of electroneutral Na transport in sheep rumen epithelium by luminal ammonia. Am J Physiol 289: G508-520, 2005.*
> ***Stumpff F and Martens H.*** *The rumen and potassium homeostasis: a model. Journal of Animal and Feed Sciences 16: 436-441, 2007.*
> ***Leonhard-Marek S, Stumpff F, and Martens H.*** *Transport of cations and anions across forestomach epithelia: conclusions from in vitro studies. Animal 4: 1037-1056, 2010.*

Whereas the uptake of potassium from the rumen has been suggested to occur via a paracellular pathway (235, 342), the expression of potassium conductances by the apical and basolateral membranes of the ruminal epithelium is supported by various investigations *in vitro* (103, 141, 198). Thus, the electrophysiological effects of high mucosal K^+ can be blocked by verapamil, which clearly argues against an efflux via a paracellular route. However, the multiple possible interactions within the intact epithelium do not amount to a proof for the expression of potassium channels by the ruminal epithelium. In particular, the problem remains as to why the secretion of potassium by the tissue is so low when the depolarizing effects of potassium on the epithelium are so high (101-103, 142, 198)? Only direct experiments on single cells can resolve the issue of whether the rumen expresses potassium channels.

6.4.1 Inwardly rectifying potassium conductance

In patch-clamp experiments on isolated cells of the ruminal epithelium, potassium conductances could be directly and clearly demonstrated both on the whole cell and on the single-channel level (4, 199). Whole cell experiments suggest that functionally, the cells express an inwardly rectifying conductance that may well correspond to a classical inward rectifyer (146). A pronounced increase in current could be observed when cells were exposed to high potassium solutions, suggesting a pronounced selectivity of the conductance for K^+ over Na^+.

Whereas the localization of channels expressed by isolated ruminal epithelial cells is not directly possible, it is reasonable to argue that the activity of the basolateral Na^+/K^+-ATPase (133, 141, 142) can only be maintained if the basolateral membrane is tight against the electrogenic influx of Na^+. The basolateral potassium conductance

(198) must therefore be highly selective for K^+ over Na^+ and may well correspond to the potassium-selective channels observed in the patch-clamp experiments (4). Conversely, the non-selective channel must correspond to an apically expressed channel.

6.4.2 Blocker sensitivity

In contrast to the non-selective cation channel of the ruminal epithelium, the potassium conductance was sensitive to Tetra-ethyl-ammonium-chloride (TEACl) (10 $mmol \cdot l^{-1}$) but could not be blocked by physiological concentrations of Ca^{2+} and Mg^{2+}. $BaCl_2$ (5 $mmol \cdot l^{-1}$) and quinidine (100 $\mu mol \cdot l^{-1}$) were also found to have effects on the inward current; however, these blockers also affected the non-selective cation channel. The expression of channels selective to K^+ by ruminal epithelial cells was confirmed using the single-channel technique (4).

6.4.3 Outwardly rectifying potassium conductance

In addition to the inwardly rectifying conductance, ruminal epithelial cells also expressed an outwardly rectifying conductance for K^+. The conductance was small in NaCl solutions containing physiological amounts of Ca^{2+} and Mg^{2+} but increased when the cells were exposed to high potassium solutions (4). The removal of divalent cations from the external medium also increased the conductance (199). Currents could be blocked by calcium, magnesium, verapamil, and quinidine, all of which also blocked the ruminal conductance for sodium in whole cell patch-clamp experiments (4, 199). This suggests that non-selective channels significantly contribute to the conductance of ruminal epithelial cells for potassium.

As mentioned above, the outwardly rectifying conductance rose with the concentration of the permeant ion (4). In the classical model, permeant ions such as K^+ enter the channel and “nudge” blocking Mg^{2+} out of the internal mouth of the channel pore of Mg^{2+} gated channels (10, 86, 148, 399). This model might explain the old paradox as to why the apical membrane of the rumen is strongly depolarized by high potassium, although the efflux of potassium from the tissue in NaCl solution is low (101-103, 142, 198).

6.4.4 A model for ruminal potassium transport

In summary, the patch-clamp experiments have led to a model of ruminal potassium transport with an outwardly rectifying conductance at the apical membrane, and an inwardly rectifying conductance at the basolateral side.

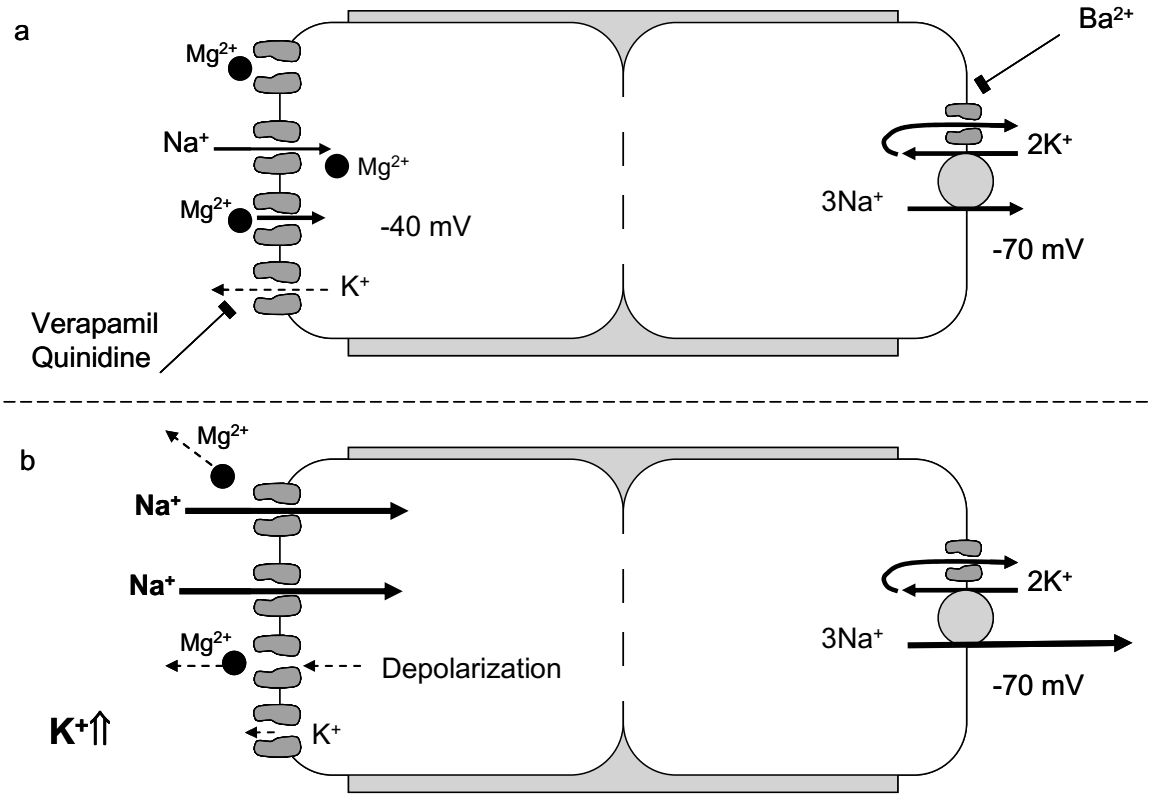

Figure 23: Model of ruminal potassium transport. a) The tissue expresses an apical conductance for potassium that is sensitive to verapamil, quinidine, and divalent cations. At least in part, the conductance is identical to the non-selective cation channels that mediate the uptake of sodium and magnesium. The uptake of Mg^{2+} through the non-selective cation channel interferes with the transport of other cations, corresponding functionally to a partial block of the conductance for Na^+ and K^+ by external and internal Mg^{2+}. Whereas the influx of Na^+ is facilitated both by the potential and the concentration gradient, the efflux of K^+ is limited by the potential across the apical membrane. The efflux of potassium taken up with the Na^+/K^+ ATPase is thus mostly mediated by basolateral channels, which are highly selective for potassium. b) The mucosal elevation of potassium will further decrease the apical efflux of K^+, resulting in a depolarization of the apical membrane. This decreases the influx of divalent cations from the mucosal side, resulting in a decrease in the cytosolic concentration of Mg^{2+}, thus freeing the internal and external mouth of the non-selective cation channel. An increase in the uptake of Na^+ down the concentration gradient should follow. Conversely, an apical influx of K^+ will only occur at high ruminal concentrations of potassium as a driving force. Ultimately, the basolateral efflux of potassium out of the epithelium into blood will depend on the activity of the Na^+/K^+ ATPase.

Basolaterally, the model follows classical outlines (373). A high cytosolic concentration of potassium is maintained by the activity of the Na^+/K^+ ATPase in conjunction with an inward rectifier. When cytosolic concentrations of potassium

drop, the efflux of K^+ across the basolateral channel drops, and the tissue is depolarized. Depolarization closes the inward rectifier, so that cytosolic K^+ concentrations can rise again because of the activity of the pump ("rectification").

Apically, the outwardly rectifying conductance plays a similar role. When ruminal potassium concentrations are low, a large "leakage" of potassium from the cytosol into the large cavity of the ruminal epithelium is prevented by the low open probability of the apical channels. When ruminal potassium concentrations rise, the apical efflux of potassium from the tissue will drop further, resulting in a depolarization of the apical membrane with stimulatory effects on sodium transport following as described above (358, 359). Due to the influx of Na^+, the apical potential will become more depolarized and limit the apical potassium influx. The implications of the model for the homeostasis of sodium, magnesium, and potassium in the ruminant will be outlined in the Discussion.

6.5 The conductance of the rumen for ammonium

Do isolated cells of the ruminal epithelium express ion channels with a conductance for the ammonium ion?
What interactions occur between ruminal ammonia and ruminal sodium transport?
How does basolateral efflux occur?

> ***Abdoun K, Stumpff F, Wolf K, and Martens H.*** *Modulation of electroneutral Na transport in sheep rumen epithelium by luminal ammonia. Am J Physiol 289: G508-520, 2005.*
> ***Abdoun K, Stumpff F, and Martens H.*** *Ammonia and urea transport across the rumen epithelium: a review. Anim Health Res Rev 7: 43-59, 2006.*

The absorption of ammonia from the rumen has to be regulated in a manner that ensures that the concentration is high enough to serve as a source of nitrogen for microbial protein synthesis but does not lead to toxic effects. As mentioned in the Introduction, the absorption of ammonia has long been postulated to occur not only in the form of NH_3, but also in the form of NH_4^+ (34, 38, 122). This pathway should be of particular importance postprandially, when ruminal pH reaches a minimum, while large amounts of ammonia are set free.

6.5.1 Permeability of the intact rumen to NH_3 and NH_4^+

The amount of ammonia taken up apically as NH_3 and NH_4^+ by the intact tissue was estimated by measuring the total flux of both forms of ammonia (J_{tot}(Am) in µeq·cm^{-2}·h^{-1}) across the tissue at various levels of mucosal pH. From this, the concentration of NH_3 (c(NH_3), in mmol·l^{-1}) could be calculated by using the Henderson Hasselbalch equation. Data could be fitted to the equation (4):

$$J_{tot}(\text{Ammonia}) = 4.1\ \text{cm}^{-2}\cdot\text{h}^{-1}\cdot c(NH_3) + 0.7\ \mu\text{eq}\cdot\text{cm}^{-2}\cdot\text{h}^{-1}\quad (r = 0.99)$$

The equation suggests that, whereas the ammount of ammonia transported by the tissue rises with pH and the concentration of NH_3, an amount of ~ 0.7 µeq·cm^{-2}·h^{-1} is transported even when the concentration of NH_3 drops to low levels. This amount corresponds to the increase in short-circuit current observed across the tissue after exposure to ammonia (4) and may thus reflect the uptake of ammonia in the form of NH_4^+.

The equation also allows a calculation of the permeability of the rumen to both forms of ammonia by dividing the respective fluxes by the concentration (P=J/C) (1), yielding

$$p(NH_3) \approx 0.001\ \text{cm}\cdot\text{s}^{-1}$$

$$p(NH_4^+) \approx 6.46 \times 10^{-6}\ \text{cm}\cdot\text{s}^{-1}$$

The rumen is thus far more permeable to NH_3 than to NH_4^+, but the concentrations of the latter are much higher. For orientation, lipid bilayer membranes have a p(NH_3) of 7.8 x 10^{-2} to 2.4 x 10^{-3}cm·s^{-1} (187), whereas permeability to cations is 10^{-11} to 10^{-13} cm·s^{-1} (256)). Of course, direct comparisons of a tissue with a bilayer are perilous.

6.5.2 Isolated cells of the ruminal epithelium express channels permeable to NH_4^+

The permeability of the cell membrane of cells of the ruminal epithelium to the ammonium ion (NH_4^+) could be confirmed by using the patch-clamp technique (4). Importantly, and as in the case of potassium, the conductance increased with the elevation of the permeant anion.

These results cannot come as a surprise. The outer diameter of the NH_4^+ ion is almost identical to that of the K^+ ion, and accordingly, the energy necessary to strip both ions of the surrounding hydration shell in order to allow passage through the pore of a channel is remarkably similar (-314 $kJ \cdot mol^{-1}$ for K^+ and -293 $kJ \cdot mol^{-1}$ for NH_4^+). The permeability of the pore of potassium channels to NH_4^+ has been demonstrated numerous times (40, 55, 146, 147, 398). The passage of NH_4^+ through non-selective cation channels (254), which allow the passage not only of K^+, but also of ions as diverse as Na^+ (-398 $kJ \cdot mol^{-1}$), Cs^+ (-256 $kJ \cdot mol^{-1}$), or even Ca^{2+} (-1577 $kJ \cdot mol^{-1}$), is equally predictable and has been demonstrated directly (47). Bödeker's hypothesis that NH_4^+ can permeate the potassium conductances of the ruminal epithelium is thus supported by our present understanding of channel-mediated transport.

The patch-clamp experiments suggest that the conductance of ruminal epithelial cells for ammonia is regulated in a complex manner and involves effects of the permeant cation on blocking cytosolic cations, such as Mg^{2+}, and effects resulting from the influx of NH_3 through other pathways with an impact on cellular volume and cytosolic pH. Thus, the acidification of the cytosol by SCFA will increase the open probability of the non-selective cation channel (360). This effect may play a role in stimulating the efflux of ammonium as NH_4^+ postprandially (37, 122, 276, 329), when the concentration of SCFA and NH_4^+ rises, while pH and NH_3 concentration drops.

6.5.3 Interaction of NH_3/NH_4^+ transport with ruminal sodium transport

The effects of NH_3/NH_4^+ on sodium transport (4) support the notion that the transport of both forms of ammonia occurs via a transcellular pathway. At high mucosal pH (> 7.0), the uptake of NH_3 predominates. Once taken up into the cell, NH_3 will predictably be protonated within the neutral pH of the cytosol, thus resulting in an alkalinization with a reduction of sodium transport via NHE.

The stimulation of NHE at low mucosal pH is not quite as straightforward. If mucosal pH is low, the amount of ammonia present as NH_3 will be negligible, and influx will occur primarily as NH_4^+, which is driven into the cell both by the concentration gradient and by the potential across the apical membrane. Within the neutral or near neutral pH of the cytosol, a certain fraction will dissociate to NH_3, which will thus be

present in the cytosol in a greater concentration than apically. Diffusive reflux down the concentration gradient back to the apical side is to be expected (40). The circulation of ammonia across the apical membrane – in as NH_4^+, out as NH_3 – will lead to a net transport of protons into the epithelium, which have to be removed via NHE. The stimulation of sodium transport by ammonia thus reflects the apical uptake of protons via the recycling of ammonia. Accordingly, the stimulation of NHE by ammonia at low pH is roughly twice as high as the net transport of NH_4^+ (4).

Of course, an acidification of the cytosol will tend to reduce the apical reflux of NH_3 and increase the amount of NH_4^+ that reaches the basolateral membrane. SCFA and CO_2 stimulate the absorption of ammonia across the ruminal epithelium *in vitro* (37) and *in vivo* (276). This may be related both to an increased influx through the apical non-selective cation channel and to a decrease in the apical reflux of NH_3.

6.5.4 The basolateral efflux of NH_4^+

A specific and highly variable fraction of ammonia taken up apically is metabolized by the tissue (37, 231, 250), with the metabolized fraction rising in response to a concentrate-based diet (6). However, considerable amounts of ammonia must pass the basolateral membrane of the ruminal epithelium, since large quantities appear in the portal blood (276), where they can lead to toxic effects when the concentrations exceed liver capacity (48, 387). Based on the observation of an increase in short-circuit current after application of ammonium, Bödeker (34) suggests that basolateral efflux primarily occurs in the form of NH_4^+, which will remove a proton from the cytosol into the blood. Conversely, and since ammonia is present primarily as NH_4^+ in the cytosol, efflux as NH_3 will set free a proton and, thus, acidify the cytosol.

The data of Abdoun (4) can be used to clarify the issue of the basolateral efflux of ammonia by using several approaches. First, if the basolateral efflux of NH_4^+ exceeds the efflux of NH_3, an *alkalinization* of the tissue at the basolateral membrane should follow, with the inhibition of basolateral pH regulatory proteins (such as NHE1 and Na-HCO_3^- cotransport (239)). Accordingly, an inhibition of serosal to mucosal sodium transport was found when tissues were exposed to ammonia. Second, the short-circuit current should equal the sum of the cations minus the sum of the anions flowing across the membrane. Since both sodium and chloride fluxes were obtained

in our study (4), the ammonium must have left the basolateral membrane in the form of NH_4^+ at pH 7.4 to balance the charge and restore electroneutrality.

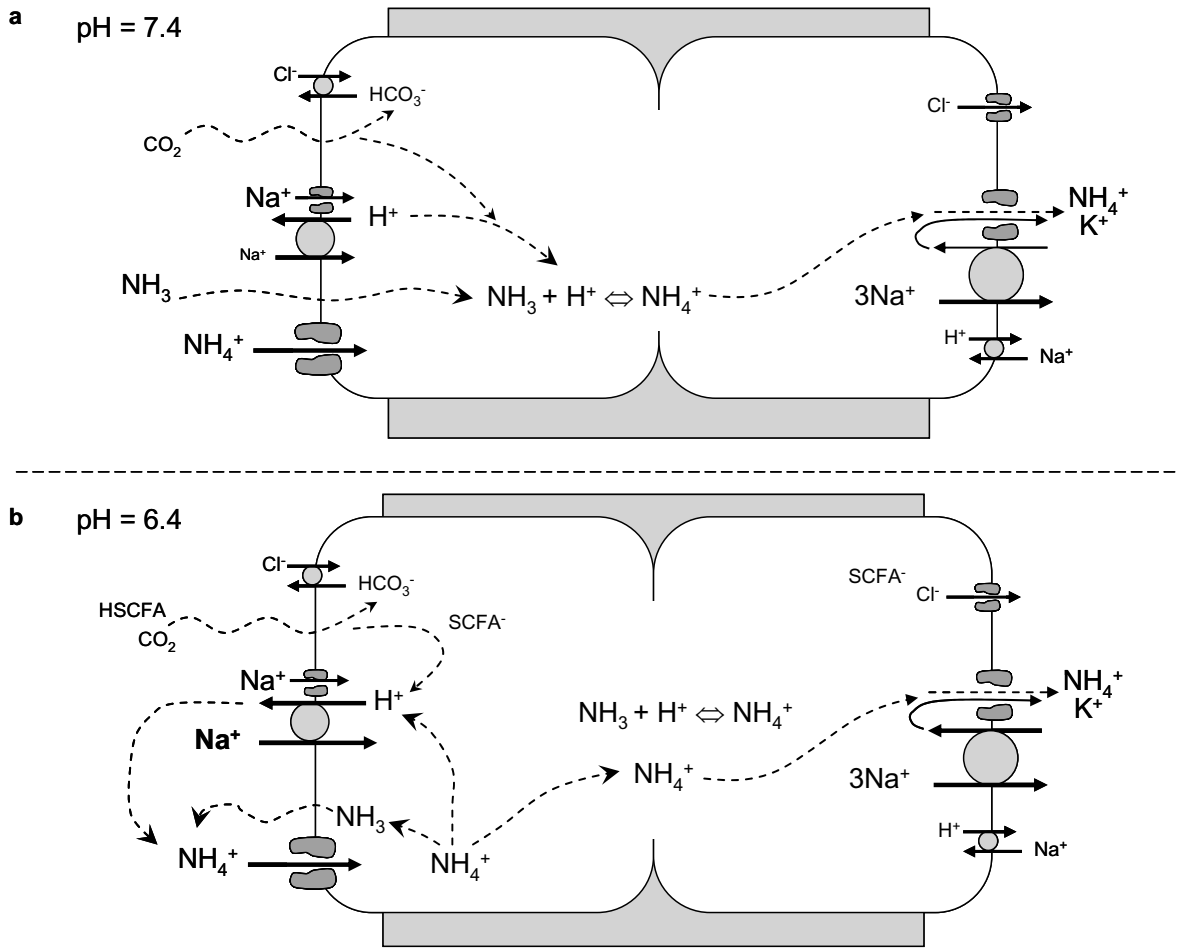

Figure 24: Model of ruminal ammonia transport. a) At high ruminal pH, apical influx of NH_3 exceeds that of NH_4^+. Inside the cell, NH_3 is protonated to NH_4^+ restoring the equilibrium between the two forms. Protons entering the cell (e.g., with CO_2) are no longer extruded in exchange for Na^+, resulting in a drop of sodium flux across the tissue. b) At low ruminal pH, the apical uptake of NH_4^+ exceeds that of NH_3. Depending on cytosolic pH, a certain fraction of this NH_4^+ will dissociate and form NH_3 so that protons are freed and stimulate the apical influx of sodium via NHE. Since NH_3 concentrations within the cell are now higher than those outside, a certain reflux of NH_3 into the luminal fluid will occur. At the low pH found on the apical side, this NH_3 will be reprotonated and flow back into the cell as NH_4^+, resulting in a cycle that increases the amount of protons in the epithelium and thus stimulates apical uptake of sodium via NHE. NH_4^+ leaves basolaterally through potassium channels, linked to the efflux of a (counter-) anion through a basolateral anion channel.

These calculations also lead to another conclusion: at pH 6.4, a balance between the flow of cations (Na^+ and NH_4^+) and anions across the tissue can only be obtained if one assumes that both Cl^- and $SCFA^-$ anions leave basolaterally through an anion

channel.[8] Notably, the efflux of $SCFA^-$ through an anion channel will depolarize the basolateral membrane and, thus, increase the driving force for the efflux of NH_4^+. The ruminal transport of ammonia is, indeed, enhanced by SCFA as this model would suggest (37, 262).

6.6 The secretion of urea by the rumen

Can the flux of urea into the rumen be explained by "lipid diffusion", or is a protein-mediated pathway mandatory?
What physiological role might the transport of urea and the reuptake as ammonia have for ruminal acid-base equilibrium?

> ***Abdoun K, Stumpff F, and Martens H.*** *Ammonia and urea transport across the rumen epithelium: a review. Anim Health Res Rev 7: 43-59, 2006.*
> ***Abdoun K, Stumpff F, Rabbani I, and Martens H.*** *Modulation of urea transport across sheep rumen epithelium in vitro by SCFA and CO_2. Am J Physiol 298: G190-202, 2010.*
> ***Aschenbach JR, Penner GB, Stumpff F, and Gäbel G.*** *Role of fermentation acid absorption in the regulation of ruminal pH. J Anim Sci (submitted), 2010.*

6.6.1 Transport of urea is mediated by a transport protein

Many studies support the expression of UT-B by the rumen (281, 283, 345). However, the conclusion that the transport of urea across the ruminal epithelium does, indeed, occur via a transport protein cannot be drawn from molecular biological investigations but requires functional data. In a recent study (2), we were able to demonstrate that:

- urea flux rates are not correlated with the flux rates for mannitol
- urea transport is modulated by maneuvers that have an impact on cytosolic pH

These observations cannot be explained by assuming a simple efflux via a paracellular pathway or via "lipid diffusion". It should be mentioned that our studies (2, 4) show that the ratio between the permeability of the rumen for urea ($7.9 \cdot 10^{-6}$ $cm \cdot s^{-1}$) and for NH_3 (0.001 $cm \cdot s^{-1}$) is over 100 times as high as corrresponding ratios from lipid bilayer membranes (187).

[8] This hypothesis was first seriously considered in the course of work on the passage of ammonia through the epithelium (4). Since the major focus of that study was related to the apical uptake pathways, this hypothesis was not followed through. However, even at the time, it was clear that balancing the cation and anion fluxes with the I_{sc} required the passage of SCFA through an electrogenic basolateral efflux pathway. These deliberations inspired the later time-consuming study on the ruminal anion channel (360).

6.6.2 Urea recycling and pH homeostasis

Urea secreted into the rumen and not used for microbial protein synthesis is rapidly degraded to CO_2 and NH_3, the latter of which is protonated and absorbed as ammonium. Since the subsequent resynthesis of urea from ammonia requires energy, this would appear to be an energetically wasteful arrangement.

However, the stimulation of electroneutral sodium absorption by NH_4^+ (4) is beneficial for ruminal osmoregulation and for the provision of Na^+ for the resecretion with salivary buffers. Basolateral efflux as NH_4^+ should remove protons from the rumen directly. Since portal flows of ammonium have been estimated to amount to 100 mmol per kg $BW^{0.75}$(255), with peak values of 25 mol·day^{-1} being found in dairy cows (64, 65), considerable quantities of protons can be removed by this mechanism. Understanding that ammonia can cross the basolateral membrane as NH_4^+ through potassium channels may thus be central to understanding one physiological purpose of urea recycling in the ruminant. However, the ability of the rumen to transport protons out of the rumen via this mechanism will be limited both by the toxicity of ammonia and possibly also by the limited transport capacity of the basolateral K^+ channels.

6.7 Apical uptake of SCFA

Do SCFA acidify the epithelium?

> ***Abdoun K, Stumpff F, Rabbani I, and Martens H.*** *Modulation of urea transport across sheep rumen epithelium in vitro by SCFA and CO_2. Am J Physiol 298: G190-202, 2010.*
> ***Aschenbach JR, Bilk S, Tadesse G, Stumpff F, and Gäbel G.*** *Bicarbonate-dependent and bicarbonate-independent mechanisms contribute to nondiffusive uptake of acetate in the ruminal epithelium of sheep. Am J Physiol 296: 1098-1107, 2009.*

SCFA have long been known to stimulate the uptake of sodium via NHE and have long been postulated to acidify the epithelium. However, this has never been shown directly. In particular, the uptake of SCFA via an apical anion channel appears theoretically possible and will lead to an alkalinization of the epithelium.

Using ion-selective microelectrodes on ruminal tissues *in vitro*, we were able to directly demonstrate the acidifying effects of an application of SCFA to the ruminal epithelium (2). *In vivo*, the effects are likely to be smaller, because of the presence of large amounts of buffering bicarbonate and a higher capacity of the epithelium for acid extrusion.

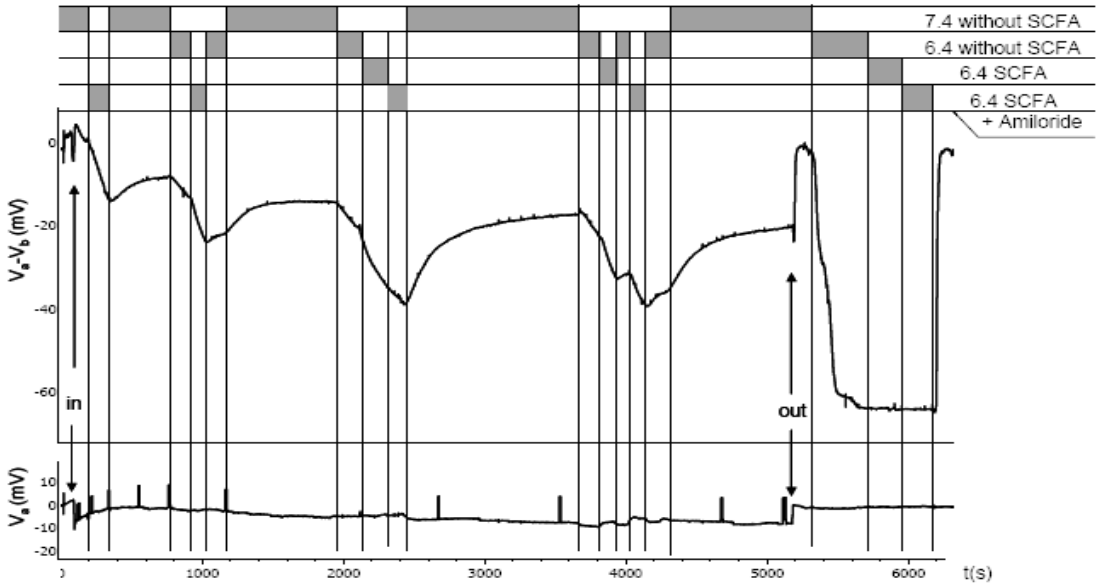

Figure 25: Short chain fatty acids (SCFA) acidify the cytosolic space of the ruminal epithelium. The figure shows the original recording of the cytosolic pH of the ruminal epithelium measured with a pH-sensitive microelectrode. After impalement of the tissue ("in"), various solutions were applied consecutively via continuous perfusion. Under bicarbonate-free conditions and at pH 6.4, addition of SCFA to the solution led to a marked acidification of the epithelium, although the apical pH remained constant. At the end of the measurement, the microelectrode was pulled out of the tissue ("out") and calibrated by using solutions with defined pH values.

A parallel study has shown that both the uptake of undissociated SCFA and the uptake of SCFA/HCO_3^- contribute to the apical uptake of SCFA (15). In this study, the stimulatory effect of a low pH on SCFA absorption has, in large part, been shown to be related to the bicarbonate gradient and not to the pH gradient *per se*. However, since this anion exchange removes buffering bicarbonate from the cytosol, both pathways should contribute to the acidification observed.

6.8 Distribution theory across epithelia or why lipid diffusion cannot work

Stumpff F, Martens H, Bilk S, Aschenbach JR, and Gäbel G. *Cultured ruminal epithelial cells express a large-conductance channel permeable to chloride, bicarbonate, and acetate. Pflugers Arch 457: 1003-1022, 2009.*

Classically, the uptake of SCFA by the rumen has been assumed to occur via “lipid diffusion”. However, no attempt has been made to estimate the accumulation of the SCFA that is to be expected within the tissue if both uptake and efflux occur via this pathway.

The distribution of weak electrolytes such as SCFA across cellular membranes has been extensively studied both theoretically and experimentally (285), and pH gradients between the cytosol and the bath are well known to lead to an inhomogenic distribution of the weak electrolyte. However, if a theory of weak electrolyte diffusion across epithelia exists in the literature, we have been unable to find it. Therefore, a mathematical model has been developed in order to answer the question as to whether lipid diffusion is a viable model for the transport of SCFA across the ruminal epithelium (360).

In the following, we will shown that, if transport of SCFA across the apical and the basolateral membranes is assumed to occur via passive diffusion only, equilibrium calculations predict an accumulation of SCFA within the cells not only of tissues bathed on all sides by a SCFA-containing solution (285), but also within a transporting epithelium in a gradient of SCFA.

We will assume that on the mucosal side, the total concentration of the SCFA (dissociated and undissociated: $[SCFA]_m^{tot}$) remains constant throughout, whereas basolaterally, the concentration remains zero (e.g., removal by the portal circulation). Mucosal uptake of the protonated undissociated SCFA ($J(HSFA)_m$) into the cell will depend on the concentration gradient between the undissociated SCFA on the mucosal side ($[HSCFA]_m$) and the cytosol ($[HSCFA]_{cyt}$) multiplied by a diffusion constant C_1: $J(HSCFA)_m = C_1 \cdot([HSCFA]_m - [HSCFA]_{cyt})$. By analogy, efflux from the basolateral side will be $J(HSCFA)_s = C_2 \cdot([HSCFA]_{cyt})$, where C_2 is the constant describing the efflux of undissociated SCFA across the basolateral membrane. The

cytosolic concentration ($[HSCFA]_{cyt}$) will rise until steady state conditions are reached and apical influx equals basolateral efflux :

$$J(HSCFA)_m = C_1 \cdot([HSCFA]_m - [HSCFA]_{cyt}) = J(HSCFA)_s = C_2 \cdot([HSCFA]_{cyt})$$

leading to : $[HSCFA]_{cyt} = C_1/(C_1 + C_2) \cdot [HSCFA]_m$

The concentration of the undissociated SCFA $[HSCFA]_m$ can be calculated from the total mucosal concentration ($[SCFA]_m^{tot}$), the mucosal pH (pH(m)), and the dissociation constant (pK) by using the Henderson-Hasselbalch equation:

$$[HSCFA]_m = [SCFA]_m^{tot} / (10^{pH(m)-pK} + 1)$$

Once in the cell and depending on the pH of the cytosol (pH(cyt)), a certain fraction of the undissociated SCFA will dissociate and accumulate until an equilibrium state between dissociation and formation is reached, leading to a total concentration of SCFA within the cytosol of:

$$[SCFA]_{cyt}^{tot} = [HSCFA]_{cyt} \cdot (10^{pH(cyt)-pK} + 1)$$

$$= C_1/(C_1 + C_2) \cdot [HSCFA]_m \cdot (10^{pH(cyt)-pK} + 1) =$$

$$= C_1/(C_1 + C_2) \cdot [SCFA]_m^{tot} \cdot (10^{pH(cyt)-pK} + 1) / (10^{pH(m)-pK} + 1)$$

For acetic acid (pK = 4.76) and by using pH(cyt) ≈ 7.4 (240) and a typical ruminal pH(m) ≈ 6.4 , we get:

$$[SCFA]_{cyt}^{tot} = 9.8 \cdot C_1/(C_1 + C_2) \cdot [SCFA]_m^{tot}$$

If we make the straightforward assumption that the apical membrane is as permeable to acetate as the basolateral membrane ($C_1 = C_2$), the accumulation of acetate will reach a catastrophic dimension of 300 $mmol \cdot l^{-1}$ at a ruminal concentration of 60 $mmol \cdot l^{-1}$. Even if we were to assume that, for some reason, basolateral permeability C_2 of the epithelium for acetate were 9 times higher than that of the apical membrane (C_1), acetate should accumulate within the ruminal epithelium to the level found within the rumen (≈ 60 $mmol \cdot l^{-1}$). The assumption of a multilayer model creates even larger problems for the apical layer of cells, as does the influx of acetate anions via electroneutral exchange.

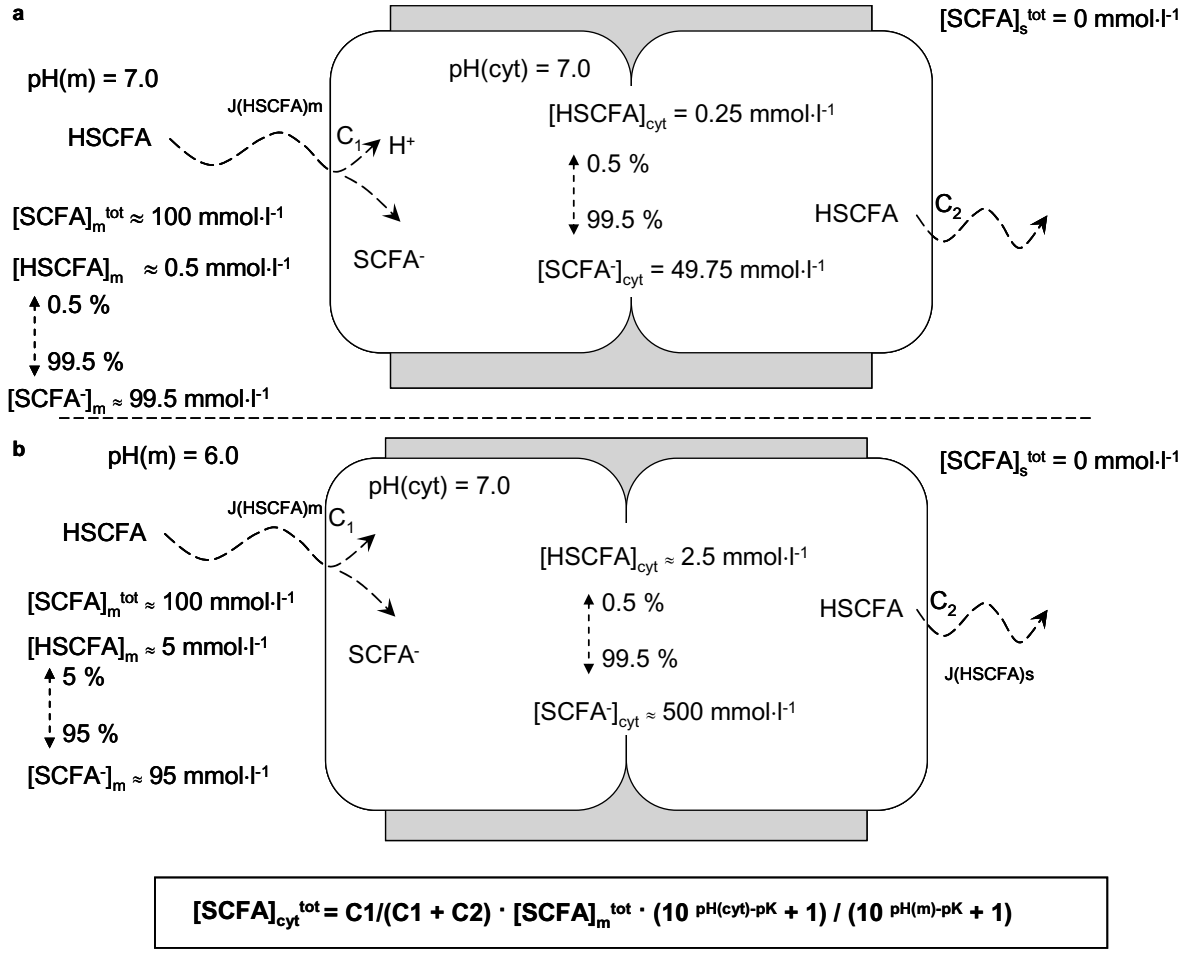

Figure 26: Distribution theory applied to the flux of SCFA across the ruminal epithelium. Assuming an equal permeability $C_1 = C_2$ of the apical and basolateral membranes and an exclusively lipid-diffusive uptake of SCFA by the rumen, steady state conditions across the epithelium (influx = efflux) will be reached when the cytosolic concentration of the permeable form (HSCFA) is half of that found mucosally. However, at neutral cytosolic pH, 99.5% of the HSCFA taken up will dissociate, and the anion will accumulate intracellularly. a) Situation at a mucosal pH of 7.0. SCFA accumulate within the epithelium to roughly half the mucosal concentration before the concentration gradient driving the efflux of HSCFA is equal to that driving the influx of HSCFA. b) At a mucosal pH of 6.0, the mucosal concentration of HSCFA is ten times higher than before. If cytosolic pH is maintained at near neutral levels, the HSCFA flowing in apically will dissociate almost completely. If efflux occurs via lipid diffusion only, SCFA will accumulate within the cytosol to 10 times the amount measured mucosally before the amount of undissociated HSCFA available for efflux reaches the level necessary to compensate for influx and steady state conditions are reached. The total osmolarity of the cytosol will rise even further, since cations must follow the anions in an equimolar amount to restore electroneutrality.

Matters become even worse if one realizes that, for every anion taken up, a cation must follow (note that the membrane potential only involves minute shifts in the concentration of cations and anions across a membrane!). The osmolarity within the epithelium should therefore rise to a level twice as high as the concentration of SCFA in our example, which clearly does not appear compatible with cellular survival. Finally, acetate only constitutes 60%-70% of the total concentration of SCFA; the problems are the same with propionate and butyrate.

To salvage lipid diffusion theory, complex models can of course be generated, such as assuming not just an apical microclimate that drives influx, but also a basolateral acidic microclimate that drives basolateral efflux. However, then a new problem will emerge: if the basolateral microclimate is acidic, then, how can ammonia efflux be explained by using a lipid diffusive uptake model? Efflux must be more efficient than influx; a protein-mediated efflux pathway is required (360, 362).

It may be mentioned that this is but one of the arguments against an efflux of SCFA via the "pure" lipid diffusion model. A further formidable argument against this hypothesis was first suggested by Danielli (62), who correctly observed that the quantity of protons present in the rumen is much too low to account for the quantities of SCFA absorbed from the organ and noted that instead, a considerable fraction of SCFA leave with Na^+ as a countercation.

6.9 Basolateral efflux of chloride and SCFA: the maxi-anion channel

What is the counter-anion for electroneutral sodium transport?
What is the basolateral efflux pathway for chloride?
Do ruminal epithelial cells express a conductance for anions of the SCFA?
Does the omasum express anion channels permeable to chloride and the anions of SCFA?
How does ruminal SCFA transport occur if protons are buffered in the rumen by saliva?

> ***Stumpff F, Martens H, Bilk S, Aschenbach JR, and Gäbel G.*** *Cultured ruminal epithelial cells express a large-conductance channel permeable to chloride, bicarbonate, and acetate. Pflugers Arch 457: 1003-1022, 2009.*
> ***Leonhard-Marek S, Stumpff F, and Martens H.*** *Transport of cations and anions across forestomach epithelia: conclusions from in vitro studies. Animal 4: 1037-1056, 2010.*

As discussed above, the electroneutral transport of NaCl (116, 217, 218) requires not only the apical uptake via NHE coupled to an anion exchanger: efflux, too, has to be electroneutral. Accordingly, a basolateral conductance for Cl^- has been postulated (4, 70). We have recently characterized the underlying channel (349, 360).

6.9.1 The large-conductance anion channel of the rumen

Patch-clamp experiments with isolated rumen epithelial cells show large-conductance channels permeable not only to Cl^- (~350 pS), but also to HCO_3^- (~120 pS), $acetate^-$ (~140 pS), and $propionate^-$ (~110 pS), with conductance for $butyrate^-$ being significantly lower (360).

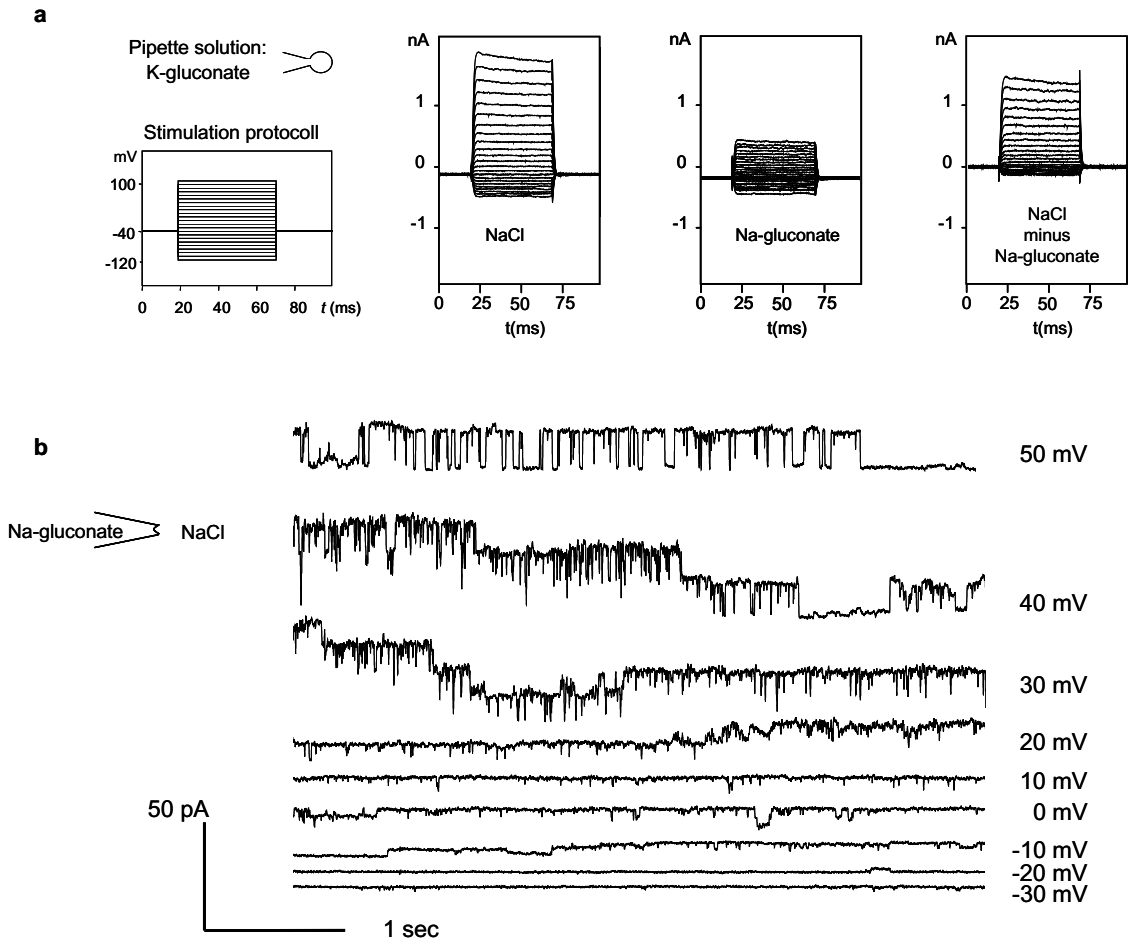

Figure 27: The ruminal anion channel. a) Original whole cell recording of a ruminal epithelial cell filled with a Na-gluconate solution and superfused with NaCl solution. Currents are outwardly rectifying and can be reduced by removal of chloride. The residual current probably reflects some membrane "leak" and the passage of Na^+(in) and K^+ (out) through the non-selective cation channel. The difference between the currents measured in NaCl and Na-gluconate solutions reflects the influx of chloride into the cell. b) Membrane patch in the outside-out configuration. Large channel events could be seen that declined with pipette potential in a manner suggesting that chloride was moving into the pipette from the bath. The channels were sensitive to the removal of chloride and to application of the anion channel blocker DIDS and could be fitted with the Goldman-Hodgkin-Katz equation for two anions, yielding a channel conductance of 350 pS in symmetrical 130 $mmol \cdot l^{-1}$ solution.

A basolateral conductance for anions can be argued to lead to a large effect of potential on the flux of anions across the tissue. However, this is not so. Both Cl^- and K^+ channels may contribute to the low basolateral resistance of the epithelium, which will typically only account for 30% of the total transcellular resistance ((189, 198) and own observations). An applied transepithelial potential will therefore mostly affect the potential across the apical membrane and thus have only a small impact on the efflux. Furthermore, since uptake is electroneutral and most likely represents the rate-limiting step, any effect of potential on transport will be small (192, 321, 322, 343).

Notably, the influx of chloride from the plasma into the tissue is prevented by the low potential of the basolateral membrane, which, at -70 mV, equals the Nernst potential for a configuration with Cl_{ex} = 105 mmol·l^{-1} and Cl_{int}= 7.6 mmol·l^{-1}. Unless intracellular chloride drops below this value, chloride will move out of the cytosol into the blood through the channel.

6.9.2 Sensitivity to blockers

At positive potentials, the conductance was highly sensitive to DIDS (200 μmol·l^{-1}). However, at negative potentials, blocking effects dropped dramatically in a classical potential-dependent manner (87). The channel could also be blocked by pCMB (1 mmol·l^{-1}). Interestingly, this mercurial derivative was found to have a negative impact on the absorption of SCFA when applied to the basolateral membrane of caprine rumen *in vivo* (173). The authors of this study (173) attributed this effect to a block of basolateral MCT; however, the effects observed may equally be related to a block of the basolateral anion channel.

Nitrate (10 mmol·l^{-1}) did not interact negatively with chloride; instead, both anions appeared to be able to permeate the channel without negative interference. The channel could not be blocked by glibenclamide (100 μmol·l^{-1}), arguing against an identity with CFTR. In line with this, cAMP had no effect either on the chloride conductance of ruminal epithelial cells (44) or on the chloride transport across the epithelium (110, 393).

6.9.3 Potential dependence and the three state gating model

Based on Boltzman statistics and a three state gating model, the voltage dependency of the open probability of the single-channel data could be fitted with a bell-shaped curve (360). The model suggests that the gating of the channel occurs via a charged particle localized in the middle of the channel. This particle moves at de- and at hyperpolarization, occluding the internal or external channel mouth, respectively. The derived equation gives a better fit of the experimental data than the simple two-state Boltzman model that has been used to fit the kinetics of other channels with a bell-shaped voltage dependency in the past (58, 106). These models cannot be used to fit the data over the entire voltage range and thus ignore the possibility that the gating

charge is asymetrically localized within the channel pore. The proposed model (360) gives a more detailed description of channel kinetics than conventional models and should also be of use for the description of other channels with a similar voltage dependency.

In the model, a charged particle with gating charge *n* lies within the channel pore. At 0 mV, the channel is open. When a negative voltage is applied, the charged gating particle moves along the field until it obstructs one end of the pore, and the channel is closed, thus changing from the open state P_o to an initial closed state $P1_c$. When a positive voltage is applied, the gating charge will move in the opposite direction until it obstructs the pore at the other end and the channel is in a second closed state $P2_c$.

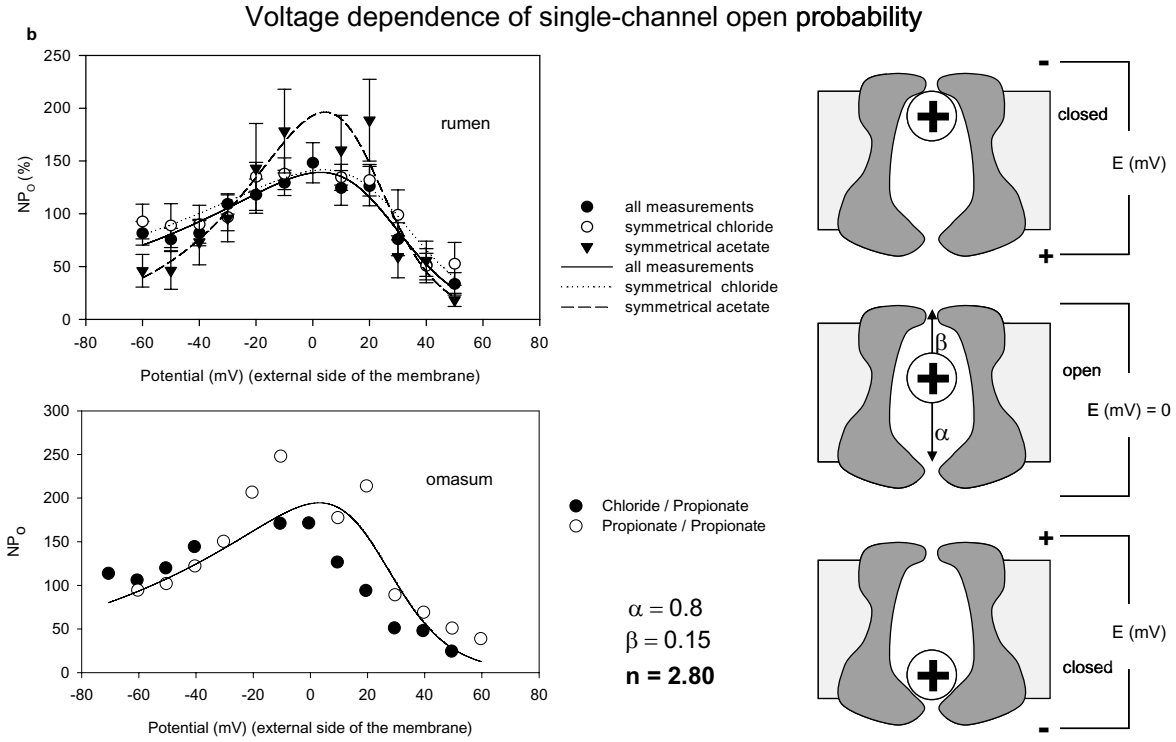

$$NP_O\,(\%)(E) = \lambda \cdot 1/[\exp(\alpha \cdot \mathbf{n} \cdot q_e \cdot E/(k_b \cdot T)) + 1 + \exp(-\beta \cdot \mathbf{n} \cdot q_e \cdot E/(k_b \cdot T))]$$

Figure 28: The voltage dependence of the open probability of the anion channel. The voltage dependence of the anion channel can be fitted with a three state gating model. The model assumes that a particle is located in the middle of the pore of the channel with a gating charge n. This particle can move within the pore to obstruct either the external or the internal mouth of the channel. The probability that the particle is in the middle position (open) is highest when no voltage is applied. The probability of finding the particle in a closed state rises with the voltage applied. No significant differences can be seen when single-channel data from measurements of the rumen or the omasum are fitted with the model, suggesting that both tissues express the same channel protein.

If a charged particle moves within a potential, the energy gained will be equal to the charge (in Coulomb) multiplied by the potential difference. If the charge moves along a fraction α of the total length of the pore in order to move from state P_o to $P1_c$, the energy difference between these two states will be proportional to the charge multiplied by the potential difference between the two states, or $\alpha \cdot n \cdot E \cdot q_e$ where E is the potential across the entire membrane, $\alpha \cdot E$ represents the fraction of the total potential that lies between the open and the closed state, and q_e is the elementary charge, while $n \cdot q_e$ represents the total charge of the gating particle. Since other potential independent interactions might hold the particle in place, a further voltage-independent term $w \cdot (k_b \cdot T)$ has been added to this energy, where k_b is the Boltzmann constant and T is the temperature. According to Boltzmann theory, the probability of finding the particle in this first open state $P1_c$ versus the probability of finding it in the closed state can be calculated from the energy difference between the two states $P_o/P1_c = \exp(w - \alpha \cdot n \cdot E \cdot q_e/(k_b \cdot T))$ (146). By analogy, $P_o/P2_c = \exp(v + \beta \cdot n \cdot E \cdot q_e/(k_b \cdot T))$ (where v is voltage independent and β designates the fractional distance between P_0 to $P2_c$). The probability that the channel is open will thus be given by

$$P_o/(P1_c+P_o+P2_c) = 1/[\exp(-(w - \alpha \cdot n \cdot E \cdot q_e/(k_b \cdot T)))+1+\exp(-(v + \beta \cdot n \cdot E \cdot q_e/(k_b \cdot T)))]$$

This function gives a bell-shaped curve and can be used to fit the experimental data, allowing a determination of the unknown constants in the equation. The gating charge appears to be asymetrically localized within the channel pore, thus resulting in a higher open probability of the channel at depolarized membrane voltages (= negative pipette potential in the inside-out configuration). The voltage-independent terms do not contribute substantially to the gating behavior.

6.9.4 Halide selectivity sequence

The permeability sequence for halides suggests that the anions have to be stripped of their hydration shell before passing through the channel pore and thus follow an Eisenman-I permeability sequence (356). No negative interactions could be seen when chloride and nitrate were both applied; unlike the many anomalous mole fraction effects observed with the non-selective cation channel and the potassium channels of the ruminal epithelium, any deviations in the passage of anions through

the ruminal anion channel were small. Although the selectivity of the channel for the various anions was poor, the channel appeared to be extremely selective for anions over cations.

The large conductance and its bell-shaped voltage dependency (360) bear a striking resemblance to the maxi-anion channels that are thought to play an important role in the flux not just of chloride, but also of much larger anions across the membranes of a multitude of tissues (29, 293). Although their molecular identity is obscure, these channels are functionally well-characterized and clearly distinct from other members of the chloride channel family. However, their functional significance is currently poorly understood. It is not unreasonable to suggest that the discovery and characterization of this channel in the ruminal epithelium represents a step forward both in the understanding of the passage of SCFA across the rumen and in an understanding of the roles that these amazingly large channels play in nature.

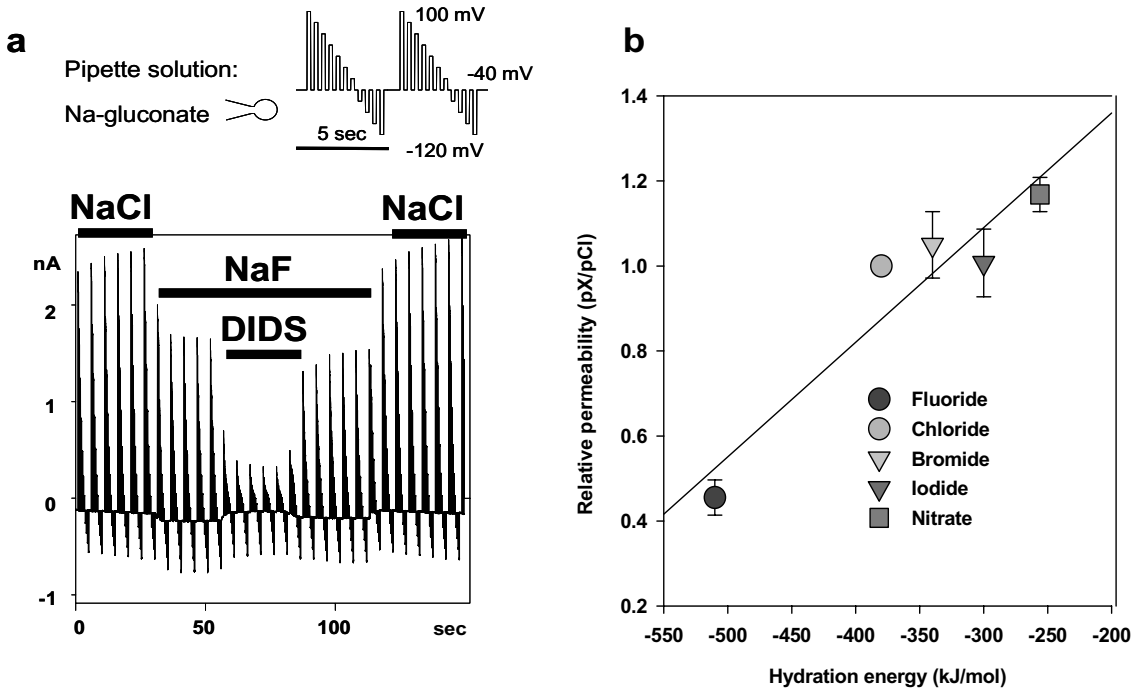

Figure 29: Permeability to halides. a) Currents mediated by halides were sensitive to DIDS (200 $\mu mol \cdot l^{-1}$). b) A weak correlation was detected between the permeability ratio versus chloride and the hydration energy, suggesting that the permeability of the channel to smaller anions is determined by the energy necessary to remove the hydration shell (channel with weak field binding site). The permeability to larger organic anions was smaller than to be expected from their hydration energies, suggesting steric interactions with the channel pore.

6.9.5 Permeability of the ruminal anion channel to the anions of SCFA

Both whole cell and single-channel experiments clearly demonstrate the permeability of the ruminal anion channel to the anions of SCFA, with the permeability ratio dropping with increasing chain length. Conductances could be blocked by DIDS and pCMB. Permeability to butyrate was low.

In the whole cell configuration, all experiments were performed in solutions containing symmetrical concentrations of Na^+. Changes in reversal potential following the replacement of chloride with SCFA anions could therefore not have been caused by a change in the permeability of the non-selective cation channel. Permeability ratios were calculated from the reversal potentials and were clearly lower than to be expected on account of the hydration energies. We suggest that with increasing chain length, steric interactions with the channel pore occur and limit permeability.

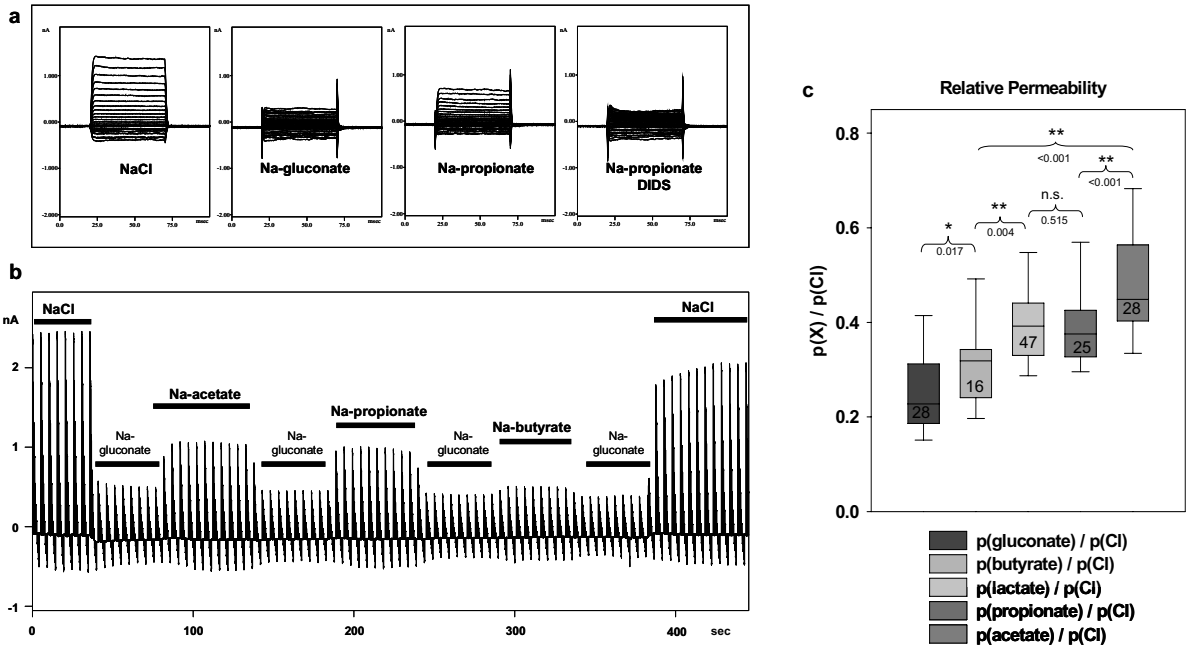

Figure 30: The anion channel of the ruminal epithelium is permeable to the anions of SCFA. a) Original recording showing a ruminal epithelial cell in the whole cell configuration of the patch clamp technique. Currents could be induced by acetate$^-$, propionate$^-$ and butyrate$^-$. b) Reversal potentials were significantly lower in solutions containing Cl^- or $SCFA^-$ anions than in gluconate solution. Relative to chloride, permeability increased with decreasing chain length. No correlation with the hydration energies was observed, suggesting steric interactions with the channel pore.

Single-channel experiments confirm the data from whole cells. The majority of the excised patches showed no channel activity. In a minority of patches, large single-channel events could be observed, the size of which changed with the dominant

anion in the bath. In symmetrical chloride solution, the channel had a large conductance of ~ 350 pS, the size of which dropped to ~ 140 pS in acetate solution. In propionate solution, conductance was ~ 100 pS (356, 360).

The permeability sequence of this channel may explain why acetate and propionate pass into the blood, whereas the larger butyrate anion is retained and extensively metabolized (181, 229). Similar patterns are observed in all parts of the gut, and physiologically, butyrate might play important roles in epithelial function, serving as a source of energy and stimulating proliferation (289).

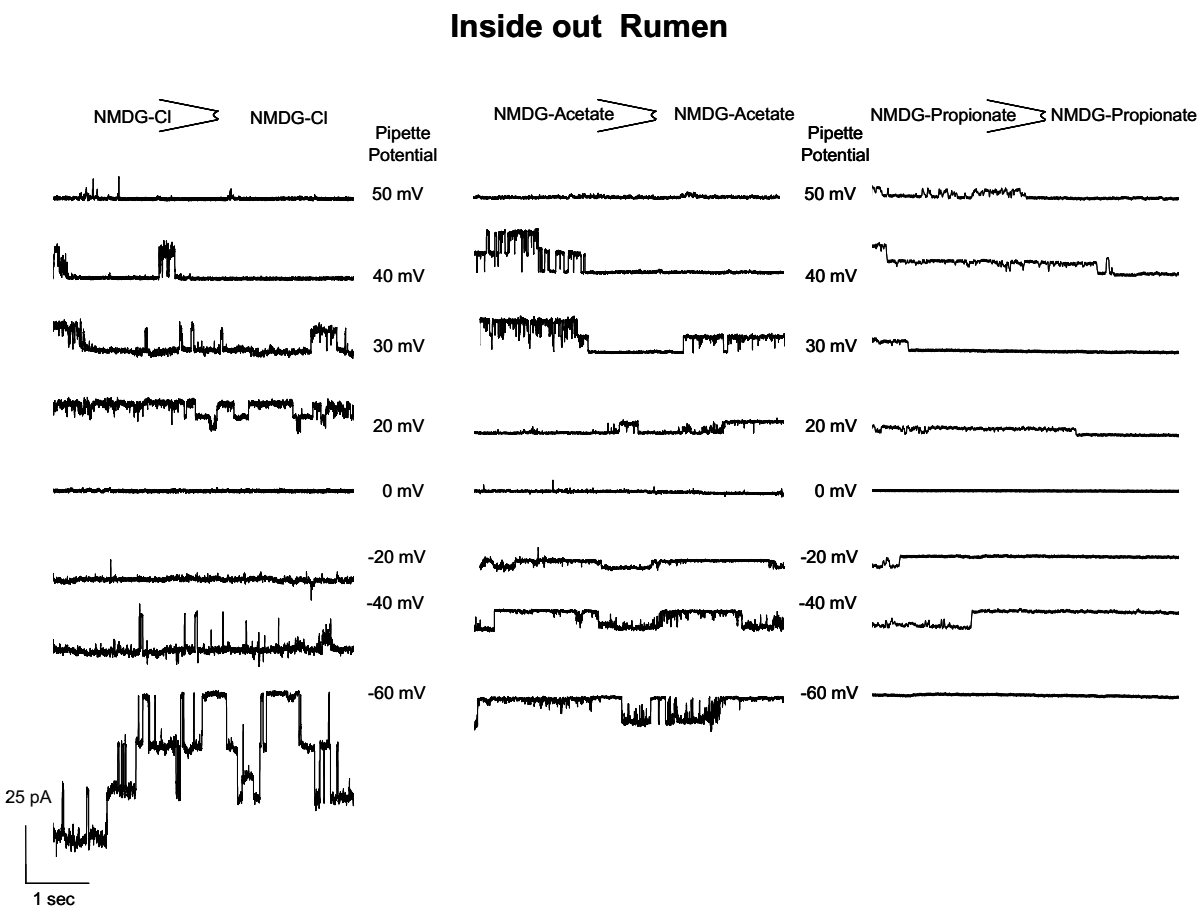

Figure 31: Single-channel recordings showing a conductance for chloride$^-$, acetate$^-$ and propionate$^-$. Original recordings of three membrane patches of the ruminal epithelium in symmetrical solutions, showing large-conductance channels with permeability to chloride$^-$ (350 pS), acetate$^-$ (140 pS), and propionate$^-$ (100 pS). The size of the channel openings changed with the dominant anion in the bath, but were not responsive to changes in the dominant cation, suggesting a high selectivity for anions over cations.

6.9.6 Interactions of SCFA with the non-selective cation channel of the rumen

It has been mentioned that when SCFA were applied to ruminal epithelial cells in the whole cell configuration, some (but by no means all) cells showed a pronounced and

variable stimulation of sodium and potassium conductances (360), in analogy to similar effects observed in cells of the colonic crypt (68, 69, 306). The reason for the activation is unclear; most likely, the perfusion of these cells with buffering pipette solution was incomplete so that the cells were acidified by the exposure to SCFA. Corresponding to this assumption, the activation of the non-selective cation conductance appeared to occur more frequently with the more lipophilic propionate and butyrate solutions; but further work is necessary to identify the signaling cascade. Interestingly, exposure to SCFA has been seen to increase significantly the short-circuit current through the ruminal epithelium in the Ussing chamber (3, 116); as in the patch clamp experiments, the effect is not consistently observed.

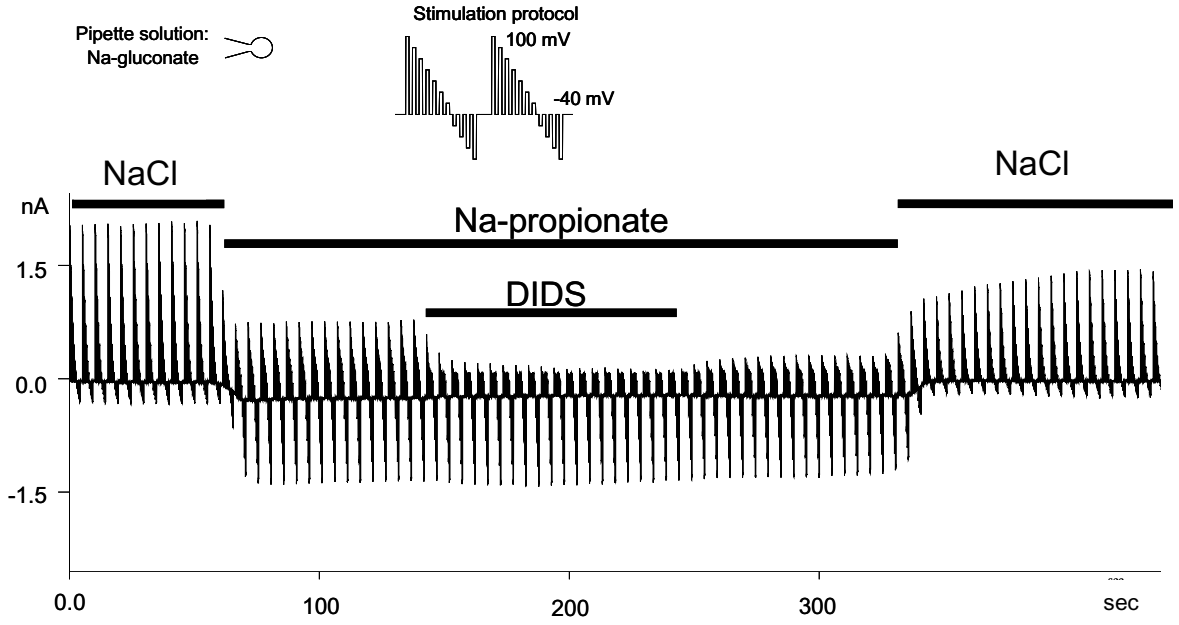

Figure 32: The interaction of SCFA with the non-selective cation channel of the ruminal epithelium. In certain cells, activation of non-selective cation channels could be observed following the exposure to SCFA. In the cell shown, exposure to propionate induces a dramatic and reversible rise in inward current that is not sensitive to DIDS and probably reflects an influx of Na^+ through the ruminal non-selective cation channel. The DIDS-sensitive outward current clearly reflects $propionate^-$ entering the cell.

6.9.7 The large-conductance anion channel of the omasum

Patch-clamp experiments with the whole cell technique show that the omasum expresses a DIDS- and pCMB-sensitive conductance with properties closely resembling that of the rumen ($p(Cl^-) > p(acetate^-) > p(propionate^-) >> p(gluconate^-)$).

The single-channel conductances of the omasal anion channel for chloride (~350 pS) and propionate (~100 pS) are not significantly different from those of the rumen (355).

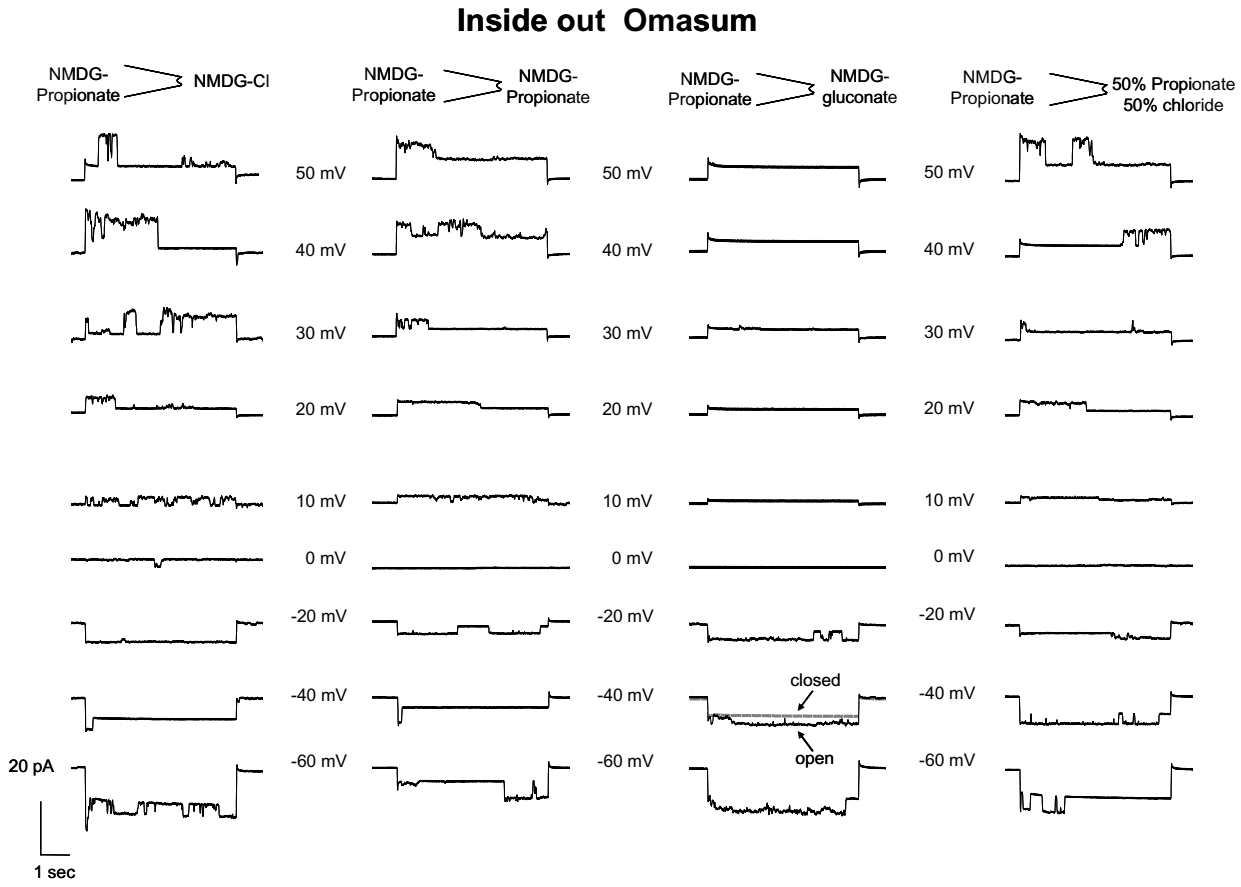

Figure 33: The anion channel of the omasum. Original recording from one membrane patch of an omasal cell showing a large-conductance channel. The size of the channel events changed with the dominant anion in the bath. Data could be fitted with the current equation of Goldman-Hodgkin-Katz theory. In particular, a mix of two anions did not show anomalous mole fraction effects, suggesting that the ions pass rapidly through the channel pore with little or no interaction or interference. Whole cell and single-channel data suggest that the omasum expresses the same large-conductance DIDS-sensitive anion channel as the rumen with $p(Cl^-) \sim 350$ pS, $p(acetate^-) \sim 140$ pS, and $p(propionate^-) \sim 100$ pS.

6.9.8 A model for the efflux of SCFA from the forestomachs

SCFA are widely believed to cross the forestomach epithelia by “lipid diffusion”. However, in its simple form, this assumption contradicts past and present *in vitro* and *in vivo* research, since the removal of protons from the rumen does not occur on a 1:1 basis with SCFA. Thus, the pH of the rumen has to be maintained via secretion of buffers with saliva, which remove large quantities of protons from the rumen. This clearly argues against a model in which the absorption of a proton is required for every SCFA removed from the rumen. We present a model for the efflux of SCFA from forestomach epithelia that resolves this contradiction.

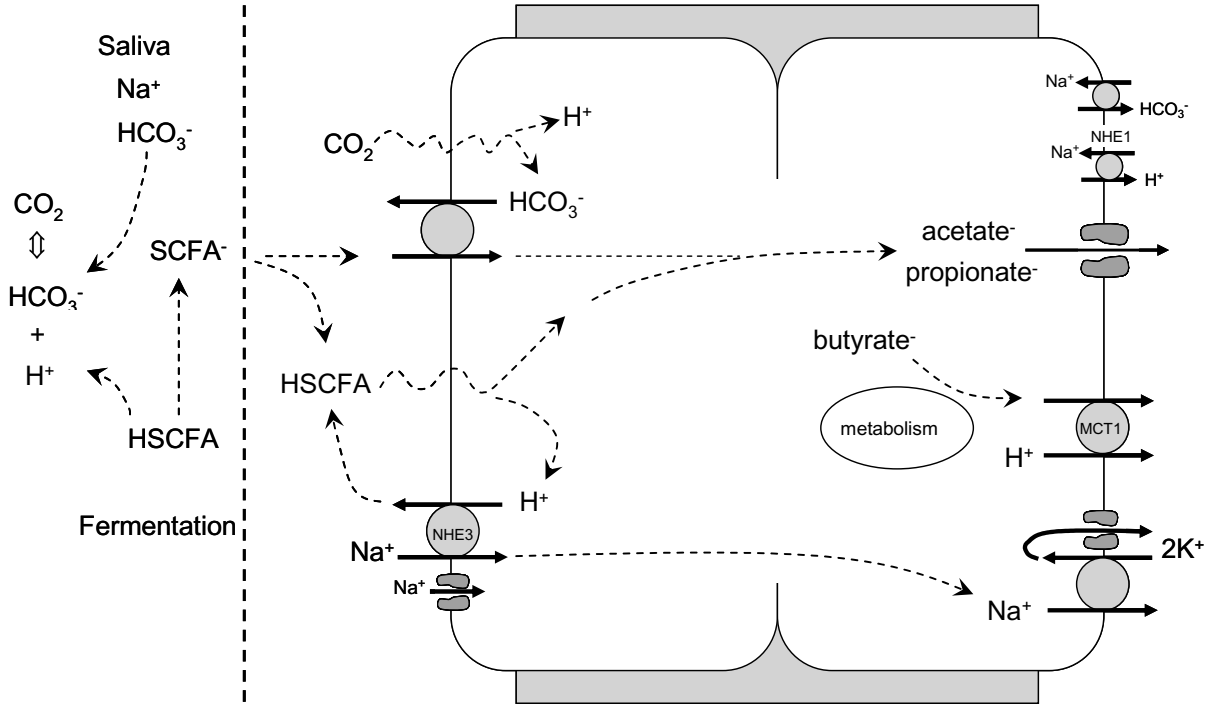

Figure 34: A model for the transport of SCFA across forestomach epithelia. Uptake of SCFA occurs via diffusion of the protonated form (HSCFA) or in exchange for HCO_3^- via an apical anion exchanger. Both pathways lead to an acidification of the cytosol and to an accumulation of $SCFA^-$ anions within the cytosol. The protons are eliminated apically in exchange for Na^+. Since basolateral efflux of Na^+ via the Na^+/K^+-ATPase is electrogenic, the efflux of SCFA anions, too, has to be electrogenic to balance the charge. The model explains the experimental finding that the uptake of $SCFA^-$ and of Na^+ from the rumen are closely correlated, whereas the secretion of HCO_3^- with saliva is essential for the removal of fermentation acids from the rumen. The model does not require an acidification of the cytosol or an accumulation of anions to drive the efflux of SCFA.
However, in situations where salivary secretion of buffer is insufficient, protons will enter the cytosol, and additional epithelial transport proteins must be expressed if epithelial damage is to be prevented. Basolateral NHE and basolateral Na-HCO_3 are prime candidates for the basolateral elimination of protons or the uptake of a base in this situation. Since both transporters lead to an influx of Na^+ into the cytosol which has to be removed electrogenically via the basolateral pump, the efflux of SCFA through the channel again occurs down the potential gradient in a secondary active manner.
The model also helps to explain why the basolateral efflux of butyrate is so low: since the permeability of the channel to butyrate is poor, this SCFA should leave more slowly, allowing time for an extensive metabolization by the epithelium.
The model suggests that monocarboxylate transporter 1 (MCT1), which requires protons to drive efflux, only plays a minor role in the efflux of $acetate^-$ and $propionate^-$. However, the protein probably plays major roles in the efflux of larger organic anions.

The influx of SCFA occurs together with a proton, with the relative contribution of the diffusive uptake of HSCFA or uptake via anion exchange being complexely regulated by factors that have as yet to be fully understood. The rate of influx strongly depends on the pH of a microclimate that is presumably located within the stratum corneum. The proton taken up with the influx of SCFA is apically removed in exchange for sodium via NHE. The basolateral efflux of $SCFA^-$ anions occurs through a large-conductance anion channel. Driven by the potential generated by the Na^+/K^+-

ATPase, the efflux of the anions of SCFA through this channel should represent a highly efficient, non-saturable pathway for the basolateral efflux of SCFA.

Since permeability to this pathway decreases with increasing chain length, butyrate predictably accumulates within the tissue, where it is extensively metabolized into substrates that may leave via MCT1 (182, 240).

In summary, we present a new model for the transport of $SCFA^-$ by the rumen and the omasum, a model that explains the well-known interactions of SCFA with the transport of Na^+ (15, 360). Unlike earlier models, the clinical observation that ruminal content has to be extensively buffered by the influx of saliva to prevent ruminal acidosis is incorporated into our model. Based on the low selectivity of the proteins that mediate the transport of anions in this tissue and others (395), transport can occur via a mechanism that closely resembles the classical and well-established electroneutral, functionally coupled uptake of NaCl by absorptive epithelia (39, 299).

7 Discussion

It was the purpose of this study to characterize the conductances of isolated cells of the ruminal epithelium. During the course of the study, it increasingly emerged that understanding these conductances and their regulation has profound implications for our understanding of ruminal transport processes in general.

7.1 The apical non-selective cation conductance of the ruminal epithelium

Over 50 years ago, it was observed that the absorption of sodium from the rumen increases with rising concentrations of potassium, which is of major importance for the regulation of ruminal osmolarity (76, 79, 159, 235, 316-318, 324, 386). A decade ago, it was discovered that the the stimulation of sodium transport across the rumen is potential-dependent (189). Since then, considerable progress has been achieved: the characterization of the ruminal sodium conductance using the patch clamp technique followed (199), suggesting an identity with channels of the TRP family, members of which have more recently been identified in the ruminal epithelium (311, 390, 391). The functional characterization of these channels has also led to other insights: we now know that the channels are gated by extracellular and intracellular divalent cations and can understand why the depolarization of the tissue opens the channels. The patch clamp data suggest that the conductance roughly follows an Eisenman-I permeability sequence dominated by the energy necessary to remove the hydration shell. Apart from Na^+, these channels thus also conduct K^+, NH_4^+, Ca^{2+}, Mg^{2+}, and possibly also other trace metals, albeit with differing permeabilities.

7.1.1 Sodium, magnesium, and the potassium homeostasis of the ruminant

Because of the blocking effects of divalent cations on the non-selective cation channel, the efflux of potassium from the cells both in the whole cell configuration of the patch-clamp technique (4, 199) and in the rumen *in vitro* and *in vivo* is small. This, of course, is of fundamental clinical significance: a large apical “leak” of potassium, driven by the basolateral pump, into the huge 100 l cavity of the bovine rumen might severely affect the potassium homeostasis of the animal.

When the animal ingests fodder with a high potassium content, ruminal potassium concentrations rise. The small efflux of potassium from the apical membrane decreases, resulting in a depolarization of the apical membrane. The potential will repell blocking Mg^{2+} and Ca^{2+} ions from the channel mouth, and the conductance for monovalent cations increases, resulting in a further depolarization of the apical membrane with a further relief of the divalent block. The consequence of this depolarization is a decrease in the uptake of Mg^{2+} via electrogenic mechanisms; this limits the digestibility of magnesium (302, 388) and can cause the clinical symptoms of grass tetany (225).

This reduced digestibility for magnesium may be of secondary importance, since in most feeding situations, the restoration of osmolarity will represent a more pressing issue. Since the influx of Mg^{2+} into the channels is prevented by the depolarized

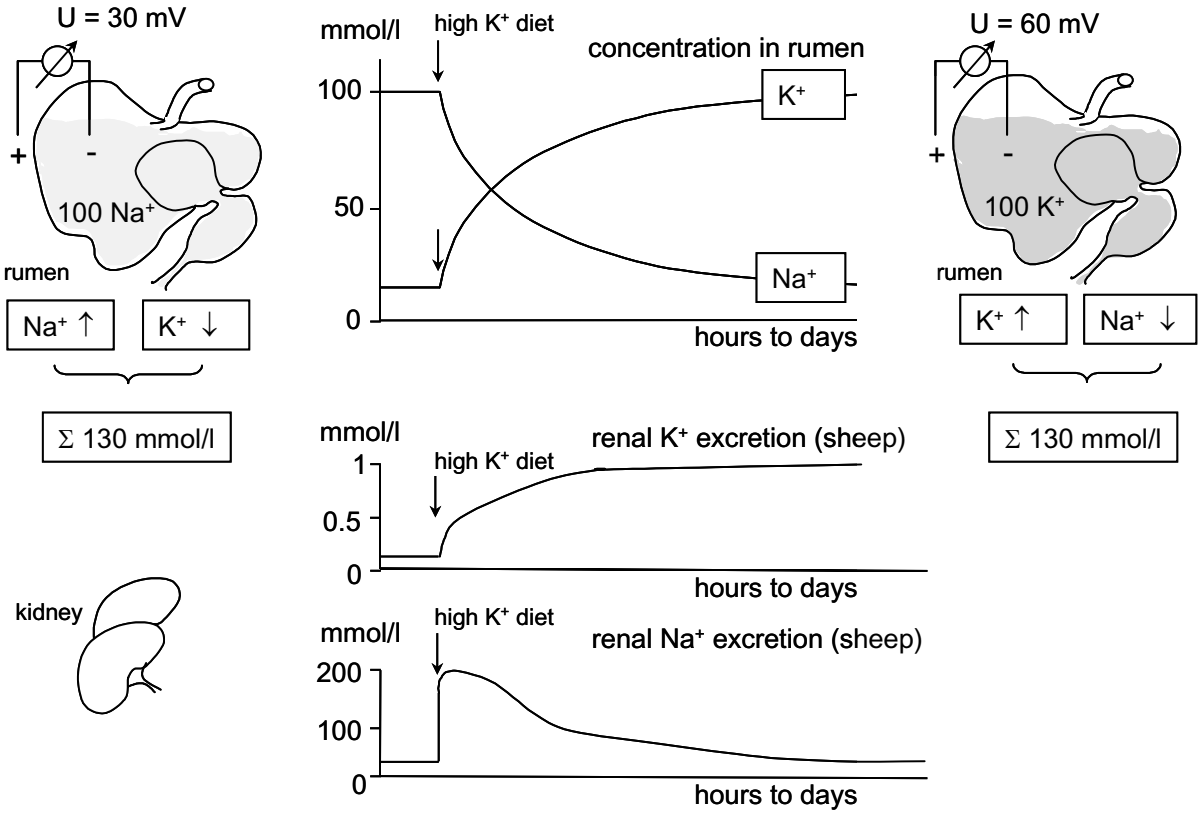

Figure 35: The potassium homeostasis of the ruminant. Stimulation of Na^+ absorption from the rumen has important consequences for the ruminant *in vivo*. When sheep are transfered from a low potassium diet (i.e., hay) to a high potassium diet (i.e., grass), the concentration of potassium in the rumen continues to rise for a period of several hours to days (76, 79, 159, 235, 316-318, 324, 386). Concomittantly, the ruminal concentration of sodium falls, so that the sum of both ions remains constant, and ruminal osmolarity is restored. *In vivo* measurements show that the transepithelial potential increases with the concentration of potassium (101, 159, 318, 324). Simultaneously, sodium excretion in urine peaks, whereas potassium excretion rises more slowly until maximum values are observed after about a week (266-269, 363). The digestibility of magnesium drops (302, 388).

potential of the cells, sodium ions can flow through the Mg^{2+}-free channels into the cytosol, driven by the concentration gradient, from where they are basolaterally extruded via the Na^+-K^+-ATPase. Osmolarity in the rumen decreases.

The mechanism might also be useful in the maintanance of potassium homeostasis. With every $3Na^+$ ions absorbed, $2K^+$ ions will be pumped back into the cytosolic space. Any efflux of potassium from the rumen will thus be limited. This model explains why the transport of sodium from the rumen increases with rising concentrations of ruminal potassium (351, 358, 359), whereas the efflux of K^+ from the organ is limited by the activity of the pump and the corresponding potential *in vivo* (101, 159, 318, 324) and *in vitro* (198, 215).

The accumulation of potassium in the rumen may be of functional significance, since it will delay entry into the blood and, thus, give the animal more time to adapt to an increase in intake. Ruminants have to be able to tolerate extremely high variations

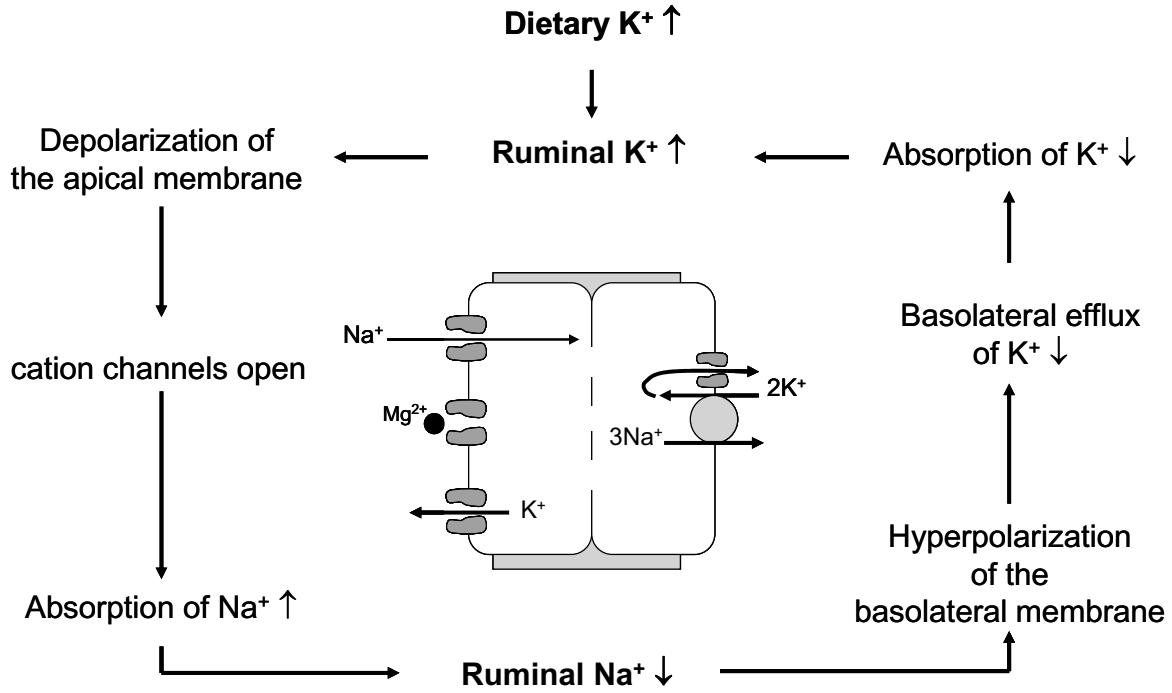

Figure 36: Model of the stimulation of sodium absorption from the rumen by the elevation of ruminal potassium. An increase in the uptake of potassium with the diet increases the concentration of potassium in the rumen. This leads to a depolarization of the apical membrane and reduces the block of the channel by divalent cations from the outside. The open probability of the non-selective cation channel increases, and more sodium can flow into the tissue and out at the basolateral membrane. This leads to a hyperpolarization of the basolateral membrane and reduces the driving force for the efflux of potassium. The absorption of Na^+ from the rumen rises, while K^+ remains within. The animal is thus given time to adjust renal excretion of K^+ to the level of uptake. A detrimental side effect is the reduction in the uptake of Mg^{2+}.

in K^+ uptake from 3.8 mmol·kg^{-1}·day^{-1} to almost 20 mmol·kg^{-1}·day^{-1} (270, 319). In comparison, the upper limit of daily voluntary human potassium intake is 1.4 mmol·kg^{-1}·day^{-1} (128). As in man, the excretion of K^+ by the kidney is under the control of aldosterone, and typically, adaptational responses will take hours or even days (266-269, 363). During this period, the rumen appears to serve as an additional space for the redistribution of K^+.

Thus, with due caution, we can state that, within a decade after work on the voltage-dependent sodium conductance of the rumen began, we know how this voltage dependence comes about, what proteins are involved, and why a mechanism that leads to such profound disturbances in magnesium homeostasis may nevertheless lead to a selective advantage for animals that express it.

7.2 Urea, ammonia and pH homeostasis

Postprandially, ruminal ammonia concentrations peak, while ruminal pH drops (193, 275, 276, 365). The rapid absorption of ammonia from the rumen that is observed in this situation has long been suggested to require pathways other than the classical diffusive efflux of NH_3. The uptake of ammonia as NH_4^+ has been discussed over many years (34, 36-38, 120-123, 236, 262, 329), but evidence showing that NH_4^+ can permeate channels in the cellular membrane of ruminal epithelial cells cannot be obtained on the basis of whole-tissue approaches and requires the study of cellular membranes in isolation via the patch-clamp technique.

The characterization of the conductances of ruminal epithelial cells for NH_4^+ has led to a model of the ruminal absorption of ammonia that helps to understand how absorption of ammonia across the ruminal wall occurs at low ruminal pH (4). The negative correlation between the ruminal concentrations of Na^+ and ammonia *in vivo* follow (235). It is now also possible to understand why SCFA have a positive impact on the absorption of ammonia (37, 262, 276). Last, but certainly not least, the efflux of ammonia from the rumen as NH_4^+ has important consequences for the maintanance of both ruminal and cytosolic pH, with implications for the functional significance of urea recycling in the ruminant (2).

7.2.1 The non-selective cation channel as a pathway for the apical uptake of NH_4^+

During the course of this study (4), isolated cells of the ruminal epithelium have been shown to express at least two different types of channels with a permeabilty to NH_4^+: channels that are highly selective for K^+ and NH_4^+, with no significant permeability to Na^+, and non-selective cation channels with a high conductance for various different cations, including NH_4^+. These findings clearly suggest that apical entry of NH_4^+ into the ruminal epithelium occurs through the same non-selective cation channels that mediate electrogenic Na^+ transport across the ruminal epithelium and that most likely belong to the TRP family. These channels open when the tissue is depolarized and should thus be ideally suited to mediate an increased efflux of NH_4^+ after a meal, since both the rise in NH_4^+ per se and the concomittant postprandial increases in the concentration of K^+ will depolarize the tissue and open the channel. In addition, the acidification of the cytosol by the postprandial rise in SCFA might increase the open probability of these channels (2, 360) and facilitate the rapid postprandial efflux of ammonia from the rumen (276, 365). The existence of further apical conductances with a permeability to NH_4^+ cannot and should not be excluded.

7.2.2 The basolateral K^+ channel as a pathway for the efflux of NH_4^+

Both the Ussing chamber data and the patch-clamp data of our study (4) clearly support an efflux of ammonium in the form of the charged ion (NH_4^+) through a channel with high permeability to K^+. The view that the ruminal epithelium expresses basolateral potassium channels for the recirculation of K^+ from the Na^+/K^+-ATPase (101, 103, 141, 142, 198) is backed by very solid evidence. Likewise, the notion that NH_4^+ can permeate K^+ channels (55, 134, 147) can be seen as classical. Ussing chamber data back the notion that a significant proportion of NH_4^+ crosses the basolateral membrane in the protonated form through potassium channels (4, 34). An additional efflux in the form of NH_3 remains a possibility at high levels of cytosolic pH, but this is probably self-limiting as the epithelium will be increasingly acidified if this manner of efflux prevails, so that cytosolic concentrations of NH_3 will drop.

7.2.3 The interactions between ammonia and ruminal Na^+ and H^+ transport

The interactions between ammonia transport and NHE can be explained by using the models outlined in Figures 24 and 37. At non-physiologically high mucosal pH (> 7.0), ammonia primarily enters as NH_3, which is protonated to NH_4^+ within the cytosol, thereby reducing the need for an apical extrusion of protons via NHE (4, 6). Na^+ absorption from the rumen is therefore reduced in this situation. At a more physiological mucosal pH (< 6.8), the uptake of NH_4^+ exceeds the uptake of NH_3. Within the cytosol, NH_4^+ will partially dissociate, forming NH_3, which can diffuse back into the lumen, resulting in an apical recycling of ammonia (in as NH_4^+, out as NH_3). Considerable amounts of protons can be transferred from the rumen into the epithelium by this mechanism, most of which will, however, be removed apically via NHE (4). Accordingly, the absorption of Na^+ from the rumen is stimulated, explaining *in vivo* observations that show a strong negative correlation between ruminal ammonium and Na^+ concentrations (235). This mechanism may thus support ruminal osmoregulation. Interestingly, the relative contribution of ammonia efflux as NH_3 or as NH_4^+ changes with dietary stimuli in a manner that facilitates the efflux of protons via NH_4^+ in animals on high energy and high protein diets (6), suggesting that the uptake of ammonia might also play a role in pH homeostasis.

The form in which basolateral efflux occurs, as NH_3 or NH_4^+, will ultimately determine the impact of ammonia on the pH of both the rumen and the cytosol of the epithelium. If efflux occurs without a proton as NH_3, ammonia will increase the uptake of protons into the epithelium without contributing to a subsequent removal and will therefore have an acidifiying effect on the cytosolic compartment. If, however, the basolateral efflux occurs in the protonated form as NH_4^+, a mole of protons will be removed from the rumen with every mole of ammonia entering the portal circulation. In this context, it may be mentioned that the portal fluxes of ammonia can reach 25 mol·day^{-1} in dairy cattle (65), so that up to one third of fermentation acids can potentially be removed via this pathway. An efflux of $SCFA^-$ anions through a basolateral anion channel should facillitate the basolateral efflux of ammonia as NH_4^+ via charge coupling, which may explain the classical observation that the absorption of ammonia is stimulated by SCFA (37, 262, 276).

In addition to providing the nitrogen needed for microbial protein synthesis, ruminal ammonia might thus represent a powerful buffer binding and removing protons as NH_4^+. A note of caution has to be added, however: if concentrations become too high, toxic effects are to be expected.

7.2.4 Urea, ammonia, and pH homeostasis

Whereas evidence that the ruminal epithelium expresses UT-B has been available for some time (212, 213, 282, 283, 345), it has been more difficult to prove that this protein is functionally expressed (71, 209, 212, 259). It has long been known that urea flux to the rumen is maximal postprandially, when ruminal pH is low and the concentrations of SCFA and CO_2 are high (140, 164, 366, 374). Furthermore, urea secretion is inversely correlated to the concentration of ruminal ammonia (140, 164, 165, 276). Our recent functional study clearly shows that these effects are not mediated by changes in blood flow (2, 207). Thus, urea does not simply "leak" into the rumen but is secreted via specifically regulated proteins that provide endogenous nitrogen for microbial protein synthesis in a manner synchronized with the dietary availability of carbohydrates and nitrogen.

However, another aspect merits some deliberation. As mentioned above, up to 10 $mol \cdot day^{-1}$ of urea can be recycled to the rumen in the bovine species (130, 140, 155, 277), an amount that greatly exceeds the requirements of microbial populations. Urea not utilized will be converted to CO_2 and $2NH_3$. NH_3 is protonated and, at the low ruminal pH seen postprandially when urea fluxes into the rumen rise, is transported across the epithelium into the portal blood as NH_4^+. Potentially, up to 20 $mol \cdot day^{-1}$ of protons can be removed from the rumen via this mechanism. The stimulation of urea flux into the rumen in response to the postprandial rise in fermentational products at physiological pH should thus be seen not only in the light of providing nitrogen for microbial protein synthesis (1, 2, 140, 164, 278), but also as a supplemental form of pH regulation[9]. The secretion of even small quantities of urea into the apical microclimate under the stratum corneum will have a profound impact

[9] In this context it is interesting to note that the ability of *Helicobacter pylori* to survive in the gastric environment at very low pH is related to the secretion of urea into a microclimate surrounding the bacterium with subsequent degradation via urease (295).

on stabilizing the pH homeostasis of the epithelium and, thus, contribute to epithelial integrity.

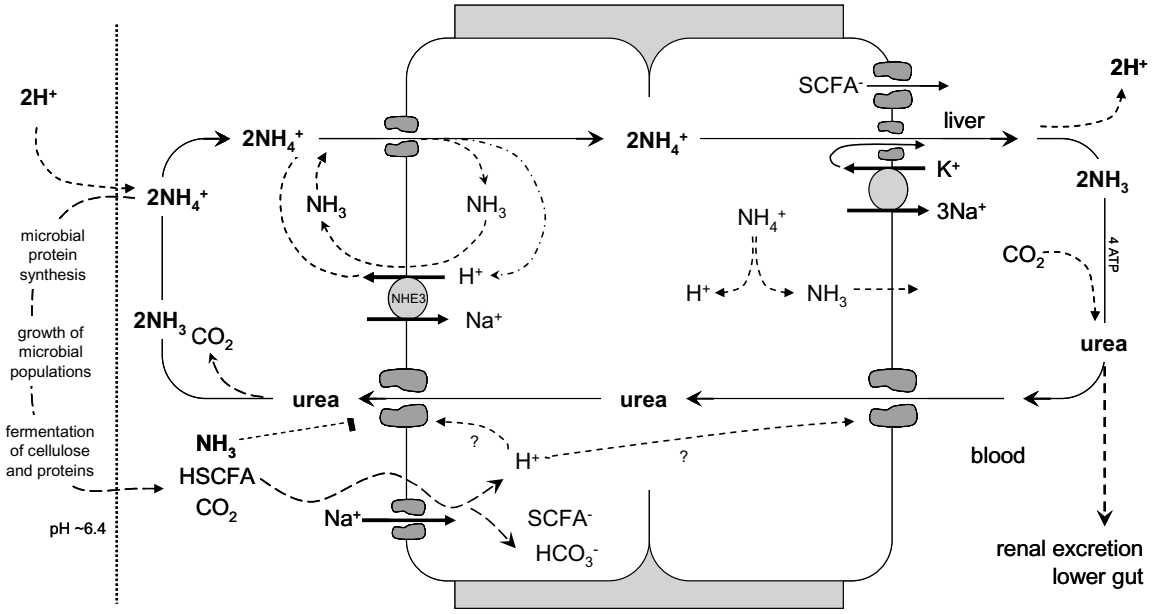

Figure 37: Ruminal recycling of urea and ammonium transport. Fermentational processes acidify the rumen and generate SCFA and CO_2 , which stimulate the secretion of urea into the rumen via a pH-regulated protein (probably UT-B) into the apical microclimate and the rumen itself. Degradation of urea in the stratum corneum releases NH_3, which buffers protons. Ammonia can be used for microbial protein synthesis, thus allowing bacteria to multiply and to ferment available carbohydrates. Excess ammonium is absorbed through the epithelium, removing a proton from the rumen as NH_4^+. When ammonia concentrations are too high, urea secretion is blocked via a mechanism yet to be identified. Urea secretion is also reduced by low mucosal pH (<6.2), possibly linked to the uptake of protons that enter the epithelium with SCFA and CO_2. The reduction of urea secretion will reduce the speed of protein synthesis by ruminal microbial populations, provided that dietary intake of nitrogen is not too high. This will in turn slow down fermentation and the rate at which fermentational acids are produced. The regulation of urea secretion should thus play an important role in the maintanance of ruminal and cellular pH homeostasis.

The inhibition of urea transport may be equally as important as its stimulation. The inhibition of urea transport by ruminal ammonia is well-documented (140, 164, 276) and may serve to prevent the rise of ruminal ammonia to toxic levels. Similarly, the permeability of the rumen to urea drops when ruminal pH is either very high or very low. Our study shows that urea secretion peaks at a mucosal pH of ~ 6.2 (2) and drops again when ruminal pH decreases further. This bell-shaped dependency between urea transport and ruminal pH may be of significant importance to ruminants on the low protein diet of their natural habitats. If carbohydrate intake is low, the decrease in urea transport seen at high values of pH will preserve energy. If carbohydrate intake is high, but nitrogen intake is insufficient, urea nitrogen will fill the gap. However, when ruminal pH drops too low, urea secretion will drop, and ruminal

fermentation will slow down until the pH recovers to a value in the optimal range. The model predicts that feeding diets high in protein will interfere with this mechanism, and thus, our model represents an interesting starting point for further investigations *in vitro* and *in vivo*.

7.3 SCFA and the basolateral anion channel

Arguably, a most striking example for the way in which a study of the ion channels expressed by isolated cells can change the perception of transport across the epithelium is the discovery of the ruminal anion channel.

When work on these cells began, the anion channel initially emerged as a “nuisance” interfering with work on the cation channels of the cells (199). As work commenced, however, it became increasingly obvious that this conductance was not accidental, but that the ruminal transport model could not function without a basolateral channel for the efflux of anions (4). The possibility of a basolateral anion channel had previously been suggested by other authors (37, 70, 321). Nevertheless, interest in the channel only commenced (196) after patch-clamp experiments had clearly demonstrated that it existed (4, 199). At this point, it is clear that this channel has fundamental consequences both for our understanding of ruminal SCFA transport and ruminal buffering of protons (16, 360).

7.3.1 Saliva is needed for ruminal buffering

Nutritionists have long known that the salivary secretion of $NaHCO_3$ is central to the maintanance of ruminal pH homeostasis. The stimulation of salivary flow by providing sufficient amounts of roughage, coupled to the addition of buffers such as $NaHCO_3$ to the diet, continues to be a major strategy in preventing ruminal acidosis and SARA (98, 174, 179, 237, 263). Models assuming that the efflux of SCFA out of the rumen occurs coupled to an equimolar removal of protons – whether via lipid diffusion, or via MCT - cannot explain why ruminal pH is clearly acidic. A transport model for the electroneutral, functionally coupled uptake of Na^+ and $SCFA^-$ across the rumen is urgently needed to explain both *in vivo* and *in vitro* observations and to lead to a clearer understanding of the regulation of ruminal pH and osmolarity in ruminants.

At physiological ruminal pH, the concentration of protons in the rumen only accounts for a very small fraction (< 1%) of the concentration of SCFA. Instead, under most feeding conditions, the dominant cation in the rumen is Na^+, which enters the rumen with saliva and is coupled to an equimolar amount of HCO_3^- and phosphate. These buffers eliminate protons generated by the fermentation process (9, 98, 176). Further protons are bound by NH_3. In addition, fermentation of already buffered organic anions (e.g. anions bound to K^+ within the cytosol of plants) will not yield a proton. Considerable amounts of SCFA must therefore be absorbed from the rumen in a net process that does not require an equimolar passage of protons and accordingly, a formidable body of evidence has shown that large quantities of SCFA anions are absorbed in a net process with Na^+ (62, 116, 235, 320) or NH_4^+ (37). The argument is even more pressing for the omasum, since the protons produced in the fermentational process have been buffered within the rumen, and are thus not available as countercations for the efflux of SCFA from the omasum.

Possibly, the issue has not been discussed in the past since there can be little doubt about the fact that SCFA cross the apical membrane of forestomach epithelia in a process that is stimulated by low mucosal pH and which acidifies the cytosol (2, 15), suggesting a transfer of SCFA with protons. However, it is equally well known that the cytosolic pH of the intact tissue is tightly controlled, and thus, the protons taken up apically are immediately extruded in exchange for the uptake of Na^+ via NHE, resulting in a functionally coupled, electrically silent, and pH-neutral uptake of Na^+ and $SCFA^-$ into the tissue (109, 113, 116, 321). Intriguingly, a similar situation is found in the colon (28, 325), where this fundamental issue also awaits clarification. In net terms, protons taken up with SCFA are apically recirculated and a coupled uptake of Na^+ and $SCFA^-$ into the epithelium takes place. The protons taken up apically with SCFA are thus not available for basolateral efflux.

7.3.2 The coupled transport of $SCFA^-$ and Na^+

Na^+ entering apically leaves basolaterally via the Na^+/K^+-ATPase with recirculation of K^+ (133, 141, 142, 217, 301). In analogy to the classical transport model for the uptake of NaCl by absorptive epithelia such as the colon, which can only function if a basolateral chloride channel is present (39, 299), the basolateral efflux of SCFA must

occur in an electrogenic manner. The demonstration that both the apical anion exchanger (15) and the basolateral anion channel (360) accept SCFA anions as a substrate allows an application of the classical model of electrically silent NaCl transport to the transport of SCFA, which represent the dominant species of anions in the rumen that have to be absorbed to reduce ruminal osmolarity.

This argument is backed by electrophysiological data: in the rumen, the flux of Na^+ across the tissue has been shown to rise more strongly than the flux of Cl^- when SCFA are added to the mucosal side (70, 116). The missing anion is clearly the $SCFA^-$ anion. The need for an additional counter-anion to balance the transport of cations across the tissue becomes even more pressing when NH_3/NH_4^+ is added to the mucosal solution (4, 37).

7.3.3 Basolateral efflux of SCFA from forestomach epithelia through a maxi anion channel

In contrast to our extensive knowledge concerning apical uptake, only a few studies have addressed the basolateral efflux of SCFA (28, 325), and no clear consensus has emerged. A basolateral exchange of $SCFA^-/HCO_3^-$ and/or cotransport of SCFA with protons via MCT (172, 173, 240) have been proposed, but require a low cytosolic pH and a high accumulation of $SCFA^-$ within the epithelium. Both models predict an alkalinization of the rumen, and fail to explain why salivary buffering is necessary. In addition, no counter-anion for the transport of cations such as Na^+ and NH_4^+ is provided. All these problems can be resolved by a model that assumes that basolateral efflux of SCFA occurs without a proton through an anion channel.

This study clearly demonstrates that isolated cells not just of the rumen, but also of the omasum express large-conductance anion channels that are permeable not only to chloride, but also to the anions of SCFA (126, 127, 355, 356, 360), with $p(Cl^-) \sim 350$ pS, $p(acetate^-) \sim 140$ pS, and $p(propionate^-) \sim 100$ pS. The characteristics of the channel, namely: the very large conductance, the permeability to large anions, the high selectivity for anions over cations, and the bell-shaped voltage dependency, are clearly distinct from chloride channels with a known molecular identity, but they closely resemble those of a group of functionally well-characterized channels generally referred to as maxi-anion channels (246, 293). Conversely, there is little to

suggest an identity of the ruminal anion channel with the cystic fibrosis transmembrane conductance regulator (CFTR). The single-channel conductance is much too high, and the channel is not blocked by glibenclamide. Since cAMP stimulates neither the chloride currents across isolated cells (44), nor the chloride fluxes across the intact epithelium (110, 393), a significant functional expression of chloride channels of the CFTR group by the rumen appears unlikely.

Maxi-anion channels of the kind expressed by the rumen and the omasum are found in numerous tissues across the body and across species. They are among the channels with the largest single-channel conductance measured to date and may be phylogenetically ancient ((246), for an extensive review, see (293)). The channels are highly selective for anions over cations but display weak electric-field selectivity with an Eisenman's selectivity sequence I dominated by the hydration energies, so that selectivity to other halides is poor. A typical trait is that the pore allows passage of large organic anions (294), including acetate, propionate, and even passage of molecules as large as glutamate or ATP has been suggested (90). To our knowledge and somewhat surprisingly, a role for these channels in the transport of SCFA across gastrointestinal epithelia has not previously been proposed, although interestingly, a functional role in SCFA transport has been suggested for *Ascaris suum* (29).

We therefore suggest that, under physiological conditions, the efflux of SCFA from the ruminal epithelium is mediated by the same channel that mediates coupled, electrically silent, Na^+ and Cl^- transport across the tissue (115, 218). The model assumes the parallel apical uptake of Na^+ and $SCFA^-$ via two separate electroneutral pathways coupled to each other by the necessity of maintaining cytosolic pH. Efflux pathways for both ions are electrogenic and coupled by charge, with the efflux of Na^+ occuring through the Na^+/K^+-ATPase and energizing the efflux of $SCFA^-$ through the basolateral anion channel. In the absence of sufficient amounts of mucosal Na^+ for cotransport, NH_4^+ can function as a counter-ion.

The selectivity sequence of the basolateral channel ($p(acetate^-) > p(propionate^-) > p(butyrate^-)$) ensures that acetate and propionate can be rapidly absorbed for utilization by the animal *in toto*, whereas butyrate remains behind to meet the energy requirements of the tissue (181, 229).

7.3.4 Multiple pathways mediate the efflux of SCFA from the rumen

Most likely, multiple pathways mediate the efflux of SCFA from the rumen. If salivary flow is ample, protons will be buffered within the rumen, and SCFA can flow out functionally coupled to the efflux of Na^+ as described above. This probably represents an ideal situation for the epithelium, since protons do not have to cross, and osmolytes are rapidly removed both from the rumen and from the cytsol.

Nitrogen should play an appreciable, if smaller, role. In vitro data suggest that the basolateral efflux of ammonia mainly occurs electrogenically as NH_4^+ through a channel (4, 34); this will remove a proton from the rumen. The corresponding potential should serve as a powerful driving force for the basolateral efflux of SCFA from the tissue. Interestingly, SCFA have been shown to stimulate the absorption of ammonia from the rumen, possibly by providing a counter-anion (37, 262).

In situations in which salivary flow is insufficient, an adaptation of the epithelium to the transport of protons has to occur. This will involve intracellular buffering systems to bind and transport protons to the basolateral side, and proteins to mediate the basolateral efflux. MCT1 (173, 240) can mediate the efflux of protons coupled to the efflux of large anions but requires an accumulation of both to energize transport. Extrusion of protons via basolateral NHE1 (131, 265) appears more likely, as does the basolateral import of HCO_3^- via Na-HCO_3 cotransport (239). Since the Na^+ taken up is recycled basolaterally via the Na^+/K^+-ATPase, the resulting potential will drive the efflux of SCFA through the large-conductance anion channel. In net terms, this represents a highly efficient, secondary active pathway for the functionally coupled basolateral efflux of $SCFA^-$ and protons, driven by the recirculation of Na^+ via the Na^+/K^+-ATPase.

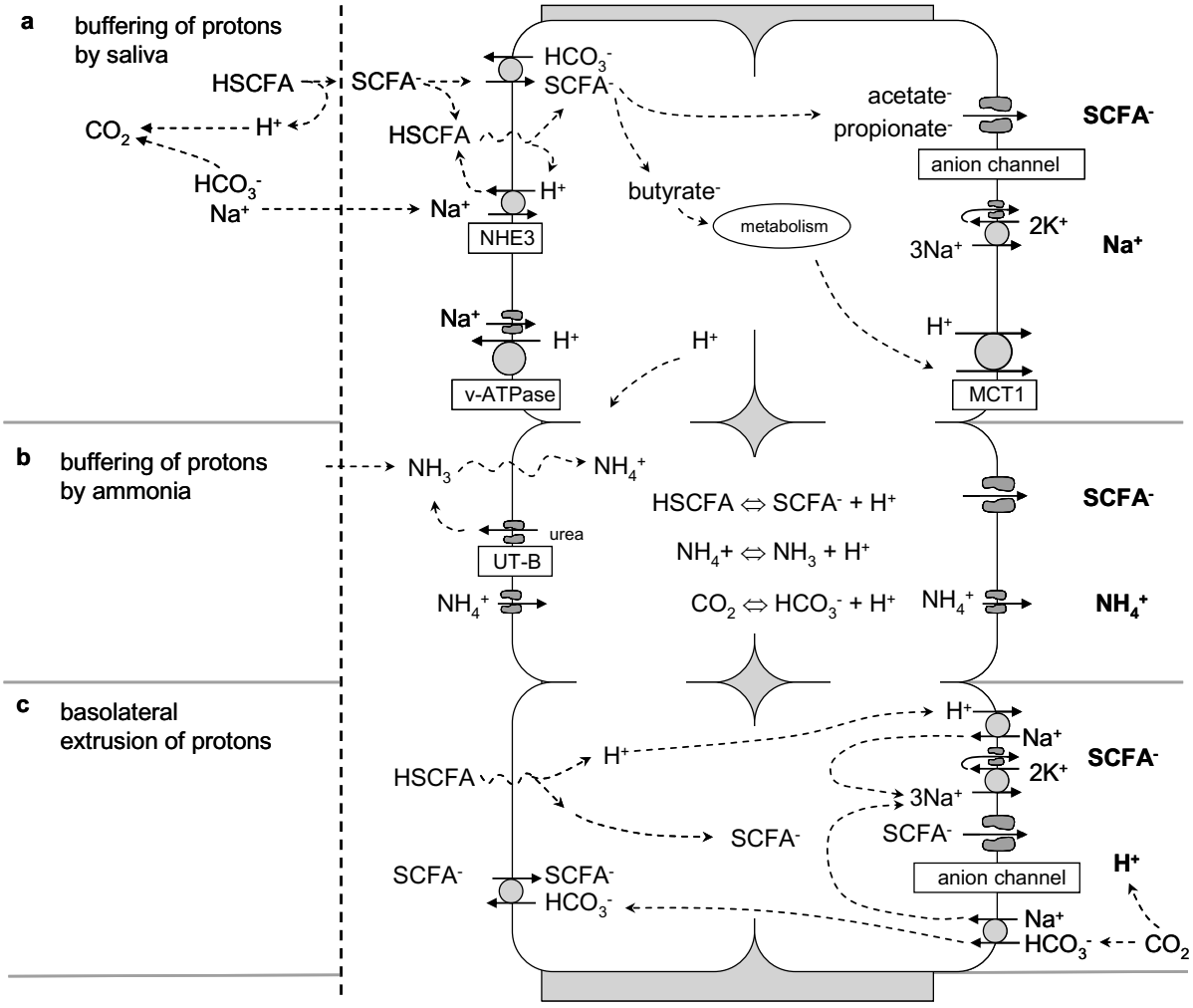

Figure 38: Multiple pathways for the efflux of SCFA from the rumen. Many different mechanisms are involved in mediating the efflux of SCFA from the rumen.
a) If salivary flow is ample, protons are buffered within the rumen. Apically, SCFA are taken up via lipid diffusion or anion exchange; the protons set free in the process are apically removed via NHE. Basolaterally, the anions of acetate$^-$ and propionate$^-$ leave through a channel. The efflux is driven by the potential generated by the efflux of Na^+ via the Na^+/K^+-ATPase. The basolateral anion channel is only poorly permeable to butyrate$^-$, and hence, this SCFA anion is extensively metabolized. Larger anions leave via MCT1.
At extremely low ruminal pH, NHE function may break down, but functional coupling of an apical H^+-ATPase with the uptake of Na^+ through the apical non-selective cation channel might compensate for NHE and restore the pH homeostasis of the tissue.
b) Ammonia from dietary and endogenous sources is also able to bind protons. $SCFA^-$ anions leave through a basolateral channel with NH_4^+ as a counter-ion.
c) If salivary secretion is insufficient, protons have to cross the epithelium and exit the basolateral membrane. Both NHE1 and Na-HCO_3 cotransport have been suggested to mediate a basolateral alkalinisation. As before, the sodium taken up via these transporters has to leave via the Na^+/K^+-ATPase, thus providing energy for the efflux of SCFA through the channel.
Efflux via MCT1 (see a) represents an alternate possibility but has to be seen as less efficient since it requires an accumulation of protons and SCFA to energetically drive the efflux.

8 Summary

Introduction: Postprandial fermentational processes in the rumen set free large quantities of SCFA, protons, K^+, and NH_3, whereas Na^+, HCO_3^- , HPO_3^{2-}, and Cl^- enter with saliva, and urea is secreted across the ruminal wall. Absorptive processes across the ruminal wall are necessary to restore osmolarity and ruminal pH.

Methods: The rumen and the omasum were studied by using various methods at the level of both the tissue and the cell (patch-clamp double-barreled pH-sensitive microelectrodes, Ussing chamber, confocal laser scanning microscopy, Western blot, PCR). A method for the isolation and cultivation of omasal cells was established.

Results and Conclusions:

Based on the findings and a careful study of the literature, a model for the efflux of osmotically active particles from the rumen was developed.

Sodium, magnesium, and potassium: we present data demonstrating that apical non-selective cation channels gated by Ca^{2+} and Mg^{2+} mediate the efflux of cations from the rumen (199).

When K^+ concentrations in the rumen rise, the cells are depolarized. The divalent cations blocking the pore of the channel are repelled by the potential, and the pore of the channel is open for the influx of Na^+, so that the absorption of this cation from the rumen is enhanced, and osmolarity is restored. The resulting transepithelial potential limits the efflux of K^+ from the rumen and into the blood, thus facillitating potassium homeostasis. Apical depolarization also limits channel-mediated uptake of Mg^{2+}, explaining the concomittant reduction in Mg^{2+} digestibility. However, the negative impact of K^+ on the uptake of Mg^{2+} is balanced by the positive effects on the absorption of Na^+, thus reducing ruminal osmolarity while maintaining systemic potassium homeostasis (351, 358, 359).

Urea and ammonium: SCFA acidify the epithelium and stimulate the secretion of urea into the rumen via a protein-mediated pathway (probably UT-B) that is regulated by cytosolic pH (2). The efflux of ammonium from the rumen can occur both as NH_3 and as NH_4^+, with differing impact on the absorption of sodium (4). Efflux of NH_4^+ occurs through apical non-selective cation channels and basolateral potassium-selective channels.

At high pH, apical uptake occurs primarily as NH_3, inhibiting sodium absorption via NHE. At acidic pH, uptake occurs as NH_4^+ through non-selective cation channels.

Since cytosolic pH is higher than ruminal pH, apical recirculation (in as NH_4^+ out as NH_3) will follow and can lead to the stimulation of Na^+ absorption via NHE, which may play a role in ruminal osmoregulation. At all values of ruminal pH, the bulk of ammonium will remain protonated and leave through potassium channels in the form of NH_4^+, removing a proton from the cytosol.

The findings suggest that the postprandial stimulation of urea secretion into the rumen occurs in response to changes of cytosolic pH and serves to the meet the nitrogen requirements of ruminal microbial populations, to regulate the speed of ruminal fermentation, and to buffer ruminal content (1).

Cl⁻ and SCFA⁻: The uptake of SCFA may be influenced by an apical microclimate, and occurs in a manner that acidifies the tissue (2). An anion exchanger can serve as an apical uptake pathway for both Cl^- and $SCFA^-$ in exchange for HCO_3^-(15). The basolateral efflux of anions (Cl^-, $SCFA^-$) is mediated by a maxi-anion channel, coupled to the charge of Na^+ leaving via the Na^+/K^+-ATPase (360).

The data confirm the classical notion that electrically silent absorption of NaCl across epithelia requires the expression of a basolateral chloride channel. The data also confirm that maxi-anion channels allow the passage of large anions. The demonstration of these channels in a transporting epithelium is new and explains why protons freed by fermentational processes have to be extensively buffered by saliva, whereas large quantities of SCFA cross the rumen coupled to the transport of Na^+ in an electrically silent manner. The permeability sequence of the channel, with $p(Cl^-) > p(acetate^-) > p(propionate^-) > p(butyrate^-)$ might explain the well-known observation that acetate and propionate enter the portal blood to meet the energy requirements of the animal, whereas butyrate is extensively metabolized within the epithelium.

It is suggested that protons taken up with SCFA are apically returned in exchange for Na^+ via NHE, where they are buffered by saliva so that epithelial function is not endangered by acidification. When ruminal pH drops, protons have to be basolaterally extruded via NHE1, or buffered by ruminal secretion of HCO_3^- entering apically in exchange for SCFA, and basolaterally via Na-HCO_3 cotransport. In all cases, the efflux of Na^+ taken up by pH regulatory proteins occurs via the Na^+/K^+-ATPase, thus efficiently energizing the efflux of $SCFA^-$ anions through a large-conductance anion channel. A cytosolic accumulation of protons or SCFA is not required.

9 References

1. **Abdoun K, Stumpff F, and Martens H.** Ammonia and urea transport across the rumen epithelium: a review. *Anim Health Res Rev* 7: 43-59, 2006.
2. **Abdoun K, Stumpff F, Rabbani I, and Martens H.** Modulation of urea transport across sheep rumen epithelium in vitro by SCFA and CO2. *Am J Physiol* 298: G190-202, 2010.
3. **Abdoun K, Stumpff F, Wolf K, and Martens H.** Ammonia inhibits urea transport across the isolated rumen epithelium by modulating cellular extrusion of protons. *XIth International Symposium on Ruminant Physiology*, edited by Chilliard Y, Glasser F, Faulconnier Y, Bocquier F, Veissier I and Doreau M, Clermont-Ferrand, France. Wageningen Academic Publishers, the Netherlands, 2009, p. 50.
4. **Abdoun K, Stumpff F, Wolf K, and Martens H.** Modulation of electroneutral Na transport in sheep rumen epithelium by luminal ammonia. *Am J Physiol* 289: G508-520, 2005.
5. **Abdoun K, Stumpff F, Wolf K, and Martens H.** Modulation of electroneutral Na transport in sheep rumen epithelium by luminal ammonia. *Am J Physiol Gastrointest Liver Physiol* 289: G508-520, 2005.
6. **Abdoun K, Wolf K, Arndt G, and Martens H.** Effect of ammonia on Na+ transport across isolated rumen epithelium of sheep is diet dependent. *Br J Nutr* 90: 751-758, 2003.
7. **Ali O.** *In vitro studies of ion transport in sheep omasum: interaction between Na, Cl and short chain fatty acids*. Berlin: Free University of Berlin, 2005.
8. **Ali O, Shen Z, Tietjen U, and Martens H.** Transport of acetate and sodium in sheep omasum: mutual, but asymmetric interactions. *J Comp Physiol (B)* 176: 477-487, 2006.
9. **Allen MS.** Relationship between fermentation acid production in the rumen and the requirement for physically effective fiber. *J Dairy Sci* 80: 1447-1462, 1997.
10. **Aqvist J and Luzhkov V.** Ion permeation mechanism of the potassium channel. *Nature* 404: 881-884, 2000.
11. **Argenzio RA, Miller N, and von Engelhardt W.** Effect of volatile fatty acids on water and ion absorption from the goat colon. *Am J Physiol* 229: 997-1002, 1975.
12. **Argenzio RA, Southworth M, Lowe JE, and Stevens CE.** Interrelationship of Na, HCO3, and volatile fatty acid transport by equine large intestine. *Am J Physiol* 233: E469-478, 1977.
13. **Aronson PS.** Ion exchangers mediating Na+, HCO3 - and Cl- transport in the renal proximal tubule. *J Nephrol* 19 Suppl 9: S3-S10, 2006.
14. **Aronson PS, Nee J, and Suhm MA.** Modifier role of internal H+ in activating the Na+-H+ exchanger in renal microvillus membrane vesicles. *Nature* 299: 161-163, 1982.
15. **Aschenbach JR, Bilk S, Tadesse G, Stumpff F, and Gäbel G.** Bicarbonate-dependent and bicarbonate-independent mechanisms contribute to nondiffusive uptake of acetate in the ruminal epithelium of sheep. *Am J Physiol* 296: 1098-1107, 2009.
16. **Aschenbach JR, Penner GB, Stumpff F, and Gäbel G.** Role of fermentation acid absorption in the regulation of ruminal pH. *J Anim Sci* (submitted), 2010.

17. **Awayda MS, Bengrine A, Tobey NA, Stockand JD, and Orlando RC.** Nonselective cation transport in native esophageal epithelia. *Am J Physiol Cell Physiol* 287: C395-402, 2004.
18. **Bailey CB.** Saliva secretion and its relation to feeding in cattle. 4. The relationship between the concentrations of sodium, potassium, chloride and inorganic phosphate in mixed saliva and rumen fluid. *Br J Nutr* 15: 489-498, 1961.
19. **Bailey CB and Balch CC.** Saliva secretion and its relation to feeding in cattle. 1. The composition and rate of secretion of parotid saliva in a small steer. *Br J Nutr* 15: 371-382, 1961.
20. **Bailey CB and Balch CC.** Saliva secretion and its relation to feeding in cattle. 2. The composition and rate of secretion of mixed saliva in the cow during rest. *Br J Nutr* 15: 383-402, 1961.
21. **Barcroft RA, McAnnally RA, and Philipson AT.** Absorption of volatile fatty acids from the alimentary tract of sheep and other animals. *J Exp Biol* 20: 120-129, 1944.
22. **Barrett KE.** New ways of thinking about (and teaching about) intestinal epithelial function. *Adv Physiol Educ* 32: 25-34, 2008.
23. **Barry PH and Lynch JW.** Liquid junction potentials and small cell effects in patch-clamp analysis. *J Membr Biol* 121: 101-117, 1991.
24. **Barry RJ, Jackson MJ, and Smyth DH.** Transfer of propionate by rat small intestine in vitro. *J Physiol* 182: 150-163, 1966.
25. **Bergman EN.** Energy contributions of volatile fatty acids from the gastrointestinal tract in various species. *Physiol Rev* 70: 567-590, 1990.
26. **Bergman EN, Reid RS, Murray MG, Brockway JM, and Whitelaw FG.** Interconversions and production of volatile fatty acids in the sheep rumen. *Biochem J* 97: 53-58, 1965.
27. **Bilk S, Huhn K, Honscha KU, Pfannkuche H, and Gäbel G.** Bicarbonate exporting transporters in the ovine ruminal epithelium. *J Comp Physiol (B)* 175: 365-374, 2005.
28. **Binder HJ.** Role of colonic short-chain fatty acid transport in diarrhea. *Annu Rev Physiol* 72: 297-313, 2010.
29. **Blair KL, Geary TG, Mensch SK, Vidmar TJ, Li SK, Ho NF, and Thompson DP.** Biophysical characterization of a large conductance anion channel in hypodermal membranes of the gastrointestinal nematode, Ascaris suum. *Comp Biochem Physiol A Mol Integr Physiol* 134: 805-818, 2003.
30. **Blair-West JR, Coghlan JP, Denton DA, Goding JR, and Wright RD.** The effect of aldosterone, cortisol, and corticosterone upon the sodium and potassium content of sheep's parotid saliva. *J Clin Invest* 42: 484-496, 1963.
31. **Blake-Palmer KG and Karet FE.** Cellular physiology of the renal H+ATPase. *Curr Opin Nephrol Hypertens* 18: 433-438, 2009.
32. **Bobulescu IA and Moe OW.** Luminal Na(+)/H (+) exchange in the proximal tubule. *Pflugers Arch* 458: 5-21, 2009.
33. **Boda JM, McDonald PG, and Walker JJ.** Effects of the Addition of Fluids to the Empty Rumen on the Flow Rate and Chemical Composition of Bovine Mixed Saliva. *J Physiol* 177: 323-336, 1965.
34. **Bödeker D and Kemkowski J.** Participation of NH4+ in total ammonia absorption across the rumen epithelium of sheep (Ovis aries). *Comp Biochem Physiol A Physiol* 114: 305-310, 1996.
35. **Bödeker D, Lamy S, Mahler M, and Höller H.** Effects of short-chain fatty acids on electrophysiological properties and permeability characteristics of sheep (Ovis aries) abomasal mucosa. *Comp Biochem Physiol A* 107: 73-79, 1994.

36. **Bödeker D, Oppelland G, and Holler H.** Involvement of carbonic anhydrase in ammonia flux across rumen mucosa in vitro. *Exp Physiol* 77: 517-519, 1992.
37. **Bödeker D, Shen Y, Kemkowski J, and Holler H.** Influence of short-chain fatty acids on ammonia absorption across the rumen wall in sheep. *Exp Physiol* 77: 369-376, 1992.
38. **Bödeker D, Winkler A, and Holler H.** Ammonia absorption from the isolated reticulo-rumen of sheep. *Exp Physiol* 75: 587-595, 1990.
39. **Boron WF and Boulpaep EL.** *Medical Physiology*. Philadelphia: Saunders, 2003.
40. **Boron WF and De Weer P.** Intracellular pH transients in squid giant axons caused by CO2, NH3, and metabolic inhibitors. *J Gen Physiol* 67: 91-112, 1976.
41. **Boron WF, Waisbren SJ, Modlin IM, and Geibel JP.** Unique permeability barrier of the apical surface of parietal and chief cells in isolated perfused gastric glands. *J Exp Biol* 196: 347-360, 1994.
42. **Bowman GR, Beauchemin KA, and Shelford JA.** Fibrolytic enzymes and parity effects on feeding behavior, salivation, and ruminal pH of lactating dairy cows. *J Dairy Sci* 86: 565-575, 2003.
43. **Bramley E, Lean IJ, Fulkerson WJ, Stevenson MA, Rabiee AR, and Costa ND.** The definition of acidosis in dairy herds predominantly fed on pasture and concentrates. *J Dairy Sci* 91: 308-321, 2008.
44. **Brinkmann I.** *Charakterisierung eines nicht selektiven Kationenkanals in Epithelzellen des Pansens von Schafen* (Dissertation). Berlin: Freie Universität Berlin, 2006.
45. **Brinkmann I, Stumpff F, and Martens H.** Effects of cAMP on the electrogenic sodium conductance on the ruminal epithelium. *Proceedings: 26. DVG Kongress, "Tierschutz, Leistung und Gesundheit"*, 2005, p. 118.
46. **Bugaut M.** Occurence, absorption and metabolism of short chain fatty acids in the digestive tract of mammals. *Comp Biochem Physiol B* 86: 439-472, 1987.
47. **Burckhardt BC and Frömter E.** Pathways of NH3/NH4+ permeation across Xenopus laevis oocyte cell membrane. *Pflugers Arch* 420: 83-86, 1992.
48. **Campagnolo ER, Kasten S, and Banerjee M.** Accidental ammonia exposure to county fair show livestock due to contaminated drinking water. *Vet Hum Toxicol* 44: 282-285, 2002.
49. **Care AD, Brown RC, Farrar AR, and Pickard DW.** Magnesium absorption from the digestive tract of sheep. *Q J Exp Physiol* 69: 577-587, 1984.
50. **Care AD, Farrar AR, and Pickard DW.** Factors affecting the absorption of magnesium from the rumen in sheep. *J Physiol* 325, 1982.
51. **Care AD and van't Klooster AT.** In Vivo Transport of Magnesium and Other Cations across the Wall of the Gastro-Intestinal Tract of Sheep. *J Physiol* 177: 174-191, 1965.
52. **Carter RR and Grovum WL.** A review of the physiological significance of hypertonic body fluids on feed intake and ruminal function: salivation, motility and microbes. *J Anim Sci* 68: 2811-2832, 1990.
53. **Cassida KA and Stokes MR.** Eating and resting salivation in early lactation dairy cows. *J Dairy Sci* 69: 1282-1292, 1986.
54. **Chien WJ and Stevens CE.** Coupled active transport of Na and Cl across forestomach epithelium. *Am J Physiol* 223: 997-1003, 1972.
55. **Choe H, Sackin H, and Palmer LG.** Permeation properties of inward-rectifier potassium channels and their molecular determinants. *J Gen Physiol* 115: 391-404, 2000.

56. **Chu S and Montrose MH.** The glow of the colonic pH microclimate kindled by short-chain fatty acids, chloride and bicarbonate. *J Physiol* 517 (Pt 2): 315, 1999.
57. **Cocimano MR and Leng RA.** Metabolism of urea in sheep. *Br J Nutr* 21: 353-371, 1967.
58. **Colombini M.** Voltage gating in the mitochondrial channel, VDAC. *J Membr Biol* 111: 103-111, 1989.
59. **Compton JS, Nelson J, Wright RD, and Young JA.** A micropuncture investigation of electrolyte transport in the parotid glands of sodium-replete and sodium-depleted sheep. *J Physiol* 309: 429-446, 1980.
60. **Coombe JB, Tribe DE, and Morrison JWC.** Some experimental observations on the toxicity of urea to sheep. *Aust J Agric Res* 11: 247-256, 1960.
61. **Cummings JH.** Colonic absorption: the importance of short chain fatty acids in man. *Scand J Gastroenterol Suppl* 93: 89-99, 1984.
62. **Danielli JF, Hitchcock WS, Marshal RA, and Phillipson AT.** The mechanism of absorption from the rumen as exemplified by the behaviour of acetic, propionic, and butyric acids. *J Exp Bio* 22: 75-84, 1945.
63. **Decker P, Gärtner K, Hörnicke H, and Hill H.** Fortlaufende Messungen von Harnstoffbildung und Harnstoffrückfluss in den Pansen in Abhängigkeit vom Harnfluss mit Hilfe von ^{14}C-Harnstoff bei Ziegen. *Pflugers Arch* 274: 289-294, 1961.
64. **Delgado-Elorduy A, Theurer CB, Huber JT, Alio A, Lozano O, Sadik M, Cuneo P, De Young HD, Simas lJ, Santos JE, Nussio L, Nussio C, Webb KE, Jr., and Tagari H.** Splanchnic and mammary nitrogen metabolism by dairy cows fed dry-rolled or steam-flaked sorghum grain. *J Dairy Sci* 85: 148-159, 2002.
65. **Delgado-Elorduy A, Theurer CB, Huber JT, Alio A, Lozano O, Sadik M, Cuneot P, De Young HD, Simas lJ, Santos JE, Nussio L, Nussio C, Webb KE, Jr., and Tagari H.** Splanchnic and mammary nitrogen metabolism by dairy cows fed steam-rolled or steam-flaked corn. *J Dairy Sci* 85: 160-168, 2002.
66. **Denton DA.** The effect of variation in the concentration of individual extracellular electrolytes on the response of the sheep's parotid gland to Na+ depletion. *J Physiol* 140: 129-147, 1958.
67. **Deveau JS, Lindinger MI, and Grodzinski B.** An improved method for constructing and selectively silanizing double-barreled, neutral liquid-carrier, ion-selective microelectrodes. *Biol Proced Online* 7: 31-40, 2005.
68. **Diener M, Helmle-Kolb C, Murer H, and Scharrer E.** Effect of short-chain fatty acids on cell volume and intracellular pH in rat distal colon. *Pflugers Arch* 424: 216-223, 1993.
69. **Diener M and Scharrer E.** The effect of short-chain fatty acids on Cl- and K+ conductance in rat colonic crypts. *Pflugers Arch* 426: 472-480, 1994.
70. **Diernaes L, Sehested J, Moller PD, and Skadhauge E.** Sodium and chloride transport across the rumen epithelium of cattle in vitro: effect of short-chain fatty acids and amiloride. *Exp Physiol* 79: 755-762, 1994.
71. **Dihn SK.** Urea-N recycling in lactating dairy cows. *Ph D Dissertation, Univ Maryland, College Park*, 2007.
72. **Dijkstra J, Boer H, Van Bruchem J, Bruining M, and Tamminga S.** Absorption of volatile fatty acids from the rumen of lactating dairy cows as influenced by volatile fatty acid concentration, pH and rumen liquid volume. *Br J Nutr* 69: 385-396, 1993.
73. **Dirksen G, Gründer HD, and Stöber M.** *Innere Medizin und Chirurgie des Rindes*. Berlin, Wien: Blackwell Verlag, 2002.

74. **Dixon RM and Nolan JV.** Nitrogen and carbon flows between the caecum, blood and rumen in sheep given chopped lucerne (Medicago sativa) hay. *Br J Nutr* 55: 313-332, 1986.
75. **Dobson A.** Active transport through the epithelium of the reticulo-rumen sac. *J Physiol* 146: 235-251, 1959.
76. **Dobson A.** *The movements of ions across the epithelium of the reticulo-rumen sac*. Aberdeen: University of Aberdeen, 1956.
77. **Dobson A and Phillipson AT.** The absorption of chloride ions from the reticulo-rumen sac. *J Physiol* 140: 94-104, 1958.
78. **Dobson A and Phillipson AT.** The forces moving chloride ions through rumen epithelium. *J Physiol* 125: 26-27P, 1954.
79. **Dobson A, Scott D, and Bruce JB.** Changes in sodium requirement of the sheep associated with changes of diet. *Q J Exp Physiol Cogn Med Sci* 51: 311-323, 1966.
80. **Dobson A, Sellers AF, and Gatewood VH.** Absorption and exchange of water across rumen epithelium. *Am J Physiol* 231: 1588-1594, 1976.
81. **Dobson A, Sellers AF, and Gatewood VH.** Dependence of Cr-EDTA absorption from the rumen on luminal osmotic pressure. *Am J Physiol* 231: 1595-1600, 1976.
82. **Dobson MJ, Brown WC, Dobson A, and Phillipson AT.** A histological study of the organization of the rumen epithelium of sheep. *Q J Exp Physiol Cogn Med Sci* 41: 247-253, 1956.
83. **Doll K, Sickinger M, and Seeger T.** New aspects in the pathogenesis of abomasal displacement. *Vet J* 181: 90-96, 2009.
84. **Dölle M.** *Charakterisierung des Na+-Transportes am isolierten Psalterepithel des Schafes.* Berlin: Freie Universität Berlin, 2008.
85. **Donowitz M and Li X.** Regulatory binding partners and complexes of NHE3. *Physiol Rev* 87: 825-872, 2007.
86. **Doyle DA.** Structural themes in ion channels. *Eur Biophys J* 33: 175-179, 2004.
87. **Droogmans G, Prenen J, Eggermont J, Voets T, and Nilius B.** Voltage-dependent block of endothelial volume-regulated anion channels by calix[4]arenes. *Am J Physiol* 275: C646-652, 1998.
88. **Dua K and Care AD.** Impaired absorption of magnesium in the aetiology of grass tetany. *Br Vet J* 151: 413-426, 1995.
89. **Dua K and Care AD.** Lack of effect of quinidine on divalent mineral absorption from the reticulorumen of sheep. *Res Vet Sci* 56: 114-115, 1994.
90. **Dutta AK, Sabirov RZ, Uramoto H, and Okada Y.** Role of ATP-conductive anion channel in ATP release from neonatal rat cardiomyocytes in ischaemic or hypoxic conditions. *J Physiol* 559: 799-812, 2004.
91. **Edlund GL and Halestrap AP.** The kinetics of transport of lactate and pyruvate into rat hepatocytes. Evidence for the presence of a specific carrier similar to that in erythrocytes. *Biochem J* 249: 117-126, 1988.
92. **Edrise BM and Smith RH.** Absorption and secretion in the omasum of the young steer. *Ann Rech Vet* 10: 354-355, 1979.
93. **Edrise BM, Smith RH, and Buttle HL.** Exchanges of digesta components in different compartments of the stomach of the young steer. *Proc Nutr Soc* 36: 8A, 1977.
94. **Edrise BM, Smith RH, and Hewitt D.** Exchanges of water and certain water-soluble minerals during passage of digesta through the stomach compartments of young ruminating bovines. *Br J Nutr* 55: 157-168, 1986.

95. **Ekman J and Sperber I.** The distribution of concentrations of bicarbonate (including carbon dioxide) and chloride in the omasum of cows. *Kungl Lantbrukshögskolans annaler* 19: 226-231, 1953.
96. **Emanuele SM and Staples CR.** Ruminal release of minerals from six forage species. *J Anim Sci* 68: 2052-2060, 1990.
97. **Engelhardt Wv and Hauffe R.** Funktionen des Blättermagens bei kleinen Hauswiederkäuern. *Zentralbl Veterinarmed A* 22: 363-375, 1975.
98. **Erdmann RA.** Dietary Buffering Requirements of the Lactating Dairy Cow: A Review. *J Dairy Sci* 71: 3246-3266, 1988.
99. **Etschmann B, Heipertz KS, von der Schulenburg A, and Schweigel M.** A vH+-ATPase is present in cultured sheep ruminal epithelial cells. *Am J Physiol* 291: G1171-1179, 2006.
100. **Etschmann B, Suplie A, and Martens H.** Change of ruminal sodium transport in sheep during dietary adaptation. *Arch Anim Nutr* 63: 26-38, 2009.
101. **Ferreira HG, Harrison FA, and Keynes RD.** The potential and short-circuit current across isolated rumen epithelium of the sheep. *J Physiol* 187: 631-644, 1966.
102. **Ferreira HG, Harrison FA, Keynes RD, and Nauss AH.** Observations on the potential across the rumen of sheep. *J Physiol* 187: 615-630, 1966.
103. **Ferreira HG, Harrison FA, Keynes RD, and Zurich L.** Ion transport across an isolated preparation of sheep rumen epithelium. *J Physiol* 222: 77-93, 1972.
104. **Finkelstein A.** Water and nonelectrolyte permeability of lipid bilayer membranes. *J Gen Physiol* 68: 127-135, 1976.
105. **Firkins JL, Yu Z, and Morrison M.** Ruminal nitrogen metabolism: perspectives for integration of microbiology and nutrition for dairy. *J Dairy Sci* 90 Suppl 1: E1-16, 2007.
106. **Forte M, Adelsberger-Mangan D, and Colombini M.** Purification and characterization of the voltage-dependent anion channel from the outer mitochondrial membrane of yeast. *J Membr Biol* 99: 65-72, 1987.
107. **Frizzell RA and Schultz SG.** Ionic conductances of extracellular shunt pathway in rabbit ileum. Influence of shunt on transmural sodium transport and electrical potential differences. *J Gen Physiol* 59: 318-346, 1972.
108. **Frömter E and Gebler B.** Electrical properties of amphibian urinary bladder epithelia. III. The cell membrane resistances and the effect of amiloride. *Pflugers Arch* 371: 99-108, 1977.
109. **Gäbel G, Aschenbach JR, and Müller F.** Transfer of energy substrates across the ruminal epithelium: implications and limitations. *Anim Health Res Rev* 3: 15-30, 2002.
110. **Gäbel G, Butter H, and Martens H.** Regulatory role of cAMP in transport of Na+, Cl- and short-chain fatty acids across sheep ruminal epithelium. *Exp Physiol* 84: 333-345, 1999.
111. **Gäbel G and Martens H.** The Effect of Ammonia on Magnesium Metabolism in Sheep. *J Anim Physiol Anim Nutr* 55: 278-287, 1986.
112. **Gäbel G, Martens H, Suendermann M, and Galfi P.** The effect of diet, intraruminal pH and osmolarity on sodium, chloride and magnesium absorption from the temporarily isolated and washed reticulo-rumen of sheep. *Q J Exp Physiol* 72: 501-511, 1987.
113. **Gäbel G and Sehested J.** SCFA transport in the forestomach of ruminants. *Comp Biochem Physiol A Physiol* 118: 367-374, 1997.
114. **Gäbel G, Suendermann M, and Martens H.** The Influence of Osmotic Pressure, Lactic Acid and pH on Ion and Fluid Absorption from the Washed and Temporarily Isolated Reticulo-Rumen of Sheep. *J Vet Med A* 34: 220-226, 1987.

115. **Gäbel G, Vogler S, and Martens H.** Mechanisms of sodium and chloride transport across isolated sheep reticulum. *Comp Biochem Physiol A* 105: 1-10, 1993.
116. **Gäbel G, Vogler S, and Martens H.** Short-chain fatty acids and CO2 as regulators of Na+ and Cl- absorption in isolated sheep rumen mucosa. *J Comp Physiol (B)* 161: 419-426, 1991.
117. **Galfi P, Gäbel G, and Martens H.** Influences of extracellular matrix components on the growth and differentiation of ruminal epithelial cells in primary culture. *Res Vet Sci* 54: 102-109, 1993.
118. **Galfi P, Neogrady S, and Gäbel G.** Na+/H+ exchange in primary, secondary and n-butyrate-treated cultures of ruminal epithelial cells: short communication. *Acta Vet Hung* 50: 211-215, 2002.
119. **Garrett EF, Pereira MN, Nordlund KV, Armentano LE, Goodger WJ, and Oetzel GR.** Diagnostic methods for the detection of subacute ruminal acidosis in dairy cows. *J Dairy Sci* 82: 1170-1178, 1999.
120. **Gärtner K.** Untersuchungen in vitro über die Ammoniakpassage durch die Pansenschleimhaut von Rindern und deren Beeinflussung durch pH-Wert und antidiuretisches Hormon. *Zbl Vet Med* A: 11-20, 1962.
121. **Gärtner K.** Untersuchungen über den Transportmechanismus von Harnstoff-Stickstoff durch die Pansenschleimhaut von Rindern in vitro. *Pflugers Arch* 276: 292-302, 1962.
122. **Gärtner K, Decker P, and Hill H.** Untersuchungen über die Passage von Harnstoff und Ammoniak durch die Pansenwand von Ziegen. *Pflugers Arch* 274: 281-288, 1961.
123. **Gärtner K and von Engelhardt W.** [Experiments concerning the resorption mechanism of ammonia through the ruminal mucosa of ruminants]. *Dtsch Tierarztl Wochenschr* 71: 57-60, 1964.
124. **Genz AK, v Engelhardt W, and Busche R.** Maintenance and regulation of the pH microclimate at the luminal surface of the distal colon of guinea-pig. *J Physiol* 517 (Pt 2): 507-519, 1999.
125. **Georgi MI, Enders, J., Mundhenk, L., Martens, H., Stumpff, F.** Isolation and Characterization of Cells of the Omasum. *Proc. Fachgruppe Physiologie und Biochemie der DVG*, Hannover. Verlag der DVG, 2010, p. 82.
126. **Georgi MI, Martens, H., Stumpff, F.** Cells of the rumen and the omasum express a conductance permeable to the anions of SCFA. *Proc. Fachgruppe Physiologie und Biochemie der DVG*, Hannover. Verlag der DVG, 2010, p. 42.
127. **Georgi MI, Stumpff, F., Martens, H.** Isolated Ruminal Epithelial Cells of the Sheep Express a Channel Permeable to the Anions of SCFA. *Proc Soc Nutr Physiol* 19: 125, 2010.
128. **Giebisch G.** Renal potassium transport: mechanisms and regulation. *Am J Physiol* 274: F817-833, 1998.
129. **Giesecke D and Engelhardt WV.** [Functions of the omasum in small domestic ruminants. II. Fermentation rate and DNA content]. *Zentralbl Veterinarmed A* 22: 177-186, 1975.
130. **Gozho GN, Hobin MR, and Mutsvangwa T.** Interactions between barley grain processing and source of supplemental dietary fat on nitrogen metabolism and urea-nitrogen recycling in dairy cows. *J Dairy Sci* 91: 247-259, 2008.
131. **Graham C, Gatherar I, Haslam I, Glanville M, and Simmons NL.** Expression and localisation of monocarboxylate transporters and sodium proton exchangers in bovine rumen epithelium. *Am J Physiol Regul Integr Comp Physiol*, 2006.
132. **Graham C, Gatherar I, Haslam I, Glanville M, and Simmons NL.** Expression and localization of monocarboxylate transporters and sodium/proton exchangers in

bovine rumen epithelium. *Am J Physiol Regul Integr Comp Physiol* 292: R997-1007, 2007.
133. **Graham C and Simmons NL.** Functional organization of the bovine rumen epithelium. *Am J Physiol* 288: R173-181, 2005.
134. **Gray DA, Frindt G, Zhang YY, and Palmer LG.** Basolateral K+ conductance in principal cells of rat CCD. *Am J Physiol Renal Physiol* 288: F493-504, 2005.
135. **Greene LW, Webb KE, Jr., and Fontenot JP.** Effect of potassium level on site of absorption of magnesium and other macroelements in sheep. *J Anim Sci* 56: 1214-1221, 1983.
136. **Grings EE and Males JR.** Effects of potassium on macromineral absorption in sheep fed wheat straw-based diets. *J Anim Sci* 64: 872-879, 1987.
137. **Han XT, Noziere P, Remond D, Chabrot J, and Doreau M.** Effects of nutrient supply and dietary bulk on O2 uptake and nutrient net fluxes across rumen, mesenteric- and portal-drained viscera in ewes. *J Anim Sci* 80: 1362-1374, 2002.
138. **Hansson A, Bloor BK, Sarang Z, Haig Y, Morgan PR, Stark HJ, Fusenig NE, Ekstrand J, and Grafstrom RC.** Analysis of proliferation, apoptosis and keratin expression in cultured normal and immortalized human buccal keratinocytes. *Eur J Oral Sci* 111: 34-41, 2003.
139. **Harmeyer J, Birk R, Varady J, and Martens H.** Kinetics of urea metabolism in protein-free fed sheep. *Zeitschr Tierphysiol Tierernähr Futtermittelkunde* 31: 239-248, 1973.
140. **Harmeyer J and Martens H.** Aspects of urea metabolism in ruminants with reference to the goat. *J Dairy Sci* 63: 1707-1728, 1980.
141. **Harrison FA.** Ion transport across rumen and omasum epithelium. *Philos Trans R Soc Lond B Biol Sci* 262: 301-305, 1971.
142. **Harrison FA, Keynes RD, Rankin JC, and Zurich L.** The effect of ouabain on ion transport across isolated sheep rumen epithelium. *J Physiol* 249: 669-677, 1975.
143. **Hauffe R and Engelhardt W.** [Functions of the omasum of small ruminants. III. Absorption of water]. *Zentralbl Veterinarmed A* 22: 283-295, 1975.
144. **Helbig H, Korbmacher C, Stumpff F, Coca-Prados M, and Wiederholt M.** Role of HCO3- in regulation of cytoplasmic pH in ciliary epithelial cells. *Am J Physiol* 257: C696-705, 1989.
145. **Herschel DA, Argenzio RA, Southworth M, and Stevens CE.** Absorption of volatile fatty acid, Na, and H2O by the colon of the dog. *Am J Vet Res* 42: 1118-1124, 1981.
146. **Hille B.** *Ion Channels of Excitable Membranes*. Sunderland, Mass.: Sinauer Associates, 2001.
147. **Hille B.** Potassium channels in myelinated nerve. Selective permeability to small cations. *J Gen Physiol* 61: 669-686, 1973.
148. **Hille B and Schwarz W.** Potassium channels as multi-ion single-file pores. *J Gen Physiol* 72: 409-442, 1978.
149. **Hinders RG and Owens FN.** Relation of ruminal parakeratosis development to volatile fatty acid absorption. *J Dairy Sci* 48: 1069-1073, 1965.
150. **Hodgkin AL.** The ionic basis of electrical activity in nerve and muscle. *Biol Rev* 26: 339-409, 1951.
151. **Hogan JP.** The absorption of ammonia through the rumen of the sheep. *Aust J Biol Sci* 14: 448, 1961.
152. **Houpt TR and Houpt KA.** Transfer of urea nitrogen across the rumen wall. *Am J Physiol* 214: 1296-1303, 1968.

153. **Huber K, Roesler U, Muscher A, Hansen K, Widiyono I, Pfeffer E, and Breves G.** Ontogenesis of epithelial phosphate transport systems in goats. *Am J Physiol Regul Integr Comp Physiol* 284: R413-421, 2003.
154. **Huhn K, Muller F, Honscha KU, Pfannkuche H, and Gäbel G.** Molecular and functional evidence for a Na(+)-HCO3(-)-cotransporter in sheep ruminal epithelium. *J Comp Physiol (B)* 173: 277-284, 2003.
155. **Huntington GB, Magee K, Matthews A, Poore M, and Burns J.** Urea metabolism in beef steers fed tall fescue, orchardgrass, or gamagrass hays. *J Anim Sci*, 2008.
156. **Hyden S.** Observations on the Absorption of Inorganic Ions from the Reticulo-Rumen of the Sheep. *Kugl Lantbrukshögkolans Annaler* 27: 273-285, 1961.
157. **Jackson MJ and Smyth DH.** Role of sodium in the intestinal active transport of organic solutes. *Nature* 219: 388-389, 1968.
158. **Jefferies KC, Cipriano DJ, and Forgac M.** Function, structure and regulation of the vacuolar (H+)-ATPases. *Arch Biochem Biophys* 476: 33-42, 2008.
159. **Jittakhot S, Schonewille JT, Wouterse HS, Yuangklang C, and Beynen AC.** The relationships between potassium intakes, transmural potential difference of the rumen epithelium and magnesium absorption in whethers. *Br J Nutr* 91: 183-189, 2004.
160. **Johnston R, Kesler EM, and McCarthy RD.** Absorption of organic acids from the omasum. *J Dairy Sci* 44: 331-339, 1961.
161. **Kay RN.** The influence of saliva on digestion in ruminants. *World Rev Nutr Diet* 6: 292-325, 1966.
162. **Kay RN.** The rate of flow and composition of various salivary secretions in sheep and calves. *J Physiol* 150: 515-537, 1960.
163. **Kemp PJ and Kim KJ.** Spectrum of ion channels in alveolar epithelial cells: implications for alveolar fluid balance. *Am J Physiol Lung Cell Mol Physiol* 287: L460-464, 2004.
164. **Kennedy P and Milligan L.** The degradation and utilization of endogenous urea in the gastrointestinal tract of ruminants: a review. *Can J Anim Sci* 60: 205-221, 1980.
165. **Kennedy PM and Milligan LP.** Transfer of urea from the blood to the rumen of sheep. *Br J Nutr* 40: 149-154, 1978.
166. **Kerschbaum HH, Kozak JA, and Cahalan MD.** Polyvalent cations as permeant probes of MIC and TRPM7 pores. *Biophys J* 84: 2293-2305, 2003.
167. **Khademi S and Stroud RM.** The Amt/MEP/Rh family: structure of AmtB and the mechanism of ammonia gas conduction. *Physiology (Bethesda)* 21: 419-429, 2006.
168. **Khorasani GR, Janzen RA, McGill WB, and Kennelly JJ.** Site and extent of mineral absorption in lactating cows fed whole-crop cereal grain silage of alfalfa silage. *J Anim Sci* 75: 239-248, 1997.
169. **Kiddle P, Marshall RA, and Phillipson AT.** A comparison of the mixtures of acetic, propionic and butyric acids in the rumen and in the blood leaving the rumen. *J Physiol* 113: 207-217, 1951.
170. **Kiela PR, Xu H, and Ghishan FK.** Apical NA+/H+ exchangers in the mammalian gastrointestinal tract. *J Physiol Pharmacol* 57 Suppl 7: 51-79, 2006.
171. **Kirat D, Inoue H, Iwano H, Hirayama K, Yokota H, Taniyama H, and Kato S.** Expression and distribution of monocarboxylate transporter 1 (MCT1) in the gastrointestinal tract of calves. *Res Vet Sci* 79: 45-50, 2005.
172. **Kirat D and Kato S.** Monocarboxylate transporter 1 (MCT1) mediates transport of short-chain fatty acids in bovine caecum. *Exp Physiol* 91: 835-844, 2006.

173. **Kirat D, Masuoka J, Hayashi H, Iwano H, Yokota H, Taniyama H, and Kato S.** Monocarboxylate transporter 1 (MCT1) plays a direct role in short-chain fatty acids absorption in caprine rumen. *J Physiol* 576: 635-647, 2006.
174. **Kleen JL, Hooijer GA, Rehage J, and Noordhuizen JP.** Subacute ruminal acidosis (SARA): a review. *J Vet Med A Physiol Pathol Clin Med* 50: 406-414, 2003.
175. **Knickelbein R, Aronson PS, Schron CM, Seifter J, and Dobbins JW.** Sodium and chloride transport across rabbit ileal brush border. II. Evidence for Cl-HCO3 exchange and mechanism of coupling. *Am J Physiol* 249: G236-245, 1985.
176. **Kohn RA and Dunlap TF.** Calculation of the buffering capacity of bicarbonate in the rumen and in vitro. *J Anim Sci* 76: 1702-1709, 1998.
177. **Kosmis K, Stumpff F, and Martens H.** Supra-apikale pH-Messungen am Blättermagenepithel des Schafes mit Hilfe der pH-sensitiven Mikroelektrode. *Proceedings 18. Tagung der DVG-Fachgruppe Physiologie und Biochemie*, 2008, p. 78.
178. **Kramer T, Michelberger T, Gurtler H, and Gäbel G.** Absorption of short-chain fatty acids across ruminal epithelium of sheep. *J Comp Physiol (B)* 166: 262-269, 1996.
179. **Krause KM and Oetzel GR.** Inducing subacute ruminal acidosis in lactating dairy cows. *J Dairy Sci* 88: 3633-3639, 2005.
180. **Krause KM and Oetzel GR.** Understanding and preventing subacute ruminal acidosis in dairy herds: A review. *Animal Feed Science and Technology* 126: 215-236, 2006.
181. **Kristensen NB.** Splanchnic metabolism of volatile fatty acids in the dairy cow. *J Anim Sci* 80: 2-9, 2005.
182. **Kristensen NB, Gäbel G, Pierzynowski SG, and Danfaer A.** Portal recovery of short-chain fatty acids infused into the temporarily-isolated and washed reticulo-rumen of sheep. *Br J Nutr* 84: 477-482, 2000.
183. **Kristensen NB and Harmon DL.** Effect of increasing ruminal butyrate absorption on splanchnic metabolism of volatile fatty acids absorbed from the washed reticulorumen of steers. *J Anim Sci* 82: 3549-3559, 2004.
184. **Kristensen NB and Harmon DL.** Splanchnic metabolism of volatile fatty acids absorbed from the washed reticulorumen of steers. *J Anim Sci* 82: 2033-2042, 2004.
185. **Kristensen NB, Pierzynowski SG, and Danfaer A.** Net portal appearance of volatile fatty acids in sheep intraruminally infused with mixtures of acetate, propionate, isobutyrate, butyrate, and valerate. *J Anim Sci* 78: 1372-1379, 2000.
186. **Kunzelmann K and Mall M.** Electrolyte transport in the mammalian colon: mechanisms and implications for disease. *Physiol Rev* 82: 245-289, 2002.
187. **Lande MB, Donovan JM, and Zeidel ML.** The relationship between membrane fluidity and permeabilities to water, solutes, ammonia, and protons. *J Gen Physiol* 106: 67-84, 1995.
188. **Lang I.** *In vitro Untersuchungen zur Charakterisierung eines spannungsabhängigen Kationenkanals in der luminalen Membran des Pansenepithels beim Schaf*. Berlin: Freie Universität Berlin, 1997.
189. **Lang I and Martens H.** Na transport in sheep rumen is modulated by voltage-dependent cation conductance in apical membrane. *Am J Physiol* 277: G609-618, 1999.
190. **Lapierre H and Lobley G.** Nitrogen Recycling in the Ruminant: A Review. *J Dairy Sci* 84: E223-E236, 2001.
191. **Lawlor MJ, Giesecke D, and Walser-Karst K.** Comparative studies on the digestive physiology of sheep fed on semi-purified or roughage-concentrate diets. 1.

Food and water intake, rumen volume and rates of parotid secretion. *Br J Nutr* 20: 373-382, 1966.
192. **Leclercq S.** *Transportphysiologische Untersuchungen am isolierten Pansenepithel des Schafes unter Berücksichtigung verschiedener osmotischer Gradienten*. Berlin: Freie Universität Berlin, 1999.
193. **Leng RA and Nolan JV.** Nitrogen metabolism in the rumen. *J Dairy Sci* 67: 1072-1089, 1984.
194. **Leonhard-Marek S.** Divalent cations reduce the electrogenic transport of monovalent cations across rumen epithelium. *J Comp Physiol (B)* 172: 635-641, 2002.
195. **Leonhard-Marek S, Breves G, and Busche R.** Effect of chloride on pH microclimate and electrogenic Na+ absorption across the rumen epithelium of goat and sheep. *Am J Physiol Gastrointest Liver Physiol* 291: G246-252, 2006.
196. **Leonhard-Marek S, Breves G, and Busche R.** Effect of chloride on pH microclimate and electrogenic Na+ absorption across the rumen epithelium of goat and sheep. *Am J Physiol* 291: G246-252, 2006.
197. **Leonhard-Marek S, Gäbel G, and Martens H.** Effects of short chain fatty acids and carbon dioxide on magnesium transport across sheep rumen epithelium. *Exp Physiol* 83: 155-164, 1998.
198. **Leonhard-Marek S and Martens H.** Effects of potassium on magnesium transport across rumen epithelium. *Am J Physiol* 271: G1034-1038, 1996.
199. **Leonhard-Marek S, Stumpff F, Brinkmann I, Breves G, and Martens H.** Basolateral Mg2+/Na+ exchange regulates apical nonselective cation channel in sheep rumen epithelium via cytosolic Mg2+. *Am J Physiol* 288: G630-645, 2005.
200. **Leonhard-Marek S, Stumpff F, and Martens H.** Transport of cations and anions across forestomach epithelia: conclusions from in vitro studies. *Animal* 4: 1037-1056, 2010.
201. **Lesmeister KE and Heinrichs AJ.** Effects of corn processing on growth characteristics, rumen development, and rumen parameters in neonatal dairy calves. *J Dairy Sci* 87: 3439-3450, 2004.
202. **Lewis D, Hill KJ, and Annison EF.** Studies on the portal blood of sheep. I. Absorption of ammonia from the rumen of the sheep. *Biochem J* 66: 587-592, 1957.
203. **Linderholm H.** Active transport of ions through frog skin with special reference to the action of certain diuretics; a study of the relation between electrical properties, the flux of labelled ions, and respiration. *Acta Physiol Scand Suppl* 27: 1-144, 1952.
204. **Lobley GE, Bremner DM, and Zuur G.** Effects of diet quality on urea fates in sheep as assessed by refined, non-invasive [15N15N]urea kinetics. *Br J Nutr* 84: 459-468, 2000.
205. **Lodemann U and Martens H.** Effects of diet and osmotic pressure on Na+ transport and tissue conductance of sheep isolated rumen epithelium. *Exp Physiol* 91: 539-550, 2006.
206. **Lopez S, Hovell FD, Dijkstra J, and France J.** Effects of volatile fatty acid supply on their absorption and on water kinetics in the rumen of sheep sustained by intragastric infusions. *J Anim Sci* 81: 2609-2616, 2003.
207. **Lu Z, Abdoun, K., Stumpff, F., Martens, H.** Inhibition of ruminal urea transport by ammonia depends on luminal pH and SCFA. *Proc. Soc. Nutr. Physiol.*, Göttingen. DLG-Verlags-GmbH, 2010, p. 122.
208. **Lucas ML, Schneider W, Haberich FJ, and Blair JA.** Direct measurement by pH-microelectrode of the pH microclimate in rat proximal jejunum. *Proc R Soc Lond B Biol Sci* 192: 39-48, 1975.

209. **Ludden PA, Stohrer RM, Austin KJ, Atkinson RL, Belden EL, and Harlow HJ.** Effect of protein supplementation on expression and distribution of urea transporter-B in lambs fed low-quality forage. *J Anim Sci*, 2008.
210. **Ludden PA, Stohrer RM, Austin KJ, Atkinson RL, Belden EL, and Harlow HJ.** Effect of protein supplementation on expression and distribution of urea transporter-B in lambs fed low-quality forage. *J Anim Sci* 87: 1354-1365, 2009.
211. **Marini J, Sands J, and Van Amburgh M.** Urea transporters and urea recycling in ruminants. In: *In: Ruminant Physiology*, edited by Sejrsen K, Hvelplund T and Nielsen M. Wageningen, The Netherlands: Wageningen Academic Publishers, 2006, p. 155-171.
212. **Marini JC, Klein JD, Sands JM, and Van Amburgh ME.** Effect of nitrogen intake on nitrogen recycling and urea transporter abundance in lambs. *J Anim Sci* 82: 1157-1164, 2004.
213. **Marini JC and Van Amburgh ME.** Nitrogen metabolism and recycling in Holstein heifers. *J Anim Sci* 81: 545-552, 2003.
214. **Martens H.** Beziehungen zwischen Fütterung, Physiologie der Vormägen und der Pathogenese der Dislocatio abomasi. In: *Ätiologie, Pathogenese, Diagnostik, Prognose, Therapie und Prophylaxe der Dislocatio abomasi.*, edited by Fürll M. Leipzig, Germany: Leipziger Universitätsverlag, 2000, p. 81-101.
215. **Martens H and Blume I.** Effect of intraruminal sodium and potassium concentrations and of the transmural potential difference on magnesium absorption from the temporarily isolated rumen of sheep. *Q J Exp Physiol* 71: 409-415, 1986.
216. **Martens H and Blume I.** Studies on the absorption of sodium and chloride from the rumen of sheep. *Comp Biochem Physiol A* 86: 653-656, 1987.
217. **Martens H and Gäbel G.** Transport of Na and Cl across the epithelium of ruminant forestomachs: rumen and omasum. A review. *Comp Biochem Physiol A* 90: 569-575, 1988.
218. **Martens H, Gäbel G, and Strozyk B.** Mechanism of electrically silent Na and Cl transport across the rumen epithelium of sheep. *Exp Physiol* 76: 103-114, 1991.
219. **Martens H, Gäbel G, and Strozyk H.** The effect of potassium and the transmural potential difference on magnesium transport across an isolated preparation of sheep rumen epithelium. *Q J Exp Physiol* 72: 181-188, 1987.
220. **Martens H and Hammer U.** [Magnesium and sodium absorption from the isolated sheep rumen during intravenous aldosterone infusion (author's transl)]. *Dtsch Tierarztl Wochenschr* 88: 404-407, 1981.
221. **Martens H and Harmeyer J.** Magnesium transport by isolated rumen epithelium of sheep. *Res Vet Sci* 24: 161-168, 1978.
222. **Martens H, Harmeyer J, Breves G, and Scholz H.** [Magnesium absorption by the rumen mucosa in sheep]. *Z Tierphysiol Tierernahr Futtermittelkd* 37: 44-52, 1976.
223. **Martens H, Heggemann G, and Regier K.** Studies on the effect of K, Na, NH4+, VFA and CO2 on the net absorption of magnesium from the temporarily isolated rumen of heifers. *Zentralbl Veterinarmed A* 35: 73-80, 1988.
224. **Martens H and Rayssiguier Y.** Magnesium metabolism and hypomagnesaemia. In: Proceedings of the 5th International Symposium on Ruminant Physiology (ed. Ruckebush, Y & Thivend, P.). 447-466, 1980.
225. **Martens H and Schweigel M.** Pathophysiology of grass tetany and other hypomagnesemias. Implications for clinical management. *Vet Clin North Am Food Anim Pract* 16: 339-368, 2000.

226. **Martens H and Stossel EM.** Magnesium absorption from the temporarily isolated rumen of sheep: no effect of hyper- or hypomagnesaemia. *Q J Exp Physiol* 73: 217-223, 1988.
227. **Mascolo N, Rajendran VM, and Binder HJ.** Mechanism of short-chain fatty acid uptake by apical membrane vesicles of rat distal colon. *Gastroenterology* 101: 331-338, 1991.
228. **Masson MJ and Philipson AT.** The composition of the digesta leaving the abomasum of sheep. *J Physiol* 116: 98-111, 1952.
229. **Masson MJ and Phillipson AT.** The absorption of acetate, propionate and butyrate from the rumen of sheep. *J Physiol* 113: 189-206, 1951.
230. **McDonald IW.** The absorption of ammonia from the rumen of the sheep. *Biochem J* 42: 584-587, 1948.
231. **McLaren GA, Anderson GC, Martin WG, and Cooper WK.** Fixation of ammonia nitrogen by rumen mucosa. *J Anim Sci* 20: 942-943, 1961.
232. **McLean AF, Buchan W, and Scott D.** Magnesium absorption in mature ewes infused intrarumenally with magnesium chloride. *Br J Nutr* 52: 523-527, 1984.
233. **Missner A and Pohl P.** 110 years of the Meyer-Overton rule: predicting membrane permeability of gases and other small compounds. *Chemphyschem* 10: 1405-1414, 2009.
234. **Monteilh-Zoller MK, Hermosura MC, Nadler MJ, Scharenberg AM, Penner R, and Fleig A.** TRPM7 provides an ion channel mechanism for cellular entry of trace metal ions. *J Gen Physiol* 121: 49-60, 2003.
235. **Mooney CS.** *Regulation of the ruminal environment by lactating dairy cows* (Dissertation). Michigan: Michigan State University, 2006.
236. **Mooney P and O'Donovan DJ.** The permeability of the rumen to simple nitrogenous compounds. *Biochem J* 119: 18P-19P, 1970.
237. **Morgante M, Stelletta C, Berzaghi P, Gianesella M, and Andrighetto I.** Subacute rumen acidosis in lactating cows: an investigation in intensive Italian dairy herds. *J Anim Physiol Anim Nutr (Berl)* 91: 226-234, 2007.
238. **Morris JG and Gartner RW.** The effect of potassium on the sodium requirements of growing steers with and without alpha-tocopherol supplementation. *Br J Nutr* 34: 1-14, 1975.
239. **Müller F, Aschenbach JR, and Gäbel G.** Role of Na+/H+ exchange and HCO3- transport in pHi recovery from intracellular acid load in cultured epithelial cells of sheep rumen. *J Comp Physiol (B)* 170: 337-343, 2000.
240. **Müller F, Huber K, Pfannkuche H, Aschenbach JR, Breves G, and Gäbel G.** Transport of ketone bodies and lactate in the sheep ruminal epithelium by monocarboxylate transporter 1. *Am J Physiol Gastrointest Liver Physiol* 283: G1139-1146, 2002.
241. **Musa-Aziz R, Chen LM, Pelletier MF, and Boron WF.** Relative CO2/NH3 selectivities of AQP1, AQP4, AQP5, AmtB, and RhAG. *Proc Natl Acad Sci U S A* 106: 5406-5411, 2009.
242. **Musa-Aziz R, Jiang L, Chen LM, Behar KL, and Boron WF.** Concentration-dependent effects on intracellular and surface pH of exposing Xenopus oocytes to solutions containing NH3/NH4(+). *J Membr Biol* 228: 15-31, 2009.
243. **Mutoh K and Wakuri H.** Early organogenesis of the caprine stomach. *Nippon Juigaku Zasshi* 51: 474-484, 1989.
244. **Nagaraja TG and Titgemeyer EC.** Ruminal acidosis in beef cattle: the current microbiological and nutritional outlook. *J Dairy Sci* 90 Suppl 1: E17-38, 2007.
245. **Nielsen AL and Bang HO.** The influence of diet on the renal function of healthy persons. *Acta Med Scand* 130: 382-388, 1948.

246. **Nilius B and Droogmans G.** Amazing chloride channels: an overview. *Acta Physiol Scand* 177: 119-147, 2003.
247. **Norlin A, Lu LN, Guggino SE, Matthay MA, and Folkesson HG.** Contribution of amiloride-insensitive pathways to alveolar fluid clearance in adult rats. *J Appl Physiol* 90: 1489-1496, 2001.
248. **Norton BW, Janes AN, and Armstrong DG.** The effects of intraruminal infusions of sodium bicarbonate, ammonium chloride and sodium butyrate on urea metabolism in sheep. *Br J Nutr* 48: 265-274, 1982.
249. **Norton BW, Mackintosh JB, and Armstrong DG.** Urea synthesis and degradation in sheep given pelleted-grass diets containing flaked barley. *Br J Nutr* 48: 249-264, 1982.
250. **Oba M, Baldwin RLt, Owens SL, and Bequette BJ.** Metabolic fates of ammonia-N in ruminal epithelial and duodenal mucosal cells isolated from growing sheep. *J Dairy Sci* 88: 3963-3970, 2005.
251. **Obara Y, Dellow D, and Nolan J.** Effects of energy-rich supplements on nitrogen kinetics in ruminants. In: *Physiological aspects of digestion and metabolism in ruminants*, edited by Tsuda T, Sasaki Y and Kawashima R. San Diego, Ca.: Academic Press, 1991, p. 551-539.
252. **Orbach E and Finkelstein A.** The nonelectrolyte permeability of planar lipid bilayer membranes. *J Gen Physiol* 75: 427-436, 1980.
253. **Owens FN, Secrist DS, Hill WJ, and Gill DR.** Acidosis in cattle: a review. *J Anim Sci* 76: 275-286, 1998.
254. **Owsianik G, Talavera K, Voets T, and Nilius B.** Permeation and selectivity of TRP channels. *Annu Rev Physiol* 68: 685-717, 2006.
255. **Parker DS, Lomax MA, Seal CJ, and Wilton JC.** Metabolic implications of ammonia production in the ruminant. *Proc Nutr Soc* 54: 549-563, 1995.
256. **Paula S, Volkov AG, Van Hoek AN, Haines TH, and Deamer DW.** Permeation of protons, potassium ions, and small polar molecules through phospholipid bilayers as a function of membrane thickness. *Biophys J* 70: 339-348, 1996.
257. **Penner GB, Aschenbach JR, Gäbel G, Rackwitz R, and Oba M.** Epithelial capacity for apical uptake of short chain fatty acids is a key determinant for intraruminal pH and the susceptibility to subacute ruminal acidosis in sheep. *J Nutr* 139: 1714-1720, 2009.
258. **Penner GB, Taniguchi M, Guan LL, Beauchemin KA, and Oba M.** Effect of dietary forage to concentrate ratio on volatile fatty acid absorption and the expression of genes related to volatile fatty acid absorption and metabolism in ruminal tissue. *J Dairy Sci* 92: 2767-2781, 2009.
259. **Peters D.** Molecular adaptation of the urea transporter (UT) in ruminal and colonic epithelia of goats as affected by dietary nitrogen and energy intake. *Ph D Dissertation, Dept of Vet Med, Hannover*, 2007.
260. **Pfeffer E, Thompson A, and Armstrong DG.** Studies on intestinal digestion in the sheep. 3. Net movement of certain inorganic elements in the digestive tract on rations containing different proportions of hay and rolled barley. *Br J Nutr* 24: 197-204, 1970.
261. **Phillipson AT and McAnnally RA.** Studies on the fate of Carbohydrates in the Rumen of Sheep. *J Exp Biol* 19: 199, 1942.
262. **Pilgrim AF, Gray FV, and Belling GB.** Production and absorption of ammonia in the sheep's stomach. *Br J Nutr* 23: 647-655, 1969.

263. **Plaizier JC, Krause DO, Gozho GN, and McBride BW.** Subacute ruminal acidosis in dairy cows: The physiological causes, incidence and consequences. *Vet J* 176: 21-31, 2008.
264. **Price NT, Jackson VN, and Halestrap AP.** Cloning and sequencing of four new mammalian monocarboxylate transporter (MCT) homologues confirms the existence of a transporter family with an ancient past. *Biochem J* 329 (Pt 2): 321-328, 1998.
265. **Rabbani I, Siegling-Vlitakis, Dölle M, Noci B, and Martens H.** Electroneutral Na transport in sheep and bovine forestomach is mediated via NHE3 and not via NHE1. *Proc. Fachgruppe Physiologie und Biochemie der DVG*, Hannover, 2010.
266. **Rabinowitz L.** Aldosterone and potassium homeostasis. *Kidney Int* 49: 1738-1742, 1996.
267. **Rabinowitz L, Green DM, Sarason RL, and Yamauchi H.** Homeostatic potassium excretion in fed and fasted sheep. *Am J Physiol* 254: R357-380, 1988.
268. **Rabinowitz L, Sarason RL, and Yamauchi H.** Effect of aldosterone on potassium excretion during potassium chloride infusion in sheep. *Am J Physiol* 249: R455-461, 1985.
269. **Rabinowitz L, Sarason RL, and Yamauchi H.** Sheep renal potassium excretion: efferent kaliuretic regulatory factors. *Am J Physiol* 247: F520-526, 1984.
270. **Rabinowitz L, Sarason RL, Yamauchi H, Yamanaka KK, and Tzendzalian PA.** Time course of adaptation to altered K intake in rats and sheep. *Am J Physiol* 247: F607-617, 1984.
271. **Rahnema SH and Fontenot JP.** Effects of intravenous infusion of high levels of potassium and sodium on mineral metabolism in sheep. *J Anim Sci* 68: 2833-2838, 1990.
272. **Raymond WA and Leong AS.** Co-expression of cytokeratin and vimentin intermediate filament proteins in benign and neoplastic breast epithelium. *J Pathol* 157: 299-306, 1989.
273. **Read B.** Chemical constituents of camel's urine. *J Biol Chem* 64: 615-617, 1925.
274. **Remond D, Bernard L, Savary-Auzeloux I, and Noziere P.** Partitioning of nutrient net fluxes across the portal-drained viscera in sheep fed twice daily: effect of dietary protein degradability. *Br J Nutr*: 1-12, 2009.
275. **Remond D, Chaise JP, Delval E, and Poncet C.** Net flux of metabolites across the ruminal wall of sheep fed twice a day with orchardgrass hay. *J Anim Sci* 71: 2529-2538, 1993.
276. **Remond D, Chaise JP, Delval E, and Poncet C.** Net transfer of urea and ammonia across the ruminal wall of sheep. *J Anim Sci* 71: 2785-2792, 1993.
277. **Reynolds CK and Huntington GB.** Partition of portal-drained visceral net flux in beef steers. 1. Blood flow and net flux of oxygen, glucose and nitrogenous compounds across stomach and post-stomach tissues. *Br J Nutr* 60: 539-551, 1988.
278. **Reynolds CK and Kristensen NB.** Nitrogen recycling through the gut and the nitrogen economy of ruminants: an asynchronous symbiosis. *J Anim Sci* 86: E293-305, 2008.
279. **Reynolds M.** Measurement of bovine plasma and blood volume during pregnancy and lactation. *Am J Physiol* 175: 118-122, 1953.
280. **Richard MH, Viac J, Reano A, Gaucherand M, and Thivolet J.** Vimentin expression in normal human keratinocytes grown in serum-free defined MCDB 153 medium. *Arch Dermatol Res* 282: 512-515, 1990.

281. **Ritzhaupt A, Breves G, Schröder B, Winckler C, and Shirazi-Beechey S.** Urea transport in gastrointestinal tract of ruminants: effect of dietary nitrogen. *Biochem Soc Trans* 25: S 490, 1997.
282. **Ritzhaupt A, Breves G, Schröder B, Winckler C, and Shirazi-Beechey SUtigtoreodnBSTSA.** Urea transport in gastrointestinal tract of ruminants: effect of dietary nitrogen. *Biochemical Society Transaction* 25: S 490, 1997.
283. **Ritzhaupt A, Wood I, Jackson A, Moran B, and Shirazi-Beechey S.** Isolation of a RT-PCR fragment from human colon and sheep rumen RNA with nucleotide sequence similarity to human and rat urea transporter isoforms. *Biochemical Society Transaction* 26: S 122, 1998.
284. **Romero MF, Fulton CM, and Boron WF.** The SLC4 family of HCO 3 - transporters. *Pflugers Arch* 447: 495-509, 2004.
285. **Roos A.** Intracellular pH and distribution of weak acids across cell membranes. A study of D- and L-lactate and of DMO in rat diaphragm. *J Physiol* 249: 1-25, 1975.
286. **Roos A and Boron WF.** Intracellular pH. *Physiol Rev* 61: 296-434, 1981.
287. **Rossier BC.** The epithelial sodium channel: activation by membrane-bound serine proteases. *Proc Am Thorac Soc* 1: 4-9, 2004.
288. **Rossier BC, Pradervand S, Schild L, and Hummler E.** Epithelial sodium channel and the control of sodium balance: interaction between genetic and environmental factors. *Annu Rev Physiol* 64: 877-897, 2002.
289. **Roy CC, Kien CL, Bouthillier L, and Levy E.** Short-chain fatty acids: ready for prime time? *Nutr Clin Pract* 21: 351-366, 2006.
290. **Rübbelke MK.** *In vitro Untersuchungen des Pansenepithels von Schafen zur Characterisierung eines elektrogenen, calcium-sensitiven Natriumtransportes*. Berlin: Freie Universität Berlin, 1998.
291. **Rübsamen K and von Engelhardt W.** Absorption of Na, H ions and short chain fatty acids from the sheep colon. *Pflugers Arch* 391: 141-146, 1981.
292. **Rupp GP, Kreikemeier KK, Perino LJ, and Ross GS.** Measurement of volatile fatty acid disappearance and fluid flux across the abomasum of cattle, using an improved omasal cannulation technique. *Am J Vet Res* 55: 522-529, 1994.
293. **Sabirov RZ and Okada Y.** The maxi-anion channel: a classical channel playing novel roles through an unidentified molecular entity. *J Physiol Sci* 59: 3-21, 2009.
294. **Sabirov RZ, Sheiko T, Liu H, Deng D, Okada Y, and Craigen WJ.** Genetic demonstration that the plasma membrane maxianion channel and voltage-dependent anion channels are unrelated proteins. *J Biol Chem* 281: 1897-1904, 2006.
295. **Sachs G, Kraut JA, Wen Y, Feng J, and Scott DR.** Urea transport in bacteria: acid acclimation by gastric Helicobacter spp. *J Membr Biol* 212: 71-82, 2006.
296. **Sands JM.** Urea transporter UT-B. *UCSD-Nature Molecule Pages*, 2006.
297. **Sargison ND, Macrae AI, and Scott PR.** Hypomagnesaemic tetany in lactating Cheviot gimmers associated with pasture sodium deficiency. *Vet Rec* 155: 674-676, 2004.
298. **Satter LD and Slyter LL.** Effect of ammonia concentration of rumen microbial protein production in vitro. *Br J Nutr* 32: 199-208, 1974.
299. **Schmidt RF, Lang F, and Thews G.** *Physiology des Menschen*. Heidelberg: Springer, 2004.
300. **Schmidt-Nielsen B and Osaki H.** Renal response to changes in nitrogen metabolism in sheep. *Am J Physiol* 193: 657-661, 1958.

301. **Schnorr B.** Histochemical, electron microscopic and biochemical studies on ATPases in the forestomach epithelium of goats. *Zeitschrift für Zellforschung Mikroskopie und Anatomie* 114, 1971.
302. **Schonewille JT, Everts H, Jittakhot S, and Beynen AC.** Quantitative prediction of magnesium absorption in dairy cows. *J Dairy Sci* 91: 271-278, 2008.
303. **Schröder B, Rittmann I, Pfeffer E, and Breves G.** In vitro studies on calcium absorption from the gastrointestinal tract in small ruminants. *J Comp Physiol (B)* 167: 43-51, 1997.
304. **Schröder B, Vossing S, and Breves G.** In vitro studies on active calcium absorption from ovine rumen. *J Comp Physiol (B)* 169: 487-494, 1999.
305. **Schröder B, Vossing S, and Breves G.** In vitro studies on active calcium absorption from ovine rumen. *J Comp Physiol [B]* 169: 487-494, 1999.
306. **Schultheiss G and Diener M.** K+ and Cl- conductances in the distal colon of the rat. *Gen Pharmacol* 31: 337-342, 1998.
307. **Schultheiss G and Martens H.** Ca-sensitive Na transport in sheep omasum. *Am J Physiol* 276: G1331-1344, 1999.
308. **Schultz SG, Zalusky R, and Gass AE, Jr.** Ion Transport in Isolated Rabbit Ileum. 3. Chloride Fluxes. *J Gen Physiol* 48: 375-378, 1964.
309. **Schwab CG, Huhtanen P, Hunt CW, and Hvelplund T.** Nitrogen requirements of cattle. In: *Nitrogen and Phosphorus Nutrition of Cattle. Reducing the Environmental Impact of Cattle Operations*, edited by Pfeffer E and Hristov A. King's Lynn, UK.: Biddles Ltd., 2005, p. 13-70.
310. **Schweigel M, Freyer M, Leclercq S, Etschmann B, Lodemann U, Bottcher A, and Martens H.** Luminal hyperosmolarity decreases Na transport and impairs barrier function of sheep rumen epithelium. *J Comp Physiol (B)* 175: 575-591, 2005.
311. **Schweigel M, Kolisek M, Nikolic Z, and Kuzinski J.** Expression and functional activity of the Na/Mg exchanger, TRPM7 and MagT1 are changed to regulate Mg homeostasis and transport in rumen epithelial cells. *Magnes Res* 21: 118-123, 2008.
312. **Schweigel M, Lang I, and Martens H.** Mg(2+) transport in sheep rumen epithelium: evidence for an electrodiffusive uptake mechanism. *Am J Physiol* 277: G976-982, 1999.
313. **Schweigel M and Martens H.** Anion-dependent Mg2+ influx and a role for a vacuolar H+-ATPase in sheep ruminal epithelial cells. *Am J Physiol* 285: G45-53, 2003.
314. **Schweigel M, Park HS, Etschmann B, and Martens H.** Characterization of the Na+-dependent Mg2+ transport in sheep ruminal epithelial cells. *Am J Physiol* 290: G56-65, 2006.
315. **Schweigel M, Vormann J, and Martens H.** Mechanisms of Mg(2+) transport in cultured ruminal epithelial cells. *Am J Physiol* 278: G400-408, 2000.
316. **Scott D.** Changes in mineral, water and acid base balance associated with feeding and diet. *Digestion and metabolism in the ruminant: Proceedings of the IV International Symposium on Ruminant Physiology (1974) ed: IW McDonald and ACI Warner*
The University of New England Publishing Unit (1975), 1975.
317. **Scott D.** The effects of potassium supplements upon the absorption of potassium and sodium from the sheep rumen. *Q J Exp Physiol Cogn Med Sci* 52: 382-391, 1967.
318. **Scott D.** The effects of sodium depletion and potassium supplements upon electrical potentials in the rumen of the sheep. *Q J Exp Physiol Cogn Med Sci* 51: 60-69, 1966.

319. **Scott D.** The effects of variations in water or potassium intake on the renal excretion of potassium in sheep. *Q J Exp Physiol Cogn Med Sci* 54: 16-24, 1969.
320. **Sehested J, Diernaes L, Moller PD, and Skadhauge E.** Interaction between absorption of sodium and acetate across the rumen epithelium of cattle. *Acta Vet Scand Suppl* 89: 107-108, 1993.
321. **Sehested J, Diernaes L, Moller PD, and Skadhauge E.** Transport of butyrate across the isolated bovine rumen epithelium--interaction with sodium, chloride and bicarbonate. *Comp Biochem Physiol A Mol Integr Physiol* 123: 399-408, 1999.
322. **Sehested J, Diernaes L, Moller PD, and Skadhauge E.** Transport of sodium across the isolated bovine rumen epithelium: interaction with short-chain fatty acids, chloride and bicarbonate. *Exp Physiol* 81: 79-94, 1996.
323. **Seidler U, Singh AK, Cinar A, Chen M, Hillesheim J, Hogema B, and Riederer B.** The role of the NHERF family of PDZ scaffolding proteins in the regulation of salt and water transport. *Ann N Y Acad Sci* 1165: 249-260, 2009.
324. **Sellers AF and Dobson A.** Studies on reticulo-rumen sodium and potassium concentration and electrical potentials in sheep. *Res Vet Sci* 1: 95-102, 1960.
325. **Sellin JH.** SCFAs: The Enigma of Weak Electrolyte Transport in the Colon. *News Physiol Sci* 14: 58-64, 1999.
326. **Sellin JH, DeSoignie R, and Burlingame S.** Segmental differences in short-chain fatty acid transport in rabbit colon: effect of pH and Na. *J Membr Biol* 136: 147-158, 1993.
327. **Seo S, Lanzas C, Tedeschi LO, and Fox DG.** Development of a mechanistic model to represent the dynamics of liquid flow out of the rumen and to predict the rate of passage of liquid in dairy cattle. *J Dairy Sci* 90: 840-855, 2007.
328. **Shen Z, Seyfert HM, Lohrke B, Schneider F, Zitnan R, Chudy A, Kuhla S, Hammon HM, Blum JW, Martens H, Hagemeister H, and Voigt J.** An energy-rich diet causes rumen papillae proliferation associated with more IGF type 1 receptors and increased plasma IGF-1 concentrations in young goats. *J Nutr* 134: 11-17, 2004.
329. **Siddons RC, Nolan JV, Beever DE, and Macrae JC.** Nitrogen digestion and metabolism in sheep consuming diets containing contrasting forms and levels of N. *Br J Nutr* 54: 175-187, 1985.
330. **Silanikove N.** The struggle to maintain hydration and osmoregulation in animals experiencing severe dehydration and rapid rehydration: the story of ruminants. *Exp Physiol* 79: 281-300, 1994.
331. **Silanikove N and Tadmor A.** Rumen volume, saliva flow rate, and systemic fluid homeostasis in dehydrated cattle. *Am J Physiol* 256: R809-815, 1989.
332. **Sjaastad OV, Hove K, and Olav S.** *Physiology of Domestic Animals*. Oslo: Scandinavian Veterinary Press, 2003.
333. **Sjollema B.** On the nature and therapy of grass staggers. *Vet Rec* 10: 425, 1930.
334. **Sjollema B.** Untersuchungen über die Ursache der Grastetanie und der großen Frequenzzunahme dieser Krankheit. *Deutsche Tierärztliche Wochenzeitschrift* 15, 1932.
335. **Sklan D and Hurwitz S.** Movement and absorption of major minerals and water in ovine gastrointestinal tract. *J Dairy Sci* 68: 1659-1666, 1985.
336. **Skou JC.** The influence of some cations on an adenosine triphosphatase from peripheral nerves. *Biochim Biophys Acta* 23: 394-401, 1957.
337. **Sperber I and Hyden S.** Transport of chloride through the ruminal mucosa. *Nature* 169: 587, 1952.

338. **Stacy BD and Warner AC.** Acute effects on hypertonicity on the potential difference across the rumen wall in sheep. *Comp Biochem Physiol A* 43: 637-641, 1972.
339. **Stacy BD and Warner AC.** Balances of water and sodium in the rumen during feeding: osmotic stimulation of sodium absorption in the sheep. *Q J Exp Physiol Cogn Med Sci* 51: 79-93, 1966.
340. **Steele MA, AlZahal O, Hook SE, Croom J, and McBride BW.** Ruminal acidosis and the rapid onset of ruminal parakeratosis in a mature dairy cow: a case report. *Acta Vet Scand* 51: 39, 2009.
341. **Stevens CE.** Transport of Sodium and Chloride by the Isolated Rumen Epithelium. *Am J Physiol* 206: 1099-1105, 1964.
342. **Stevens CE and Hume ID.** *Comparative Physiology of the Vertebrate Digestive System*. Cambridge, England: Cambridge Univ. Press, 1995.
343. **Stevens CE and Stettler BK.** Transport of fatty acid mixtures across rumen epithelium. *Am J Physiol* 211: 264-271, 1966.
344. **Stevens MH, Thirlby RC, and Feldman M.** Mechanism for high PCO2 in gastric juice: roles of bicarbonate secretion and CO2 diffusion. *Am J Physiol* 253: G527-530, 1987.
345. **Stewart GS, Graham C, Cattell S, Smith TP, Simmons NL, and Smith CP.** UT-B is expressed in bovine rumen: potential role in ruminal urea transport. *Am J Physiol Regul Integr Comp Physiol* 289: R605-R612, 2005.
346. **Stone WC.** Nutritional approaches to minimize subacute ruminal acidosis and laminitis in dairy cattle. *J Dairy Sci* 87: E13-E26, 2004.
347. **Storeheier PV, Sehested J, Diernaes L, Sundset MA, and Mathiesen SD.** Effects of seasonal changes in food quality and food intake on the transport of sodium and butyrate across ruminal epithelium of reindeer. *J Comp Physiol (B)* 173: 391-399, 2003.
348. **Stumpff F, Bondzio A, Einspanier R, and Martens H.** Effects of the Bacillus thuringiensis toxin Cry1Ab on membrane currents of isolated cells of the ruminal epithelium. *J Membr Biol* 219: 37-47, 2007.
349. **Stumpff F, Brinkmann I, and Martens H.** Isolated cells of the ruminal epithelium express chloride channels. *Proc Soc Nutr Physiol* 14: 100, 2005.
350. **Stumpff F, Brinkmann I, and Martens H.** Regulation of a non-selective cation channel in cells of the ovine rumen epithelium by PGE2 and Forskolin. *Pflugers Arch*, 2005, p. P-16-14.
351. **Stumpff F, Brinkmann I, Schweigel M, and Martens H.** High potassium diet, sodium and magnesium in ruminants: the story is not over. In: *Production diseases in farm animals*, edited by Joshi NP and Herdt TH, 2004, p. 284-285.
352. **Stumpff F, Brinkmann I, Schweigel M, and Martens H.** Regulation of electrogenic sodium transport across the ruminal epithelium involves a divalent sensitive cation channel. *Pflugers Arch* 447: O-28, 2004.
353. **Stumpff F, Georgi MI, and Martens H.** The ruminal anion channel: a pathway for the efflux of SCFA. *XIth International Symposium on Ruminant Physiology*, edited by Chilliard Y, Glasser F, Faulconnier Y, Bocquier F, Veissier I and Doreau M, Clermont-Ferrand, France. Wageningen Academic Publishers, the Netherlands, 2009, p. 366.
354. **Stumpff F, Georgi MI, Martens H, and Gäbel G.** Ruminal epithelial cells express a conductance for Propionate. *Acta Physiol*, 2009, p. P175.
355. **Stumpff F, Georgi, M.I., Martens, H.** Isolated cells of the omasum express tight junction proteins and maxi-anion channels with a conductance for acetate and propionate. *Acta Physiol.*, 2010, p. O-Sun-6-8.

356. **Stumpff F, Georgi, M.I., Martens, H.** The permeability of the large conductance anion channel of the ruminal epithelium decreases with increasing chain length. *Acta Physiol*, 2010, p. P-Mon-90.
357. **Stumpff F, Leonhard-Marek S, and Martens H.** Forskolin affects Na, but not K currents across the membrane of isolated ruminal epithelial cells in the whole cell configuration J. Physiol. Biochem. 61 (4): 582, 200. *J Physiol. Biochem.*, 2005, p. 581.
358. **Stumpff F and Martens H.** A role for magnesium in the regulation of ruminal sodium transport. In: *Focus on signal transduction research*, edited by McAlpine G. New York: New Nova Science Publishers, Inc. (ISBN 13 978-1-60021-376-2), 2006, p. 37-66.
359. **Stumpff F and Martens H.** The rumen and potassium homeostasis: a model. *Journal of Animal and Feed Sciences* 16: 436-441, 2007.
360. **Stumpff F, Martens H, Bilk S, Aschenbach JR, and Gäbel G.** Cultured ruminal epithelial cells express a large-conductance channel permeable to chloride, bicarbonate, and acetate. *Pflugers Arch* 457: 1003-1022, 2009.
361. **Stumpff F, Martens H, and Schweigel M.** A patch-clamp and furaptra study of electrodiffusive Mg uptake into cells of the ruminal epithelium. *Acta Physiol*, 2006, p. 232 (PW203A-217).
362. **Stumpff F, Martens, H., Gäbel, G.** Ruminal transport of SCFA. *Proc. Fachgruppe Physiologie und Biochemie der DVG*, Hannover. Verlag der DVG, 2010, p. 36-41.
363. **Suttle NF and Field AC.** Studies on magnesium in ruminant nutrition. 8. Effect of increased intakes of potassium and water on the metabolism of magnesium, phosphorus, sodium, potassium and calcium in sheep. *Br J Nutr* 21: 819-831, 1967.
364. **Svendsen P.** Etiology and pathogenesis of abomasal displacement in cattle. *Nordisk Veterinärmedizin 21* (Suppl. 1): 1-60, 1969.
365. **Thompson DJ, Beever DE, Lonsdale CR, Haines MJ, Cammell SB, and Austin AR.** The digestion by cattle of grass silage made with formic acid and formic acid-formaldehyde. *Br J Nutr* 46: 193-207, 1981.
366. **Thorlacius SO, Dobson A, and Sellers AF.** Effect of carbon dioxide on urea diffusion through bovine ruminal epithelium. *Am J Physiol* 220: 162-170, 1971.
367. **Tiling C.** *In vitro Untersuchungen zum Chloridionentransport des Blättermagenepithels von Schafen*. Berlin: Free University, 1997.
368. **Tomakidi P, Fusenig NE, Kohl A, and Komposch G.** Histomorphological and biochemical differentiation capacity in organotypic co-cultures of primary gingival cells. *J Periodontal Res* 32: 388-400, 1997.
369. **Tomas FM and Potter BJ.** The site of magnesium absorption from the ruminant stomach. *Br J Nutr* 36: 37-45, 1976.
370. **Tosteson DC.** Halide transport in red cells. *Acta Physiol Scand* 46: 19-41, 1959.
371. **Trautmann A.** Beiträge zur Physiologie des Wiederkäuermagens. VI. Mitteilung. Über die Resorption in Wiederkäuermägen. *Arch Tierernähr Tierz* 9: 178-193, 1933.
372. **Uppal SK, Wolf K, Khahra SS, and Martens H.** Modulation of Na+ transport across isolated rumen epithelium by short-chain fatty acids in hay- and concentrate-fed sheep. *J Anim Physiol Anim Nutr (Berl)* 87: 380-388, 2003.
373. **Ussing HH and Zerahn K.** Active transport of sodium as the source of electric current in the short-circuited isolated frog skin. *Acta Physiol Scand* 23: 110-127, 1951.

374. **v. Engelhardt W and Nickel W.** Factors influencing the endogenous urea-N secretion and utilization in the gastrointestinal tract. In: *Ruminants digestion and feed evaluation*, edited by Osboum D, Beever D and Thomson D. London: Agricultural Research Council, 1978, p. 4.1-4.12.
375. **van der Velden LA, Manni JJ, Ramaekers FC, and Kuijpers W.** Expression of intermediate filament proteins in benign lesions of the oral mucosa. *Eur Arch Otorhinolaryngol* 256: 514-519, 1999.
376. **Van Driessche W and Zeiske W.** Ionic channels in epithelial cell membranes. *Physiol Rev* 65: 833-903, 1985.
377. **Vanhatalo A, Kuoppala K, Ahvenjarvi S, and Rinne M.** Effects of feeding grass or red clover silage cut at two maturity stages in dairy cows. 1. Nitrogen metabolism and supply of amino acids. *J Dairy Sci* 92: 5620-5633, 2009.
378. **Vidyasagar S, Barmeyer C, Geibel J, Binder HJ, and Rajendran VM.** Role of short-chain fatty acids in colonic HCO(3) secretion. *Am J Physiol* 288: G1217-1226, 2005.
379. **Voets T, Janssens A, Prenen J, Droogmans G, and Nilius B.** Mg2+-dependent gating and strong inward rectification of the cation channel TRPV6. *J Gen Physiol* 121: 245-260, 2003.
380. **Waisbren SJ, Geibel JP, Modlin IM, and Boron WF.** Unusual permeability properties of gastric gland cells. *Nature* 368: 332-335, 1994.
381. **Wakabayashi S, Hisamitsu T, Pang T, and Shigekawa M.** Kinetic dissection of two distinct proton binding sites in Na+/H+ exchangers by measurement of reverse mode reaction. *J Biol Chem* 278: 43580-43585, 2003.
382. **Walter A and Gutknecht J.** Permeability of small nonelectrolytes through lipid bilayer membranes. *J Membr Biol* 90: 207-217, 1986.
383. **Walter A, Hastings D, and Gutknecht J.** Weak acid permeability through lipid bilayer membranes. Role of chemical reactions in the unstirred layer. *J Gen Physiol* 79: 917-933, 1982.
384. **Warner AC and Stacy BD.** Intraruminal and systemic responses to variations in intake of sodium and potassium by sheep. *Q J Exp Physiol Cogn Med Sci* 57: 89-102, 1972.
385. **Warner AC and Stacy BD.** Solutes in the Rumen of the Sheep. *Q J Exp Physiol Cogn Med Sci* 50: 169-184, 1965.
386. **Warner AC and Stacy BD.** Water, sodium and potassium movements across the rumen wall of sheep. *Q J Exp Physiol Cogn Med Sci* 57: 103-119, 1972.
387. **Webb DW, Bartley EE, and Meyer RM.** A comparison of nitrogen metabolism and ammonia toxicity from ammonium acetate and urea in cattle. *J Anim Sci* 35: 1263-1270, 1972.
388. **Weiss WP.** Macromineral digestion by lactating dairy cows: factors affecting digestibility of magnesium. *J Dairy Sci* 87: 2167-2171, 2004.
389. **Wickersham TA, Titgemeyer EC, Cochran RC, Wickersham EE, and Gnad DP.** Effect of rumen-degradable intake protein supplementation on urea kinetics and microbial use of recycled urea in steers consuming low-quality forage. *J Anim Sci* 86: 3079-3088, 2008.
390. **Wilkens M, Kunert-Keil C, Brinkmeier H, and Schröder B.** Expression of calcium channel TRPV6 in ovine epithelial tissue. *Veterinary Journal (Epub)*, 2008.
391. **Wilkens M, Kunert-Keil C, and Schröder B.** Expression of the epithelial Ca^{2+} channels TRPV5 and TRPV6 in ovine Ca^{2+} transporting tissues. *Acta Physiol* 186(Suppl): 232 (PW203A-215), 2006.
392. **Winkler FK.** Amt/MEP/Rh proteins conduct ammonia. *Pflugers Arch* 451: 701-707, 2006.

393. **Wolffram S, Frischknecht R, and Scharrer E.** Influence of theophylline on the electrical potential difference and ion fluxes (Na, Cl, K) across the isolated rumen epithelium of sheep. *Zentralbl Veterinarmed A* 36: 755-762, 1989.
394. **Woodford ST, Murphy MR, and Davis CL.** Water dynamics of dairy cattle as affected by initiation of lactation and feed intake. *J Dairy Sci* 67: 2336-2343, 1984.
395. **Wright EM and Diamond JM.** Anion selectivity in biological systems. *Physiol Rev* 57: 109-156, 1977.
396. **Wylie MJ, Fontenot JP, and Greene LW.** Absorption of magnesium and other macrominerals in sheep infused with potassium in different parts of the digestive tract. *J Anim Sci* 61: 1219-1229, 1985.
397. **Yang MG and Thomas JW.** Absorption and secretion of some organic and inorganic constituents and the distribution of these constituents throughout the alimentary tract of young calves. *J Nutr* 87: 444-458, 1965.
398. **Yellen G.** Permeation in potassium channels: implications for channel structure. *Annu Rev Biophys Biophys Chem* 16: 227-246, 1987.
399. **Yellen G.** The voltage-gated potassium channels and their relatives. *Nature* 419: 35-42, 2002.
400. **Zachos NC, Tse M, and Donowitz M.** Molecular physiology of intestinal Na+/H+ exchange. *Annu Rev Physiol* 67: 411-443, 2005.
401. **Zitnan R, Voigt J, Schonhusen U, Wegner J, Kokardova M, Hagemeister H, Levkut M, Kuhla S, and Sommer A.** Influence of dietary concentrate to forage ratio on the development of rumen mucosa in calves. *Arch Tierernahr* 51: 279-291, 1998.

10 Abbreviations

NHE	Sodium proton exchanger (= Na^+/H^+ exchanger) pH regulatory protein that exchanges extracellular sodium for intracellular protons
NHE3	Subtype of NHE; found apically in the rumen
NHE1	Subtype of NHE; found basolaterally in the rumen
MCT1	Monocarboxylate transporter 1: cotransport of protons and large anions
CFTR	Cystic Fibrosis Transmembrane Conductance Regulator: cAMP regulated anion channel
ENaC	Epithelial sodium channel
cAMP	Cyclic adenosine monophosphate. Intracellular second messenger
DIDS	Blocker of anion-transporting proteins (transporters and channels) 4,4' - Diisothiocyanatostilbene - 2,2' - disulfonic acid, disodium salt
HEPES	2-(4-(2-Hydroxyethyl)- 1-piperazinyl)-ethansulfonic acid: Buffer
NMDG	N-Methyl-D-glucamine: large cation used as a substitute for e.g. Na^+
pH_i	Intracellular pH
Σx_i	Sum of the arguments x_i (= $x_1 + x_2 + x_3 + x_4 + x_5$……)

R	Gas constant (= 8.314 $J \cdot K^{-1} \cdot mol^{-1}$). (ideal gas theory; $p \cdot V = R \cdot n \cdot T$)
T	Absolute temperature (in Kelvin)
z	Valency of an ion
F	Faraday constant (= 96485 $A \cdot s \cdot mol^{-1}$); electrical charge per mole
SCFA	Short chain fatty acid (= VFA) (both protonated and unprotonated form)
VFA	Volatile fatty acid (= SCFA)
HSCFA	Protonated short chain fatty acid (acetic, propionic, or butyric acid)
$SCFA^-$	Anion of the short chain fatty acid (acetate, propionate or butyrate)
SARA	Subacute ruminal acidosis (see 2.1.4)
Φ	Flux of ions, measured as a current (in $A \cdot cm^{-2}$)
J(X)	Molar flux of ion “X” (in $\mu eq \cdot cm^{-2} \cdot h^{-1}$)
$J_{ms}(X)$	Flux of ion “X” from the mucosal side to the serosal (blood) side
$J_{sm}(X)$	Flux of ion “X” from the serosal (blood) side to the mucosal side
G_t	Tissue Conductance (= I/E) (in $mS \cdot cm^{-2}$)
I	Current
I_{sc}	Short circuit current. (Current needed to clamp potential across a tissue to 0 mV); measured in $\mu A \cdot cm^{-2}$ or in the molar form as $\mu eq \cdot cm^{-2}$
PD_t	Transepithelial potential difference as measured in Ussing Chambers
E	Potential (in mV)
$[X]_i$	Intracellular concentration of the ion “X”
$[X]_i$	Extracellular concentration of the ion “X”
P_x or p(X)	Permeability constant of the substance “X”
C	Single-channel conductance (= I/E)(in pS)(patch clamp)
V_a	Potential across the apical membrane of the tissue (microelectrode)
V_t	Potential across the entire tissue (microelectrode)

11 Acknowledgments

First and foremost, I want to thank Prof. Holger Martens for his endless support, enthusiasm, help, advice, ideas and formidable knowledge of the literature on the rumen. Prof. Gotthold Gäbel and Prof. Jörg Aschenbach introduced me to the topic of SCFA transport; without their encouragement, I could not have entered this fascinating field. Dr. Khalid Abdoun is a wonderful friend and co-worker; both his data, and the discussions with him were truly inspiring. I have also profited greatly from the intellectually stimulating exchanges with PD Dr. Sabine Leonhard-Marek.

My sincerest thanks goes to PD Dr. Dorothee Günzel, without whose extensive help I would not have been able to characterize the cells in this study. Prof. Michael Fromm supported our collaboration and gave excellent advice. Prof. McGuigan introduced me to a whole new dimension of patience, precision - and friendship - in science.

I would also like to thank Dr. Lars Mundhenk and Jana Enders for their willingness to stain countless pieces of omasum until we had the incubation times right, not to mention their help in cytokeratin staining. Prof. Gruber is thanked for his support.

Dr. Inge Brinkmann and Maria Georgi not only contributed excellent patch clamp data and excellent ideas, but also endless time and patience – and laughs! The members of the Journal Club also deserve to be mentioned, in particular, Osama Ali, Imtiaz Rabbani, and Driton Caushi, without whom the study of the rumen would not have been as enjoyable.

The staff of the Institute of Veterinary Physiology were wonderful. Katharina Wolf, always friendly, enthusiastic, tireless and full of ideas. Bernd Anders, who until his death, tirelessly supported me in more ways than I can mention. Thanks to Gabriele Kiselowski for the cells. Carola Behm deserves praise for her friendly efficiency.

Many thanks also to the Margarete Markus Charity and the Deutsche Forschungsgemeinschaft and BMBF (Fugato-*plus*) for funding.

Finally, thanks to my father, Prof. Dr. Peter Stumpff, and to my mother, Brigitte Remertz-Stumpff, for being the best parents imaginable and for laying the foundation for my fascination with science. Prof. Samuel and Carol Goldstein were also of importance in this regard and others. Very special thanks to my “Doktorvater”, Prof. Michael Wiederholt, who got me started in physiology and supported me throughout.

Finally, thanks to all of those whom I have not mentioned, last but not least for their understanding that this list must come to an end. But before that happens, I must thank my family, Günter, Yamina and Nils. They deserve much, much more credit than I can express in this context.

12 Appendix

Diese Habilitationsschrift stellt eine Zusammenfassung der folgenden, kumulativ erfolgten Originalarbeiten dar:

Der Anteil der an den aufgeführten Publikationen beteiligten Autorinnen und Autoren wird nach folgenden Kriterien gegliedert:

a) Idee und Versuchsplanung
b) Versuchsdurchführung
c) Auswertung
d) Erstellen des Manuskriptes

In den Fällen, in denen der Zweit-Autor im gleichen Umfang zur Arbeit beigetragen hat wie der Erst-Autor wurde der Name unterstrichen.

1. **Leonhard-Marek S, Stumpff F, and Martens H.** Transport of cations and anions across forestomach epithelia: conclusions from in vitro studies. Animal 4: 1037-1056, 2010.
DOI: 10.1017/S1751731110000261

a) Idee und Versuchsplanung	*Leonhard-Marek, S, Stumpff, F, Martens, H.*
b) Versuchsdurchführung	*Leonhard-Marek, S, Stumpff, F, Martens, H.*
c) Auswertung	*Leonhard-Marek, S, Stumpff, F, Martens, H.*
d) Erstellen des Manuskripts	*Leonhard-Marek, S, Stumpff, F, Martens, H.*

2. **Abdoun K, Stumpff F, Rabbani I, and Martens H.** Modulation of urea transport across sheep rumen epithelium in vitro by SCFA and CO_2. Am J Physiol 298: G190-202, 2010.
DOI: 10.1152/ajpgi.00216.2009

a) Idee und Versuchsplanung	*Stumpff F, Abdoun, K, Martens, H.*
b) Versuchsdurchführung	*Abdoun, K, Stumpff, F, Rabbani, I.*
c) Auswertung	*Abdoun, K, Stumpff, F.*
d) Erstellen des Manuskripts	*Stumpff, F, Rabbani, I, Martens, H.*

3. **Stumpff F, Martens H, Bilk S, Aschenbach JR, and Gäbel G.** Cultured ruminal epithelial cells express a large-conductance channel permeable to chloride, bicarbonate, and acetate. Pflugers Arch 457: 1003-1022, 2009.
DOI: 10.1007/s00424-008-0566-6

a) Idee und Versuchsplanung	*Stumpff, F.*
b) Versuchsdurchführung	*Stumpff, F.*
c) Auswertung	*Stumpff, F.*
d) Erstellen des Manuskripts	*Stumpff, F, Martens, H, Bilk, S, Aschenbach, JR, Gäbel, G.*

4. **Aschenbach JR, Bilk S, Tadesse G, Stumpff F, and Gäbel G.** Bicarbonate-dependent and bicarbonate-independent mechanisms contribute to nondiffusive uptake of acetate in the ruminal epithelium of sheep. Am J Physiol 296: 1098-1107, 2009.

DOI: 10.1152/ajpgi.90442.2008

a) Idee und Versuchsplanung	*Aschenbach, JR, Gäbel, G.*
b) Versuchsdurchführung	*Bilk, S, Tadesse, G.*
c) Auswertung	*Bilk, S, Tadesse, G; Aschenbach, JR.*
d) Erstellen des Manuskripts	*Aschenbach, JR, Gäbel, G, Stumpff, F.*

5. **Bondzio A, Stumpff F, Schön J, Martens H, and Einspanier R.** Impact of Bacillus thuringiensis toxin Cry1Ab on rumen epithelial cells (REC) - a new in vitro model for safety assessment of recombinant food compounds. *Food Chem Toxicol* 46: 1976-1984, 2008.

DOI:10.1016/j.fct.2008.01.038

a) Idee und Versuchsplanung	*Bondzio, A, Stumpff F, Einspanier, R.*
b) Versuchsdurchführung	*Bondzio, A, Schön, J.*
c) Auswertung	*Bondzio, A.*
d) Erstellen des Manuskripts	*Bondzio, A, Stumpff, F, Einspanier, R.*

6. **Stumpff F, Bondzio A, Einspanier R, and Martens H.** Effects of the Bacillus thuringiensis toxin Cry1Ab on membrane currents of isolated cells of the ruminal epithelium. J Membr Biol 219: 37-47, 2007.

DOI: 10.1007/s00232-007-9059-3

a) Idee und Versuchsplanung	*Stumpff, F, Einspanier, R.*
b) Versuchsdurchführung	*Stumpff, F.*
c) Auswertung	*Stumpff, F.*
d) Erstellen des Manuskripts	*Stumpff, F,Bondzio,A,Einspanier,R,Martens, H.*

7. **Stumpff F and Martens H.** The rumen and potassium homeostasis: a model. Journal of Animal and Feed Sciences 16: 436-441, 2007.

ISSN 1230-1388

a) Idee und Versuchsplanung	*Stumpff, F, Martens, H.*
b) Versuchsdurchführung	*Stumpff, F.*
c) Auswertung	*Stumpff, F.*
d) Erstellen des Manuskripts	*Stumpff, F, Martens, H.*

8. **Abdoun K, Stumpff F, and Martens H.** Ammonia and urea transport across the rumen epithelium: a review. Anim Health Res Rev 7: 43-59, 2006. *DOI: 10.1017/S1466252307001156*

a) Idee und Versuchsplanung	*Stumpff, F, Abdoun, K, Martens, H.*
b) Versuchsdurchführung	*Abdoun, K, Stumpff, F.*
c) Auswertung	*Abdoun, K, Stumpff, F.*
d) Erstellen des Manuskripts	*Stumpff, F, Abdoun, K, Martens, H.*

9. **Stumpff F and Martens H.** A role for magnesium in the regulation of ruminal sodium transport. In: Focus on signal transduction research, edited by McAlpine G. New York: New Nova Science Publishers, Inc. 2006, p. 37-66. *ISBN 1-60021-376-6*

a) Idee und Versuchsplanung	*Stumpff, F.*
b) Versuchsdurchführung	*Stumpff, F.*
c) Auswertung	*Stumpff, F.*
d) Erstellen des Manuskripts	*Stumpff, F, Martens, H.*

10. **Leonhard-Marek S, Stumpff F, Brinkmann I, Breves G, and Martens H.** Basolateral Mg^{2+}/Na^{+} exchange regulates apical nonselective cation channel in sheep rumen epithelium via cytosolic Mg^{2+}. Am J Physiol 288: G630-645, 2005.

DOI: 10.1152/ajpgi.00275.2004

a) Idee und Versuchsplanung	*Stumpff, F, Leonhard-Marek, S, Martens, H.*
b) Versuchsdurchführung	*Stumpff, F, Brinkmann, I, Leonhard-Marek, S.*
c) Auswertung	*Stumpff, F, Leonhard-Marek, S.*
d) Erstellen des Manuskripts	*Stumpff, F, Leonhard-Marek, S.*

11. **Abdoun K, Stumpff F, Wolf K, and Martens H.** Modulation of electroneutral Na transport in sheep rumen epithelium by luminal ammonia. Am J Physiol 289: G508-520, 2005.

DOI: 10.1152/ajpgi.00436.2004

a) Idee und Versuchsplanung	*Stumpff, F, Abdoun, K, Martens, H.*
b) Versuchsdurchführung	*Stumpff, F, Abdoun, K.*
c) Auswertung	*Stumpff, F, Abdoun, K.*
d) Erstellen des Manuskripts	*Stumpff, F, Martens, H.*